AD-A033 682 DAYTON UNIV OHIO RESEARCH INST F/G 1/2
DAYTON AIRCRAFT CABIN FIRE MODEL. VOLUME I. BASIC MATHEMATICAL --ETC(U)
JUN 76 J B REEVES, C D MACARTHUR DOT-FA74WA-3532
UNCLASSIFIED FAA-RD-76-120-1 NL

1 OF 2
AD A033682

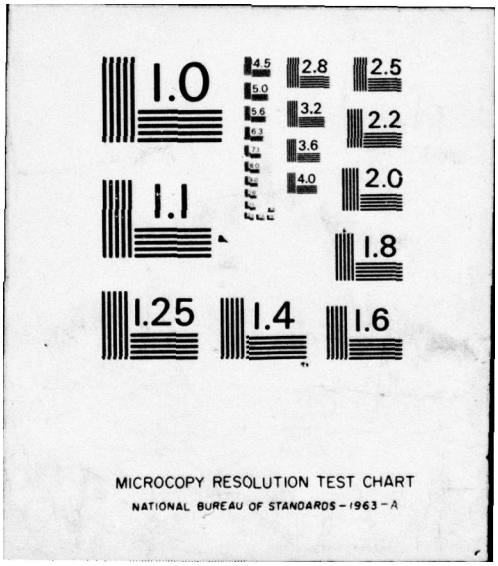
1.0
1.1
1.25
1.4
1.6
1.8
2.0
2.2
2.5
2.8
3.2
3.6
4.0
4.5
5.0
5.6
MICROCOPY RESOLUTION TEST CHART
NATIONAL BUREAU OF STANDARDS - 1963 - A

Report No. FAA-RD-76-120, I

DAYTON AIRCRAFT CABIN FIRE MODEL

Volume I - Basic Mathematical Model

Jerry B. Reeves
Charles D. MacArthur
University of Dayton
Research Institute
Dayton, Ohio 45469

June 1976

Final Report

Prepared for

U.S. DEPARTMENT OF TRANSPORTATION
FEDERAL AVIATION ADMINISTRATION
Systems Research & Development Service
Washington, D.C. 20590

NOTICE

This document is disseminated under the sponsorship of the Department of Transportation in the interest of information exchange. The United States Government assumes no liability for its contents or use thereof.

Technical Report Documentation Page

1. Report No.	2. Government Accession No.	3. Recipient's Catalog No.
FAA-RD-76-120-1		

4. Title and Subtitle
Dayton Aircraft Cabin Fire Model, Volume I. Basic Mathematical Model.

5. Report Date
June 1976

6. Performing Organization Code

7. Author(s)
J. B. Reeves and C. D. MacArthur

8. Performing Organization Report No.

9. Performing Organization Name and Address
University of Dayton Research Institute
300 College Park Drive
Dayton, Ohio 45469

10. Work Unit No. (TRAIS)

11. Contract or Grant No.
DOT-FA74WA-3532

13. Type of Report and Period Covered
Final Report.
July 1974 — March 1976

12. Sponsoring Agency Name and Address
Department of Transportation
Federal Aviation Administration
Systems Research and Development Service
Washington, D.C. 20590

14. Sponsoring Agency Code

15. Supplementary Notes
141 p.

Jerry B. Reeves
Charles D. MacArthur

16. Abstract

A basic mathematical model and computer simulation program have been developed to assess the smoke and toxic gas emissions resulting from the burning of cabin interior materials of a wide-body transport aircraft in a full-scale fire based on laboratory test data on these materials. The mathematical model employs a technique of approximating the distribution of burning or smoldering regions on combustible materials by dividing the surface of the material into square area elements. The combustion behavior of a material is modeled by the allowing of the area elements to exist in one of seven discrete states. The four primary states are the following: virgin (the original, unignited condition), smoldering (nonflaming thermal degredation), flaming (burning with open flaming), or charred (burned-out or inert). The other three states are intermediate states in the transition to or from one of the four primary states. Fire ignition; flame spread; release of heat, smoke, and toxic combustion products; and the eventual extinction of a fire are all predicted by specifying times of transition between the four primary states and by specifying flame spread rates. Transition times, flame spread rates and the smoke, heat, and toxic gas release rates are assumed to be known as functions of imposed heat flux from laboratory measurements on the specific materials and assemblies of an aircraft cabin interior. Smoke and toxic gas concentration within the cabin section of the fire origin are computed by a one-dimensional, dynamic, stratified model of the cabin atmosphere which includes buoyancy driven flow out of the cabin section through one or more doorways. The results of two sample runs of the simulation program are presented and analyzed. The significance of the various interior materials' contribution to the cabin fire is shown. Recommendations for validation of the model are given. This report consists of three volumes: Volume I is entitled "Laboratory Test Program" and Volume III is entitled "Computer Program User's Guide".

END

17. Key Words	18. Distribution Statement
aircraft fire safety, aircraft interior materials, smoke and toxic gases, aircraft cabin fires, wide-body aircraft, room fire, mathematical model, computer simulation, fire research	Document is available to the public through the National Technical Information Service, Springfield, Virginia 22151

19. Security Classif. (of this report)	20. Security Classif. (of this page)	21. No. of Pages	22. Price
Unclassified	Unclassified	143	

Form DOT F 1700.7 (8-72) Reproduction of completed page authorized

105400
LB

METRIC CONVERSION FACTORS

Approximate Conversions to Metric Measures

Symbol	When You Know	Multiply by	To Find	Symbol
		LENGTH		
in	inches	*2.5	centimeters	cm
ft	feet	30	centimeters	cm
yd	yards	0.9	meters	m
mi	miles	1.6	kilometers	km
		AREA		
in^2	square inches	6.5	square centimeters	cm^2
ft^2	square feet	0.09	square meters	m^2
yd^2	square yards	0.8	square meters	m^2
mi^2	square miles	2.6	square kilometers	km^2
	acres	0.4	hectares	ha
		MASS (weight)		
oz	ounces	28	grams	g
lb	pounds	0.45	kilograms	kg
	short tons (2000 lb)	0.9	tonnes	t
		VOLUME		
tsp	teaspoons	5	milliliters	ml
Tbsp	tablespoons	15	milliliters	ml
fl oz	fluid ounces	30	milliliters	ml
c	cups	0.24	liters	l
pt	pints	0.47	liters	l
qt	quarts	0.95	liters	l
gal	gallons	3.8	liters	l
ft^3	cubic feet	0.03	cubic meters	m^3
yd^3	cubic yards	0.76	cubic meters	m^3
		TEMPERATURE (exact)		
°F	Fahrenheit temperature	5/9 (after subtracting 32)	Celsius temperature	°C

*1 in = 2.54 (exactly). For other exact conversions and more detailed tables, see NBS Misc. Publ. 286, Units of Weights and Measures, Price $2.25, SD Catalog No. C13.10:286.

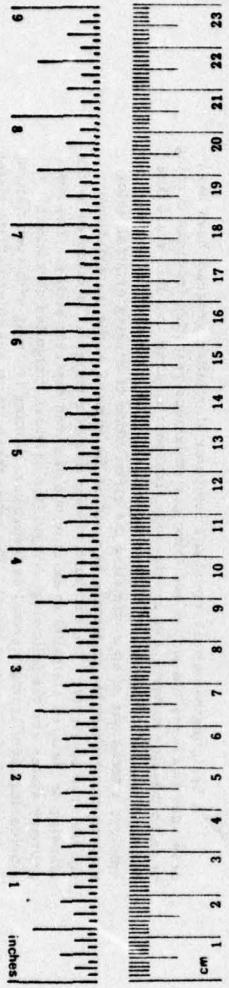

Approximate Conversions from Metric Measures

Symbol	When You Know	Multiply by	To Find	Symbol
		LENGTH		
mm	millimeters	0.04	inches	in
cm	centimeters	0.4	inches	in
m	meters	3.3	feet	ft
m	meters	1.1	yards	yd
km	kilometers	0.6	miles	mi
		AREA		
cm^2	square centimeters	0.16	square inches	in^2
m^2	square meters	1.2	square yards	yd^2
km^2	square kilometers	0.4	square miles	mi^2
ha	hectares (10,000 m^2)	2.5	acres	
		MASS (weight)		
g	grams	0.035	ounces	oz
kg	kilograms	2.2	pounds	lb
t	tonnes (1000 kg)	1.1	short tons	
		VOLUME		
ml	milliliters	0.03	fluid ounces	fl oz
l	liters	2.1	pints	pt
l	liters	1.06	quarts	qt
l	liters	0.26	gallons	gal
m^3	cubic meters	35	cubic feet	ft^3
m^3	cubic meters	1.3	cubic yards	yd^3
		TEMPERATURE (exact)		
°C	Celsius temperature	9/5 (then add 32)	Fahrenheit temperature	°F

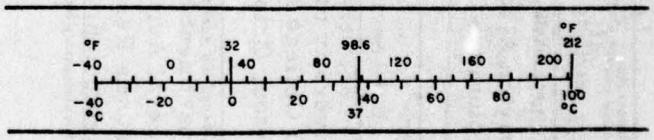

PREFACE

This report was prepared by the University of Dayton Research Institute for the Federal Aviation Administration Systems Research and Development Service under Contract FA74WA-3532 during the period July 1974 to March 1976. The report describes the development of a basic mathematical model of a fire within the cabin of a wide-body commercial transport category aircraft. The report is divided into three volumes of which this is the first. Volume I, entitled "Basic Mathematical Model", describes the development and presents example results of the model. Volume II, "Laboratory Test Program", presents the results of a laboratory test and data collection program conducted in support of the development of the model. Volume III, "Computer Program User's Guide", is a guide for use of the computer program which implements the mathematical model.

This contract was administered under the direction of Mr. Robert C. McGuire and Mr. Charles C. Troha of the Systems Research and Development Service, ARD 520. Work was performed at the University of Dayton under the supervision of Mr. Nicholas A. Engler, supervisor of the Applied Systems Analysis Section. Other personnel at the University who have contributed to this program include Mr. James K. Luers and Mr. Peter M. Kahut. The authors wish to express their gratitude to all those mentioned for their support, encouragement, and valuable technical contributions. The authors also wish to thank Ms. Jacquelin Aldrich and Ms. Peggy Cummings for their patient assistance in preparing the manuscript.

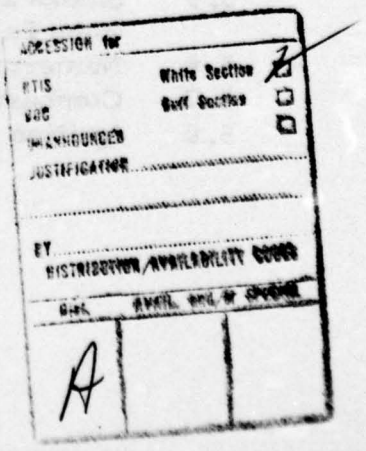

TABLE OF CONTENTS

LIST OF TABLES

LIST OF FIGURES

SECTION 1

INTRODUCTION

1.1 PURPOSE

This report describes the Dayton Aircraft Cabin Fire (DACFIR) Model, a basic mathematical model of a growing fire in the cabin of a wide-body commercial transport aircraft. The model was developed to enable the smoke and toxic gas emissions resulting from the burning of interior materials in a full-scale cabin fire to be predicted from laboratory test data on the same materials. The model is implemented as a computer simulation program which uses the geometric description of the cabin section in which the fire originates, laboratory test data on the furnishing materials, and a description of the ignition source to compute the smoke, toxic gas, and temperature levels in the cabin at selected times during the development of the fire.

1.2 BACKGROUND

Any fire which may start in or intrude into the cabin of a commercial transport aircraft presents a serious threat to passengers and crew. On the ground, effective emergency evacuation may be impeded or prevented by the toxic products of combustion and large quantities of smoke generated by burning cabin interior materials. To insure that cabin interior materials present the least possible danger in this respect the smoke and toxic gas generation properties of these materials may be determined by subjecting samples of the materials to standard laboratory fire tests. However, setting regulations based solely upon the results of laboratory tests often raises the question of the ability of the test procedures to duplicate conditions that might arise in a full-scale fire. Flammability, smoke generation, or other combustion tests normally measure the combustion behavior of a single material or fabricated unit of a given size; in a given orientation;

and under specific ignition, ventilation, and input heat flux conditions. In some tests, one or more of the above conditions or other important parameters may be varied to improve the knowledge obtained about the fire safety, or lack thereof, of the test specimen. As fire safety technology advances more tests of this type are being developed and adopted, reflecting the realization that the complexity of the combustion process demands testing to cover a wide range of possible fire exposure conditions and consequent burning behavior.

If a material's combustion behavior is known for most fire exposure situations by laboratory testing, how may the fire behavior of a number of different materials arranged in a complex geometry such as an aircraft passenger cabin be predicted? One method of obtaining an answer to this question is to construct a full-scale test enclosure, outfit it in as complete a manner as possible with the materials of interest, and conduct a fire test. This method is expensive, especially for enclosures the size of a wide-body cabin; and, since cabin interiors have a large variety of possible furnishing materials, more than one test may be required further compounding the expense. Fortunately, recent advances in experimental and theoretical fire safety research are making an alternative approach possible: computer simulation of enclosed fires. By employing simple yet powerful techniques to describe fuel and fire geometry, flame spread, enclosure gas flow behavior, and other combustion phenomena, a mathematical model can be constructed of the fire process. The implementation of the model as a computer simulation program effects vast savings over full-scale burn tests by allowing many material combinations, geometries, and ignition modes to be examined. Computer simulation must still be verified and supplemented by some full-scale or related testing since theoretical fire science is not yet sufficiently advanced to confidently predict complex fire behavior totally from theoretical principles. Fire modeling must still be very empirical in many areas. The model described in this report has

been developed to make the best use of laboratory data and other empirical results and of appropriate theoretical analyses to produce a predictive tool for evaluating the fire safety of transport category aircraft cabins.

SECTION 2
MODELING TECHNIQUES

Fire is a dynamic phenomenon whose nature is dictated in part by the type and distribution of fuel that is burning. In an aircraft cabin the fuel can include the materials comprising all the surfaces in the cabin (carpets, sidewalls, stowage bin walls, seat upholstery and padding, etc.) as well as external fuel brought into the cabin (magazines, blankets, coats, etc.) The mathematical model described in this report is concerned only with the materials that are part of the cabin structure including seats. The problem of predicting the smoke and toxic gas levels resulting from a fire in this fuel configuration can be divided into two parts: (1) predicting the amounts of smoke, toxic gases, and heat released as a function of time; and (2) determining the distribution of these quantities within the aircraft cabin. The first part of the problem can be further divided into two parts: (1) determining the area on the various surfaces on fire as a function of time; and (2) determining the amount of smoke, toxic gases, and heat release per unit area per unit time. The approach taken to solve each of these problems is discussed in Sections 2.1, 2.2, and 2.3 below. Section 2.4 contains a discussion of the availability of data defining the material parameters needed to implement these approaches.

2.1 MODELING FIRE GROWTH

As stated above, the mathematical model considers fires originating on and propagating over the fixed interior surface of the cabin. The rate at which a fire develops depends upon the type of material of which these surfaces are constructed upon the surfaces' orientation, and upon the thermal conditions in the cabin. The surfaces within a wide-body aircraft are approximated as being either vertical or horizontal in orientation. This assumption simplifies calculations determining the fire growth while retaining the important features of the cabin. Even with this simplification,

the three dimensional curves defining the boundary of a fire on a surface cannot be easily described by algebraic equations. Further, even if these equations were available at a given time, the calculation of the area within the curve and the determination of the way in which the curve would change with time as the fire grows would be very difficult. To avoid such difficulties a grid scheme which "discritizes" the fuel surface has been devised to facilitate these calculations. Under this scheme each surface within the cabin is divided into equal size squares using imaginary vertical and/or horizontal lines. A convenient dimension for the square size for a wide-body cabin is six inches on a side. These fuel squares are referred to as "elements" in the model. The details of this scheme as applied to a wide-body cabin are presented in Section 3.

The area that is burning within a cabin is designated by noting that certain elements are burning. A single fire is defined as a number of contiguous burning elements. Other elements might be smoldering (undergoing non-flaming degradation) while still others might be either unaffected by the fire or be burned out or "charred". The spread of the fire is simulated by igniting at appropriate times elements adjacent to burning elements or by igniting elements touched by the flames of a fire which does not involve immediately adjacent elements. The problem of tracking the development of a fire then becomes one of determining when and if elements change from a non-burning to a burning condition. This transition is a function of the fire situation at a given time and the characteristics of materials comprising the various surfaces within the cabin. The important material characteristics include the flame spread rates, ignition times, and burning times. The variation of these parameters with incident heat flux must be considered.

2.2 EMISSION OF SMOKE, TOXIC GASES, AND HEAT

It has been assumed that elements that are smoldering can emit smoke and toxic gases while elements that are burning can emit smoke, toxic gases, and heat. The amount that is emitted during a given time interval depends

upon the emission rates, i.e. the amount emitted per unit time. These rates are functions of the chemical and thermal properties of the material undergoing combustion as well as the size of the fire, and the amount of oxygen available. Theories which describe the thermal and chemical reactions are very complex and not yet very well defined for most of the materials in an aircraft cabin. However, these rates may be measured directly in laboratory experiments. The aircraft cabin fire model has been developed assuming that these rates are supplied as input. It is further assumed that the rates for a given material are only dependent upon the externally applied heat flux to which the material is subjected. The rates are assumed to be measured in units of amount per unit time per unit area. The amount of smoke, toxic gas, or heat emitted during a given time interval can be found by multiplying the appropriate rate by the time step of the simulation and the area of a given material that is emitting.

Associated with each material are two emission rates, one for a smoldering condition and the other for a burning condition. The smoldering condition is initiated when the heat flux to the element reaches a specified level and the material decomposes without open flaming. Smoke and toxic gases are emitted at a constant level until (1) the heat flux is reduced below the specified level, (2) the element changes to the burning state by the propagation of the fire, or (3) the element is charred. Once the material begins flaming combustion, it is assumed to emit smoke, toxic gases, and heat until the material is charred. The emission rates for flaming combustion and the time of burning are assumed to be functions of incident heat flux.

2.3 DISTRIBUTION OF SMOKE, TOXIC GASES, AND HEAT

The smoke and hot gases generated by a fire rise toward the ceiling before dispersing laterally. This results in a stratified cabin atmosphere, that is, a layer of smoke and hot gases existing above a layer of relatively cool air. The depty and stability of the hot gas layer depends upon the size of the fire and upon the ventilation of the cabin. An atmosphere model has been

developed to determine the depth of this upper layer, the density of smoke and the concentration of various toxic gases in the layer, and the average temperature of the gas in the layer. This model is described in Section 5.

2.4 AVAILABILITY OF DATA DEFINING MATERIAL PROPERTIES

During its development, certain material properties were identified as necessary input to the model. These material properties are the following.

f_h	Horizontal flame spread rate, on a horizontal surface or in a horizontal direction on a vertical surface.
f_u	Upward flame spread rate on a vertical surface.
f_d	Downward flame spread rate on a vertical surface.
t_f	Time interval from the time of contact with a flame to the time the material begins flaming combustion.
t_{fc}	Time interval from the time the material begins flaming combustion to the time the material becomes charred.
r_h	Heat release rate per unit area while the material is undergoing flaming combustion.
r_{sf}	Smoke release rate per unit area while the material is undergoing flaming combustion.
$r_{f(i)}$	Release rate per unit area of the i^{th} toxic gas while the material is undergoing flaming combustion.
q_p	Heat flux at which the material begins to smolder.
t_p	Time interval from the time the heat flux to the material reaches q_p and the time at which smoldering begins.
t_{pc}	Time interval from the time the material begins to smolder to the time it becomes charred.

t_{pe} Time required for smoldering to stop after the heat flux falls below q_p.

r_{ss} Smoke release rate per unit area when the material is smoldering.

$r_s(i)$ Release rate per unit area of the i^{th} toxic gas when the material is smoldering.

The quantities f_h, f_u, f_d, t_f, t_{fc}, r_h, r_{sf}, $r_f(i)$, and t_{pe} are to be known as a function of heat flux over the expected range of values in an aircraft cabin fire.

Combustion properties of several aircraft interior materials have been measured by researchers at the National Aviation Facilities Experimental Center and at the National Bureau of Standards [1, 2, 3, 4]. Materials were subjected to the following tests and analyses:

Horizontal Flame Spread Test (Test Method 5906)
Vertical Flame Spread Test (Test Method 5902)
Vertical Flammability Test (Test Method 5903T)
NBS Radiant Panel Test (ASTM E-162)
NBS Smoke Chamber Test
Thermogravimetric and Calorimetric Analysis

A review of the test methods and the reported data led to the following conclusions.

---

[1] Marcy, J.F., Nicholas, E.B., and Damaree, J.E., "Flammability and Smoke Characteristics of Aircraft Interior Materials," Federal Aviation Administration, FAA-ADS-3, January 1964.

[2] Marcy, J.F., "A Study of Air Transport Passenger Cabin Fires and Materials," National Aviation Facilities Experimental Center, FAA-ADS-44, December 1965.

[3] Gross, D., Loftus, J.J., Lee, T.G., and Gray, V.E., "Smoke and Gases Produced by Burning Aircraft Interior Materials," National Bureau of Standards, June 1968.

[4] "Flaming and Self-Extinguishing Characteristics of Aircraft Cabin Interior Materials," National Aviation Facilities Experimental Center, Report No. NA-68-30, July 1968.

1. The vertical and horizontal flame spread tests were conducted with no externally applied heat flux, and many of the materials were shown to be self-extinguishing under this condition. The resulting data were useful for comparing one material to another but could not be used to determine how the material would behave in a cabin fire.

2. The flame spread property of materials from the radiant panel tests is defined in terms of a flame spread index which may be used for the intercomparison of materials but is not a parameter that can be used to define the actual flame spread velocity. Also, the test was run at only one heat flux level with the flame traveling in only one direction (down a specimen oriented at 30° angle with respect to the vertical).

3. The data reported from the NBS Smoke Chamber tests was not sufficient to determine an average smoke or toxic gas release rate. This data was developed at only one heat flux level (2.5 W/cm^2).

4. In some cases the tests were conducted on individual material components of a structure rather than on the composite structure as it appears in the cabin.

5. The data generated by the above tests could be used to provide rough estimates of some of the needed material properties, but more accurate data could be generated from tests specifically designed to measure the properties of interest.

The aforementioned tests were designed primarily to compare one material to another and do indeed accomplish that purpose. This comparative data is not adequate to develop a physical model of a fire in an aircraft cabin since the test result usually cannot be converted to appropriate physical parameters.

One material characteristic which is not measured by the above test methods is the variation in flammability properties with variation in the applied heat flux. This variation significantly effects the development of a fire in an enclosure such as an aircraft cabin. An apparatus to measure flammability properties with variation in heat flux has been developed by Smith [5, 6, 7]. This device, known as the Ohio State University (OSU) Combusion Analyzer, is well suited to generate the proper input data for the DACFIR Model. The Boeing Company under subcontract employed the OSU Combustion Analyzer and other auxiliary apparatus to test a representative selection of wide-body aircraft cabin materials. A description of this test program and a compilation of the data generated is contained in Volume II of this report. Volume II also contains a discussion of how the data was used to develop specific tabulations of material properties for input to the DACFIR computer program. The data obtained by Boeing served to: (1) verify assumptions made in the model development about the variation of material properties with applied heat flux; (2) indicated the nature of these variations; and (3) provided specific input data for the simulation program to evaluate its performance.

2.5 SUMMARY OF THE MODELING TECHNIQUES

The DACFIR Model employs a grid scheme on all the surfaces in the cabin in order to determine the development of the fire. Laboratory measurements of flame spread rates, ignition times, the heat flux at the on-set of smoldering, smoldering times, and burning times are used in this determination. The emissions of smoke, heat, and toxic

---

[5] Smith, E.E., "Measuring Rate of Heat, Smoke, and Toxic Gas Release," Fire Technology, Vol. 8, No. 3, 1972, pp. 237-245.

[6] Smith, E.E. "Model for Evaluating Fire Hazard," Journal of Fire and Flammability, Vol. 5, July 1974, pp. 185-195.

[7] Smith, E.E., "Application of the Ohio State Release Rate Apparatus to Combustion Gas Studies," JFF/Combustion Toxicology, Vol. 1, May 1974, pp. 95-103.

gases during any time interval are determined by multiplying the area of each material undergoing smoldering or flaming by the laboratory measured emission rates for each material. The smoke, heat, and gases emitted by a fire or fires rise to the ceiling in the cabin creating a stratified cabin stmosphere. Finally, the material parameters needed by the model can be measured in the laboratory and, in fact, were measured by the Boeing Company for representative wide-body cabin materials.

The details of applying the grid scheme to a wide-body aircraft cabin are presented in Section 3. The logic for changing elements from one state to another are discussed in Section 4. The equations defining the distribution of smoke, heat, and toxic gases with the cabin are presented in Section 5. This is followed by a discussion of the flow of calculations within the model (Section 6), an example of the application of the model to a particular fire situation (Section 7), and conclusions reached in this study (Section 8).

SECTION 3

APPLICATION OF THE ELEMENT GRID SCHEME TO A WIDE-BODY AIRCRAFT

There are currently three wide-body aircraft certified by the FAA: the Boeing 747, the L-1011, and the CD-10. The cabin cross-section in each of these aircraft is approximately twenty feet wide and eight feet from floor to ceiling. The grid scheme discussed in the previous section has been applied to a representation of a three seat row section of a wide-body aircraft cabin. A length of three seat rows was chosen because during the time frame of interest (the first five minutes or so after a fire in the cabin begins) it is not likely that a survivable fire will spread beyond this region. All of the cabin could be included in the grid scheme but most of the elements would never enter into the calculations and thus unnecessarily increase computer time and storage requirements.

The application of the grid scheme to cabin lining surfaces and to seat surfaces is discussed below.

3.1 CABIN LINING SURFACES

The lining surfaces in an aircraft cabin include the carpet, sidewalls, window reveals and transparencies, passenger service units (PSU's), stowage bins and ceiling panels. The cross section of the cabin is assumed to be of the shape shown in Figure 3.1 which is basically a rectangle with indentions for the stowage bins and PSU's. The lining surfaces are assumed to be oriented either vertically or horizontally. Twenty individual lining surfaces are identified. Each surface runs the length of the cabin section of interest which in this case is three seat rows (7.5 feet). The twenty surfaces are numbered in Figure 3.1. The surfaces corresponding to these numbers are listed in Table 3.1. Each surface within the cabin is assumed to be constructed of one of seven material groups. Typically these seven would be the following.

TABLE 3.1

WIDE-BODY CABIN LINING SURFACES

Surface Number	Description
1	Carpet
2	Lower Right Sidewall Panel
3	Right Window Reveals and Window Transparencies (considered one surface)
4	Upper Right Sidewall Panel
5	Right Side Passenger Service Unit
6	Right Side Stowage Bin Bottom
7	Right Side Stowage Bin Face
8	Right Ceiling Panel
9	Right Center Stowage Bin Face
10	Right Center Stowage Bin Bottom
11	Left and Right Center Passenger Service Units
12	Left Center Stowage Bin Bottom
13	Left Center Stowage Bin Face
14	Left Ceiling Panel
15	Left Side Stowage Bin Face
16	Left Side Stowage Bin Bottom
17	Left Side Passenger Service Unit
18	Upper Left Sidewall Panel
19	Left Window Reveals and Window Transparencies (considered one surface)
20	Lower Left Sidewall Panel

Note: The definition of left and right with respect to the cabin interior assumes that the viewer is looking to the rear of the cabin as in Figure 3.1. This definition is opposite that which would be given by passengers seated in the aircraft.

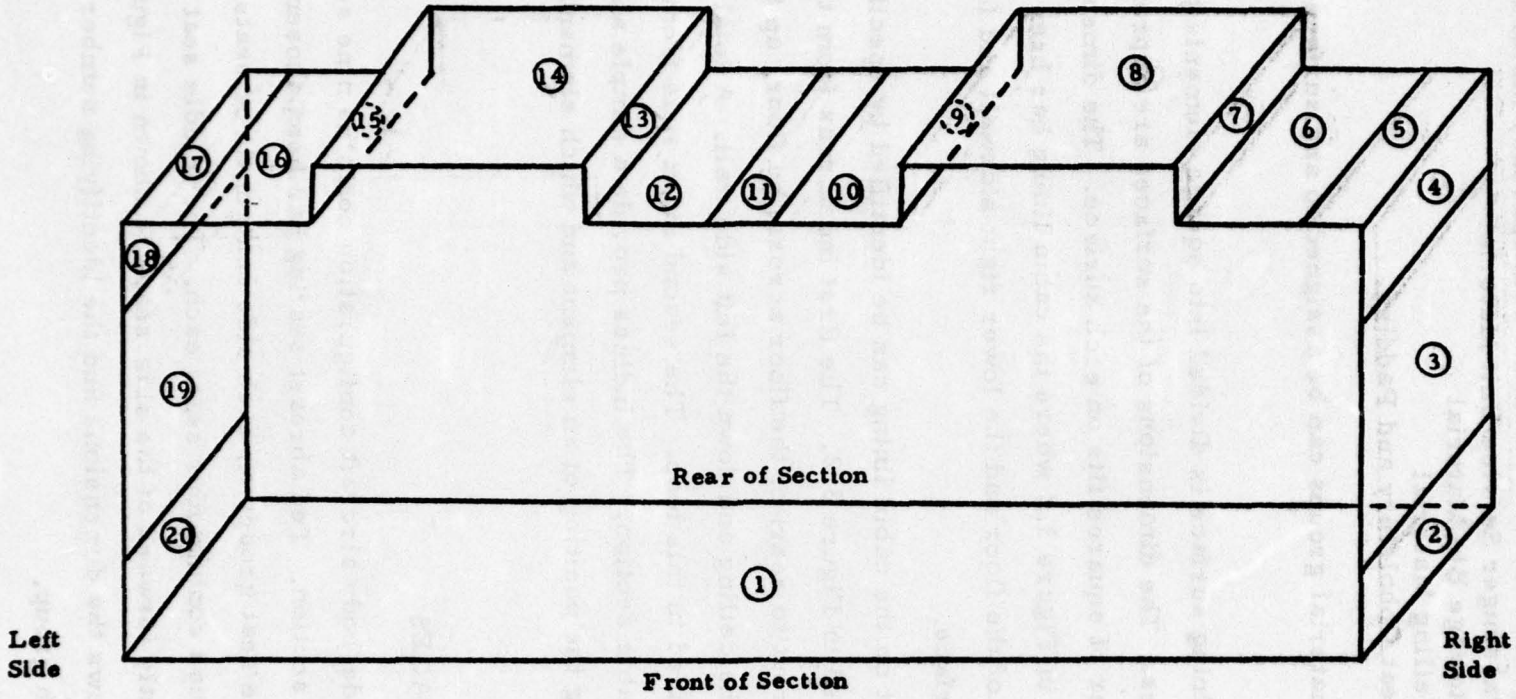

Figure 3.1 Location of Cabin Lining Surfaces

1. Carpet and Pad
2. Sidewall Material
3. Window Reveal - Window Transparency Material
4. Passenger Service Unit Material
5. Stowage Bin Material
6. Ceiling Material
7. Seat Upholstery and Padding.

Any of the seven material groups can be assigned to any surface in the cabin.

Each cabin lining surface is divided into square elements that are six inches by six inches. The dimensions of the surfaces are approximated such that a whole number of squares fits on each surface. The dimensions of each surface are shown in Figure 3.2 where the cabin lining has been disconnected at the intersection of the floor and the lower right sidewall and folded out to form a plane surface.

Each element on the cabin lining can be identified by specifying two indices as illustrated in Figure 3.2. The first index runs from the left side (facing from front to rear) of the floor across the floor, up the right side wall, across the ceiling and down the left side wall. A total of 116 elements are contained in this loop. The second index runs from the front to the rear of the cabin section. The indices provide a simple and convenient means of identifying the position of an element and which elements are adjacent to it.

3.2 SEAT SURFACES

A typical wide-body aircraft configuration contains nine seat groups in a three seat row section. Ten abreast seating has been chosen for the present model. The seat groups on each side contain three seats each; the middle seat groups contain four seats each. The middle seat groups are positioned slightly forward of the side seats as shown in Figure 3.3. This figure also shows the dimensions and the identifying number associated with each group.

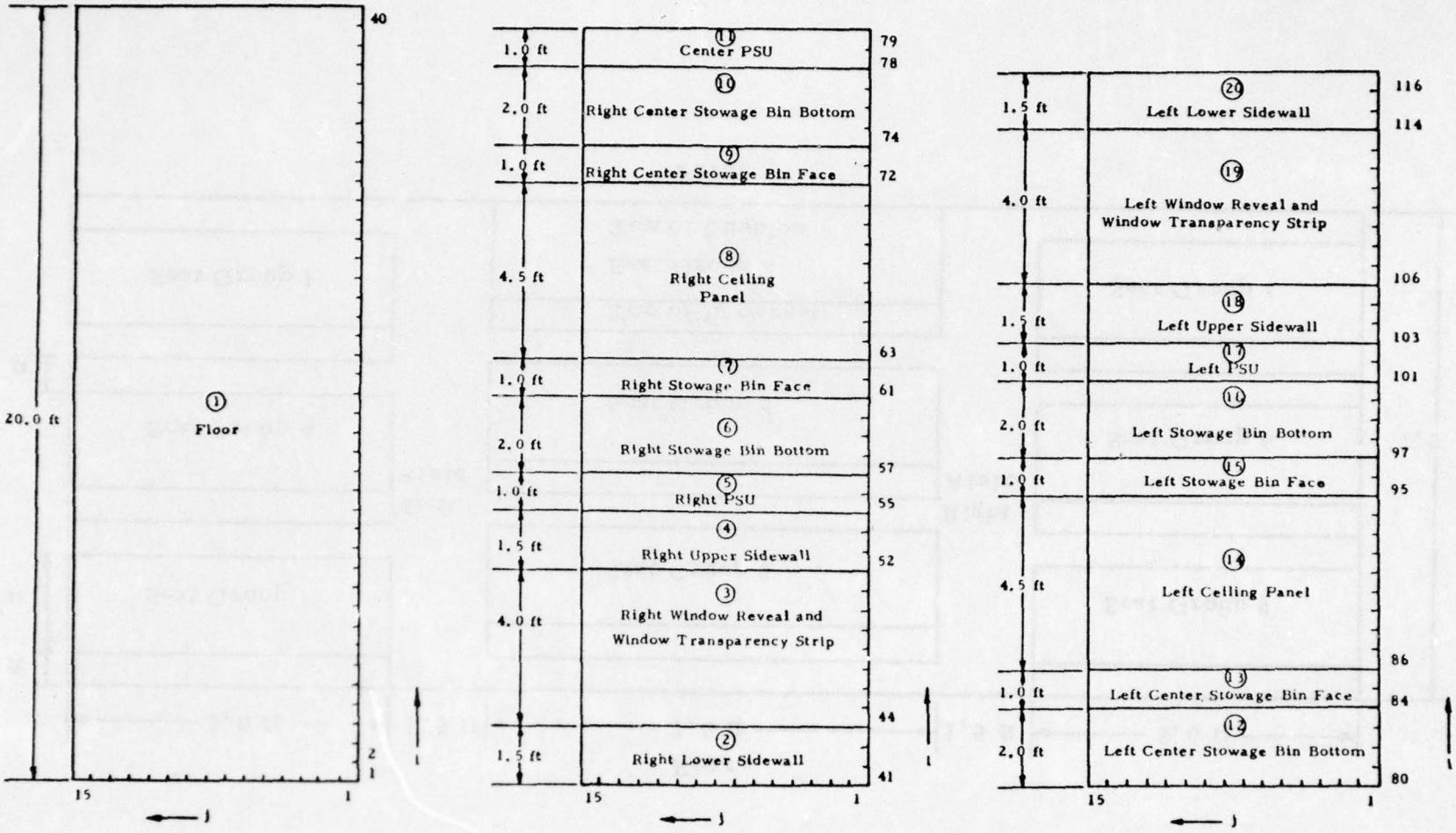

Figure 3.2 Indexing Scheme and Dimensions for Cabin Lining Surfaces

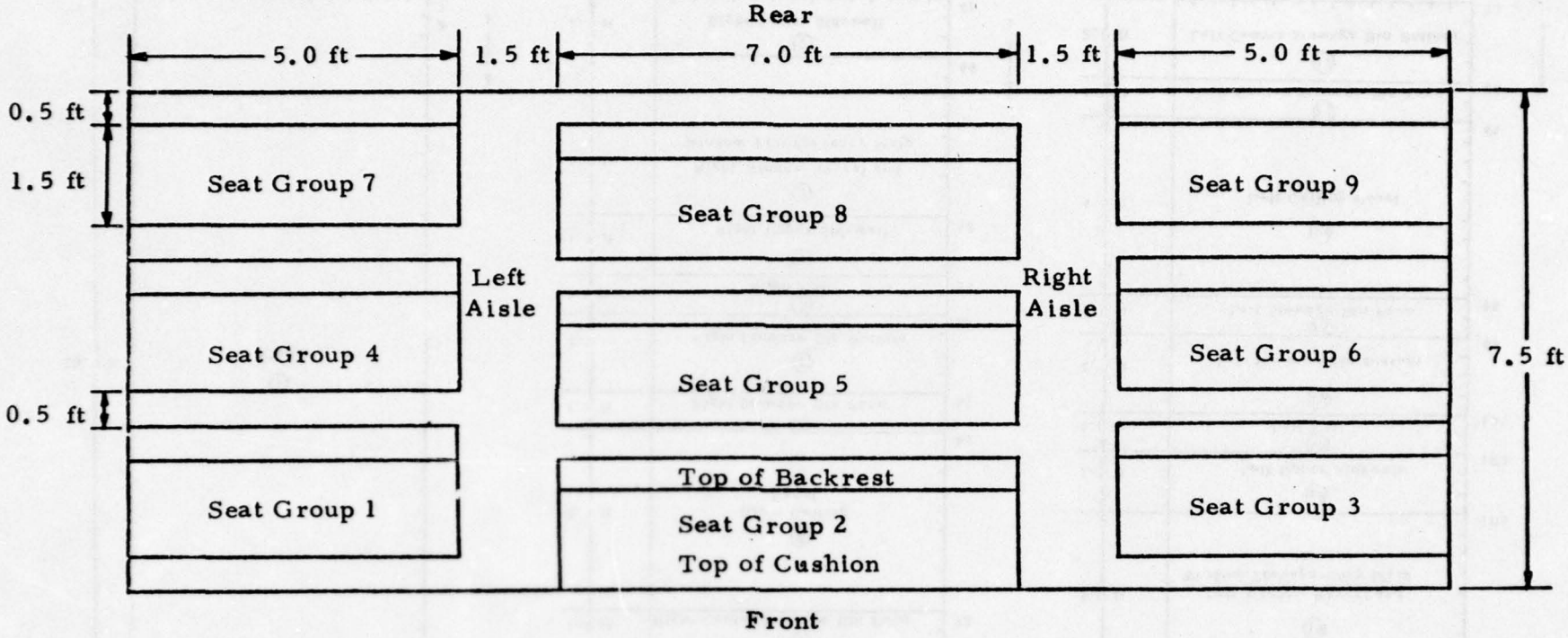

Figure 3.3 Location and Dimensions of Seat Groups (Top View)

Seven surfaces are defined on each seat group. These are shown in Figure 3.4. The seat surfaces are

Surface Number	Description
1.	Bottom of the Cushion
2.	Lower Section of the Back of the Backrest
3.	Upper Section of the Back of the Backrest
4.	Top of the Backrest
5.	Front of the Backrest
6.	Top of the Cushion
7.	Front of the Custion

Each of these surfaces can be assigned any of the seven material groups listed above. It should be noted that the sides of the seats and the arm rests are not considered in the present model.

Each surface on each of the seat groups is divided into square elements six inches on a side. The dimensions of the seat groups are adjusted so that each surface is covered by a whole number of elements. The seat elements are identified by three indices. The first index specifies the seat group (see Figure 3.3). The second two indices are illustrated in Figure 3.5 which shows the seven surfaces of a seat group folded out into a plane as was done for the lining surfaces. The second of the three seat indices begins at the left side of the seat group and runs to the right side. (Here the reference to "left" and "right" assumes that the viewer is in front of the seat facing it.) The third index begins at the back edge of the bottom of the seat cushion. This index runs from the back to the front of the cushion bottom, up the front of the cushion, from the front to the back of the cushion top, up the front of the backrest, over the top of the backrest, and down the backrest.

The seat groups are positioned above the floor such that the elements on each cusion bottom are directly aligned with elements on the floor. This facilitates the procedure for tracking a fire which propagates from the floor to a seat.

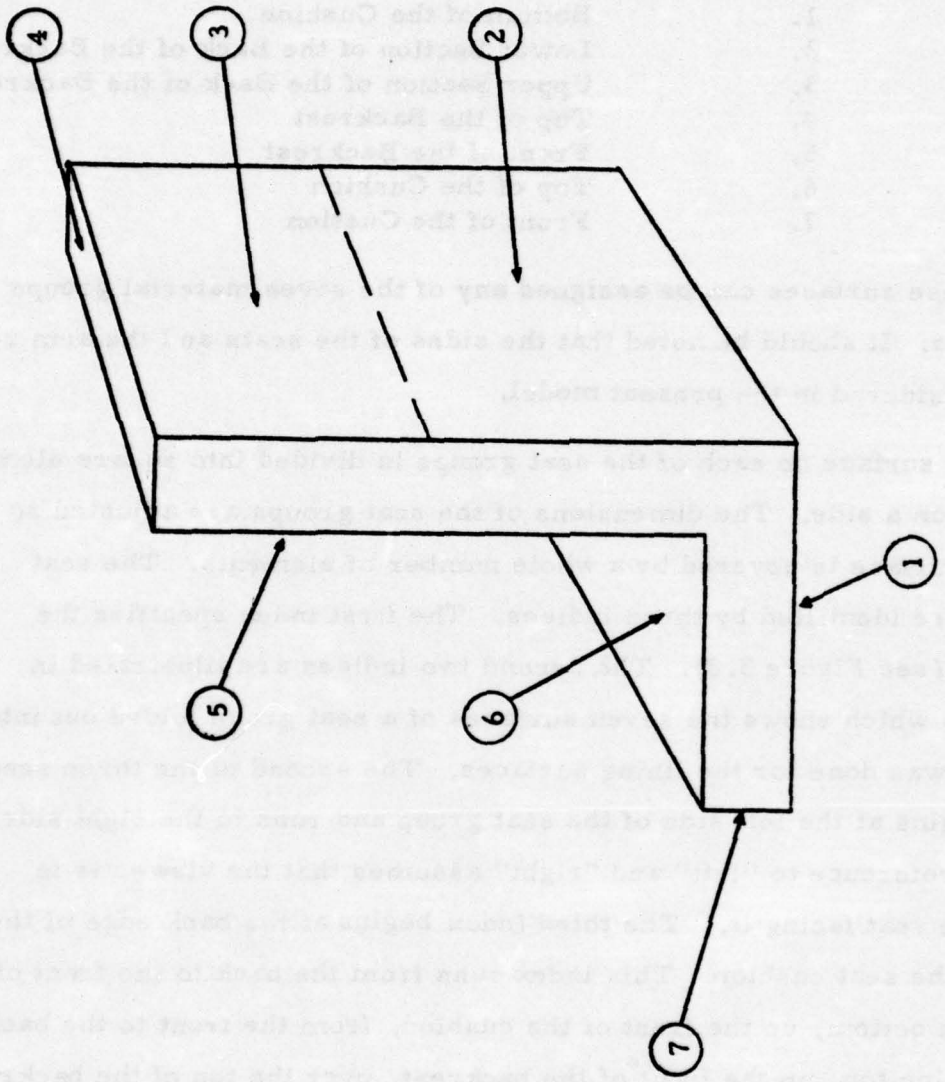

Figure 3.4 Location of the Surfaces on a Seat Group

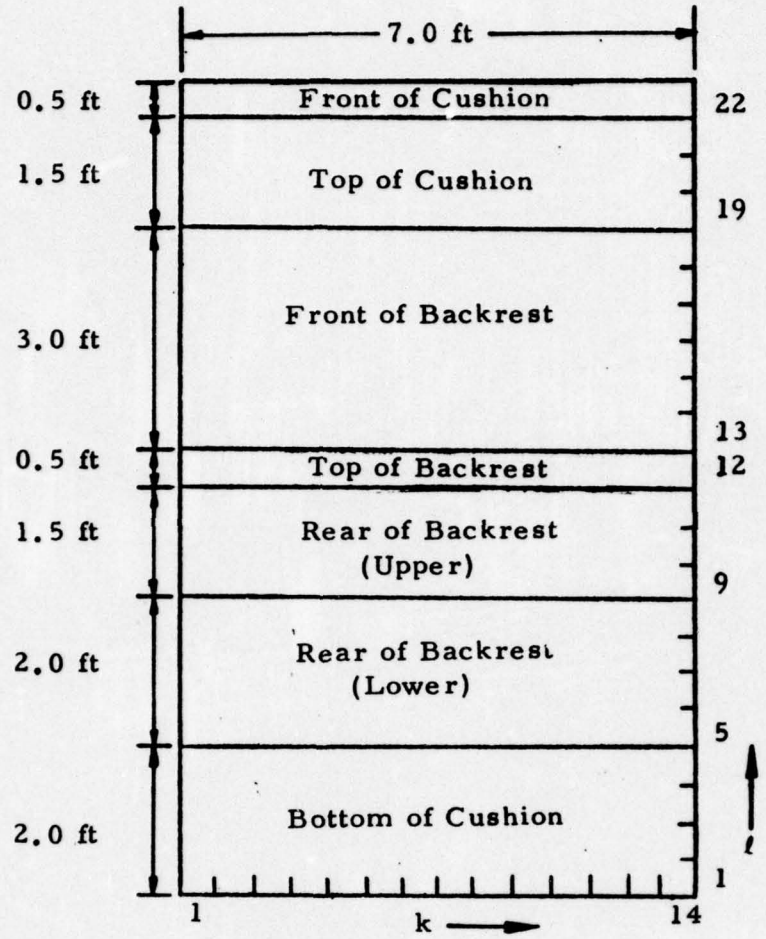

Figure 3.5 Indexing Scheme and Dimensions of One of the Middle Seat Groups (The side seat groups are only 5.0 feet wide, so the k index runs from 1 to 10 for these groups.)

SECTION 4

FIRE DEVELOPMENT MODEL

The fire situation in the cabin at any point in time is defined by the states associated with each surface element. As time progresses the states of various elements change to simulate the development or decline of a fire. The element states and the possible state transitions are described below.

4.1 ELEMENT STATES

Each element in the cabin is designated as being in one of seven states. The state of an element may change with time depending upon the size and location of the fire or fires in the cabin and upon the properties of the material associated with the surface upon which the element is located. The seven element states are as follows.

State 1 - The material comprising the element is in its virgin state; that is, it has not been affected by the fire or fires.

State 2 - The material comprising the element is smoldering; (undergoing nonflaming decomposition).

State 3 - The material comprising the element is undergoing flaming combustion.

State 4 - The material comprising the element is charred (burned out) and will no longer smolder or burn.

State 5 - The material comprising the element is receiving heat flux sufficient to cause it to smolder but because of the element's thermal inertia smoldering has not yet begun.

State 6 - The material comprising the element is being touched by the flames of a fire but has not started to burn because of the element's thermal inertia.

State 7 - The material comprising the element began smoldering when the heat flux to the element reached a specified level; the heat flux has now dropped below that level but the material is still smoldering. The element will continue to smolder for a specified time and then transform to the charred state (State 4).

There are two emission rates associated with each material: a smoldering rate and a flaming rate. The elements in States 2 and 7 emit smoke and toxic gases at the smoldering rates. The elements in State 3 emit smoke, heat, and toxic gases at the flaming rate. It should be noted that smoldering is assumed to be an endothermic reaction with no heat being released to the cabin atmosphere.

Element State 1 is a beginning state in which no state transitions have yet occurred. State 4 is a final state in which no additional state transitions can occur. States 5 and 6 are intermediate states in the transitions to States 2 and 3. The criteria governing state transitions are described in the next section.

4.2 ELEMENT STATE TRANSITIONS

An element's transition from one state to another is governed by the properties of the material associated with the element and by the element's relationship to the fire or fires in the cabin. A fire is defined by a set of contiguous elements in State 3. A fire is assumed to have a flame volume whose height is a function of the effective radius of the fire base and various properties of the fuel and the ambient atmosphere. (The equations describing a fire are discussed in Section 5.) At any point in time there are four sets of elements that are candidates for state transitions. These four sets are

1. Nonburning elements adjacent to elements that are in flaming. These elements are candidates for immediate ignition (transition to flaming combustion).

2. Elements that are inside the flame volume of a fire. All such elements are candidates for immediate ignition.

3. Elements in the general vicinity of a fire. These elements are not in danger of immediate ignition but are candidates for transition to smoldering.

4. Elements that are smoldering or flaming. These elements are candidates for transitions to the charred state.

The criteria for the state transitions that can occur to the elements within each of these sets are described below.

4.2.1 Ignition of Non-Burning Elements Adjacent to Flaming Elements

The rate at which a flame front propagates depends upon several factors. The factors considered in this work are the type of material at the edge of the fire, the size of the fire, orientation of the surface, and the background radiation level. The flame spread rates for a given material are input to the model in tabular form as functions of heat flux. The heat flux to elements adjacent to flaming elements is calculated based on the size of the adjacent fire and the overall background radiation level. Three flame spread rates are associated with a vertical surface: vertical up (f_u), vertical down (f_d) and horizontal (f_h). One flame spread rate (f_h) is associated with horizontal surfaces. The rates and directions are shown in Figure 4.1.

The state of an element adjacent to a flaming element (one in State 3) will be changed to State 3 after the original flaming element has been in State 3 for a time interval equal to or greater than d/f_i where d is the distance between the center of one element and the center of an adjacent element (six inches) and f_i is the flame spread rate in the appropriate direction for the flaming material for a given heat flux. Thus the flame front progresses in steps of six inches at a rate determined by the material characteristics and the radiation environment. By this process, called "conduction" to distinguish it from the jumping of fire across nonconnected

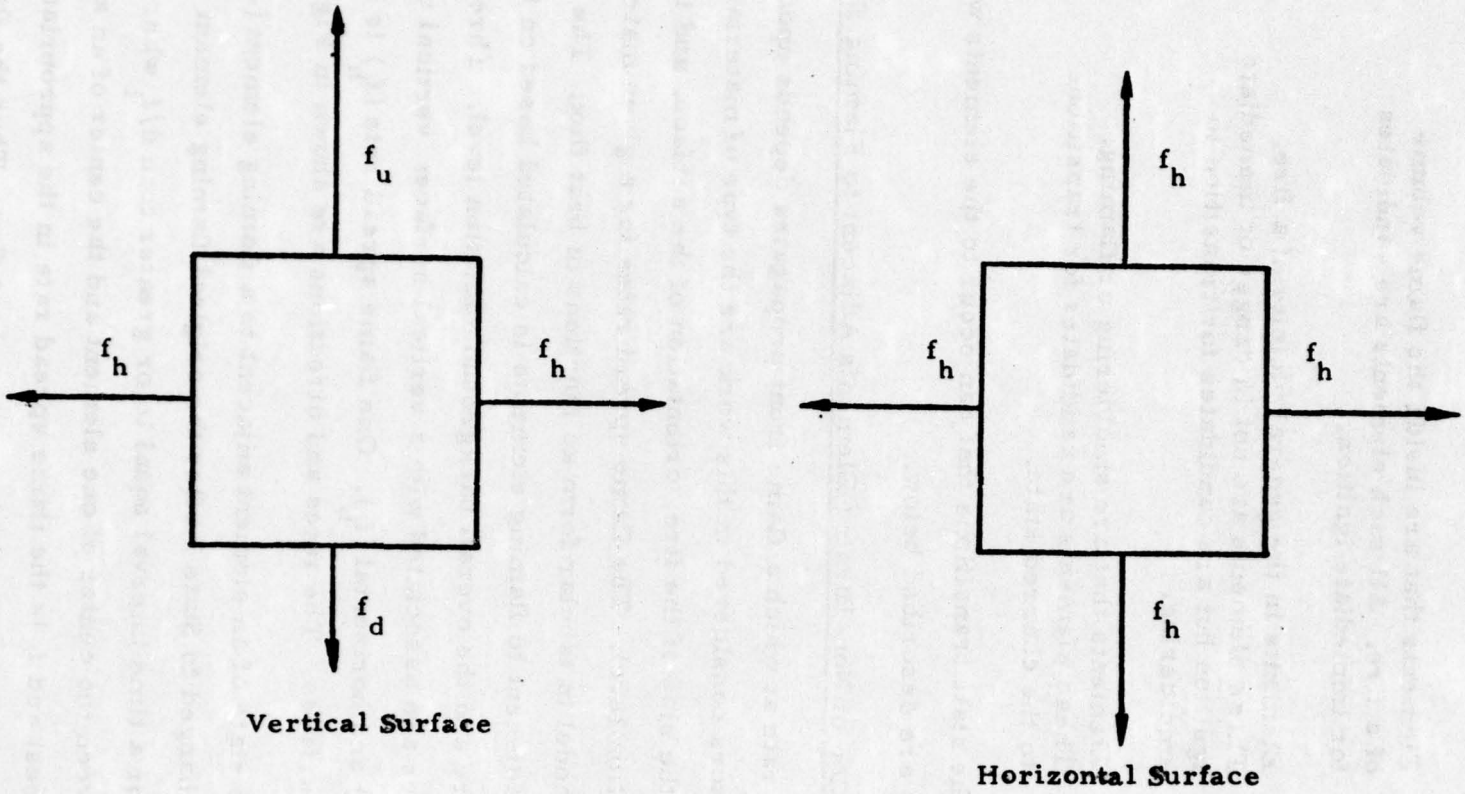

Figure 4.1 Flame Spread Rates for Vertical and Horizontal Surfaces

surfaces, a fire can propagate around the lining of the cabin or around a seat. The fire can also propagate by this process from a seat adjacent to a sidewall to the sidewall and vice versa. If a given material will not burn, the flame spread rate can be input as zero and the fire will not propagate over that material. The fire also will not propagate to an element that is in State 4 (charred). The state transitions which can occur under the above process are:

- Elements in State 1 can go to State 3
- Elements in State 2 can go to State 3
- Elements in State 5 can go to State 3
- Elements in State 6 can go to State 3

The state transitions are shown in Figure 4.2.

The flame spread rates used in determining if a state transition occurs are functions of the heat flux arriving at the material at the edge of the fire. The radiation intensity, q_1, from a fire arriving at an element area on the same plane as the fire base is

$$q_1 = \frac{e_b \alpha y_0 f^2 / \pi}{\frac{\alpha y_0 f_\ell^2}{\alpha_c \pi} + \left(\frac{\alpha f_\ell^2}{\alpha_c y_0 \pi} - y_0\right)\left(y_0 + \ell\right)^2 + \left(y_0 + \ell\right)^3} \qquad (4\text{-}1)$$

where

e_b is the black body emissive power,

α is the emissivity of the gas composing the flame,

y_0 is the effective radius of the fire, (see Section 5.2)

f_ℓ is the height of the flame volume, (see Section 5.3)

ℓ is the distance of the element from the edge of the fire, and

α_c is the percentage of blackbody radiation arriving at the center of the base of the fire.

This equation was derived by Dayan and Tien [8] for a cylindrically shaped fire on a horizontal surface facing upward. However, it is used in the

---

[8] Dayan, A. and Tien, C.L. "Radiant Heating from a Cylindrical Fire Column," Combustion Science and Technology, Vol. 9, 1974, pp. 41-47.

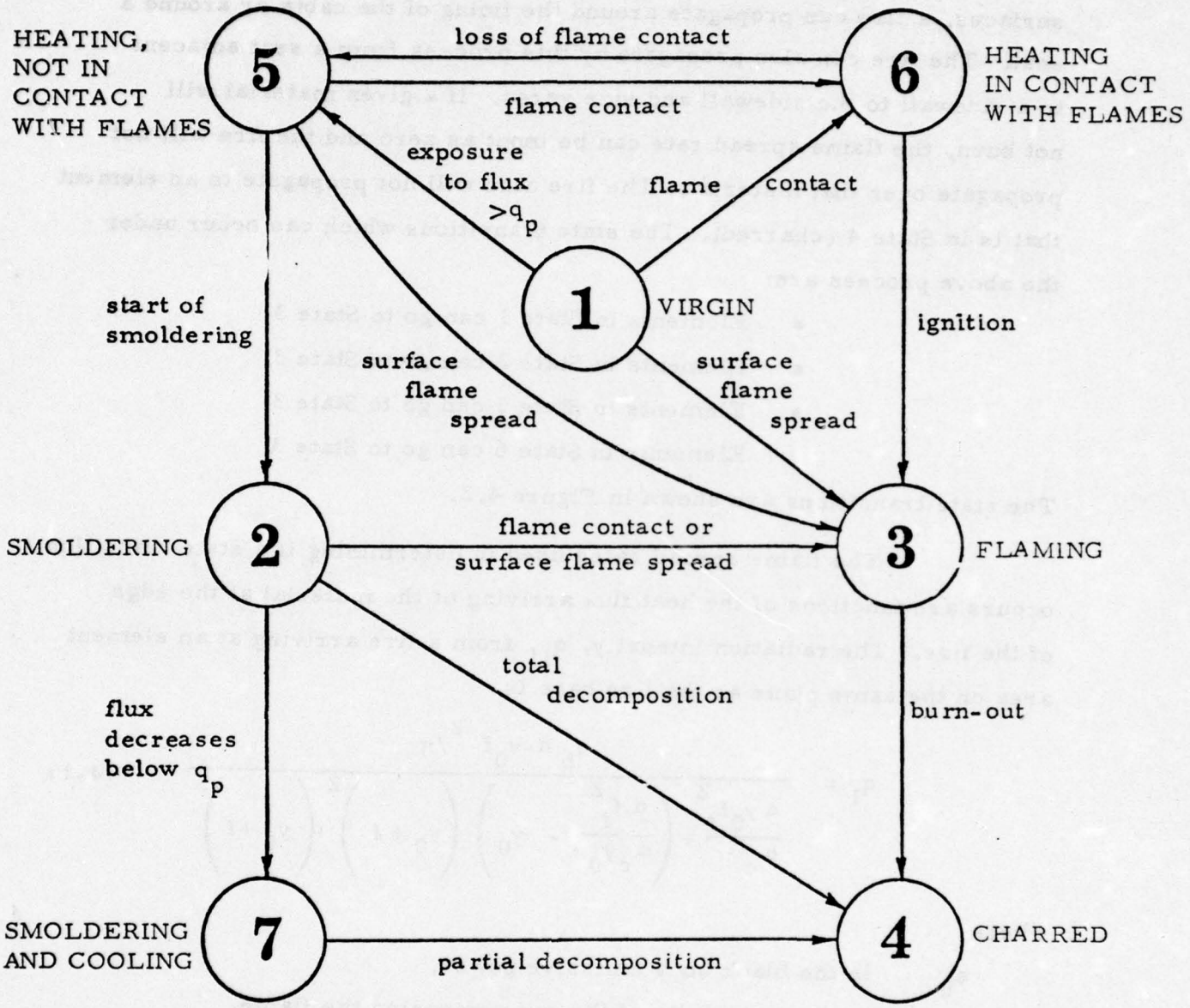

Figure 4.2 State Transitions

present model to compute the radiation level at the edge of any fire base at a value of ℓ of 0.25 feet (one half the length of an element square). The value of e_b used in the model is 16.3 Btu/(ft^2 · sec) which corresponds to blackbody radiation at 1959°R. This value of e_b corresponds to the value Fu [9] derived by extrapolating radiometer data to estimate the radiative heat flux at the flame boundary of an aircraft fuel fire. It is assumed that this value is representative of the radiative heat flux at the flame boundary of a fire in an aircraft cabin. A value of α of 1.0 is used and the value of α_c is computed by the equation

$$\alpha_c = \begin{cases} 0.4 + 0.08y_0 & \text{when } y_0 \leq 5 \text{ feet} \\ 0.8 & \text{when } y_0 > 5 \text{ feet} \end{cases} . \qquad (4\text{-}2)$$

This equation was derived based on the assumption that the radiative heat flux generated by a fire will increase with fire radius up to a given radius and then become constant. This assumption in turn is based on the findings of Blinov and Khudiakov [10, 11] who demonstrated that the mass burning rate of liquid pool fires of hydrocarbon fuels increases with radius up to base radius of about five feet and then becomes very nearly constant. It might be noted that the smallest fire in the DACFIR Model corresponds to one element burning and has an effective radius of 0.25 feet (see Section 5.2).

The value of q_1 computed from Equation 4-1 is added to the background radiation, q_b, and this sum is used to determine the values of flame spread rates (f_h, f_u, and f_d) associated with the fire under consideration. The flame spread rates are derived by linear interpolation from tables of flame spread rates for the various materials as a function

---

[9] Fu, T.T., "Aviation Fuel Fire Behavior Study," U.S. Naval Civil Engineering Laboratory, AGFSRS 72-2, February 1972.

[10] Blinov, V.I. and Khudiakov, G.N. "Certain Laws Governing Diffusive Burning of Liquids," Academiia Nauk, SSR Doklady, Vol. 113, 1957, pp. 1094-1098.

[11] Hottel, H.C., "Review-Certain Laws Governing Diffusive Burning of Liquids by V.I. Blinov and G.N. Khudiakov," Fire Research Abstracts and Reviews, Vol. 1, No. 2, January 1959, pp. 41-44.

of heat flux. The background radiation is made up of two components: the radiation from the hot gas layer in the upper portion of the cabin and a constant level of radiation input by the user. This latter component allows the user to investigate situations in which there is an external source of radiation into the cabin, such as, an external fuel fire near an opening in the fuselage.

4.2.2 Ignition of Elements Inside the Flame Volume of a Fire

The flames of a fire on one surface may contact other surfaces that are not physically connected to the surface containing the base of the fire. Elements on the surface contacted by the flames may eventually ignite. This process is referred to here as fire propagation by "flame contact" and is distinct from fire propagation from an element to an adjacent element (conduction) as discussed in the previous section. In the DACFIR Model fires can propagate by flame contact in the following manner.

- A fire on the floor can propagate to the bottom of a seat cushion.
- A fire on a seat backrest can propagate to the material on the ceiling directly above it. (This can be a PSU, a stowage bin, or a ceiling panel).
- A fire on a sidewall (including upper and lower sidewall panels or the window revel-window transparency strip) can propagate to the PSU directly above it.

The equation for computing the height of a fire is presented in Section 5.3. For a fire on the floor the height is, of course, measured from the floor. For a fire on the sidewall the height is measured from the midpoint between the upper and lower extremes of the fire. For a fire on a seat, the height is measured from a point which is a weighted average of the midpoints of four surfaces which make up the seat backrest; the weight for each surface is the number of elements on that surface in State 3 divided by the total number of elements in State 3 on the seat backrest.

If the height of a fire on the floor is sufficient to reach the bottom of a seat, the elements of the seat cushion directly above the flaming elements on the floor are identified as being in the flame volume. If the height of the fire on a seat backrest is sufficient to reach the ceiling, the elements on the ceiling directly above the top of the backrest are designated as being in the flame volume. If the height of the fire on a sidewall is sufficient to reach the ceiling, those elements at the edge of the ceiling along the sidewall are identified as being in the flame volume.

The state transitions which occur for elements identified in the flame volume are the following.

- Elements in State 1 go to State 6
- Elements in State 2 go to State 3
- Elements in State 5 go to State 6
- Elements in State 6 go to State 3, if the element has been in State 6 longer than a time interval t_f.

The time t_f is input to the model for each material as a tabular function of heat flux.

In the DACFIR Model the heat flux level inside a fire, q_2, is given by the equation

$$q_2 = 3/4\ e_b \alpha_c . \tag{4-3}$$

According to Dayan and Tien [8], the radiation level at the center of a fire at its base is $e_b \alpha_c$ while at its edge at the base of the fire the radiation level is approximately $1/2\ e_b \alpha_c$. The value of q_2 in Equation 4-3 is the average of these two and should be representative of the heat flux levels inside the fire.

The value of q_2 is added to the background radiation and used to compute values of t_f. It is also used to compute the heat release rate, smoke release rate, and toxic gases release rates for materials undergoing flaming combustion. These parameters are determined by linear interpolation in tables which show their variation with heat flux for each material.

4.2.3 Transition to Smoldering by Elements in the Vicinity of a Fire

Elements in the vicinity of a fire may receive sufficient heat flux from the flame volume to begin smoldering. In the DACFIR Model, this phenomenon is considered for elements on the floor in the vicinity of a fire on the floor, elements on the top of a seat cushion in the vicinity of a fire on the seat cushion, elements on the bottom of a seat cushion above a fire on the floor, and elements on the ceiling (PSU, stowage bin, or ceiling panel) above a fire on a seat. Associated with each material is an input parameter, q_p, which defines the heat flux level above which the material will begin to smolder within a few (0 to 20) seconds.

Elements on the floor in the vicinity of a fire on the floor and elements of a seat cushion in the vicinity of a fire on the seat cushion top will receive a heat flux level greater than or equal to q_p if they are within a distance x_p of the fire. This distance is referred to as the "smoldering range" of the fire. The equation for computing x_p which is measured from the edge of a fire is

$$x_p = x - y_0 \tag{4-4}$$

where x is found by numerically solving the cubic equation

$$x^3 + \left(\frac{a f_\ell^2}{a_c \pi y_0} - y_0 \right) x^2 + \frac{a y_0 f_\ell^2}{a_c \pi} - \frac{e_b a y_0 f_\ell^2}{\pi (q_p - q_b)} = 0. \tag{4-5}$$

The quantity q_b is the background radiation. It should be noted that q_p is different for each material and, therefore, x_p is a function of the type of material under consideration. Equation 4-5 was derived from an equation of Dayan and Tien [8] which gives the heat flux at a differential area facing upward on the plane containing the base of the fire. Equation 4-5 implies that there could be more than one value of x_p at which the value of heat flux is q_p. This is not physically true. The equation of Dayan and Tien was derived by curve fitting data with a cubic equation. Only

one segment of the cubic curve corresponds to the region of interest. If there is more than one real solution to Equation 4-5, the larger one is used to compute x_p, since this value is the one which is physically correct.

The heat flux at an element area on a surface above a fire is given by

$$q_3 = \frac{e_b}{2}\left[1 - \frac{\frac{4Z^2}{y_0^2} - 3}{\sqrt{\left(\frac{4Z^2}{y_0^2} + 9\right)\left(1 + \frac{4Z^2}{y_0^2}\right)}}\right] + h_c\left(2.25\,T_\ell - T_s\right) \quad (4\text{-}6)$$

where

- Z is the height of the surface above the flame top,
- y_0 is the effective radius of the fire,
- T_ℓ is the ambient temperature in the lower portion of the cabin (see Section 5.2),
- T_s is the temperature of the surface, and
- h_c is the convective heat transfer coefficient.

The first term on the right side of this equation defines the radiative heat flux. It was derived from Siegel and Howell [12] for a differential area above a cylindrically shaped fire at a distance $1/2\ y_0$ from the axis of the cylinder. The second term on the right defines the convective heat transfer where $2.25\,T_\ell$ is approximately the temperature at the tip of the flame (see Section 5.3). A value of 1.38×10^{-3} Btu/(ft^2 · sec · $^\circ$R) is used for h_c. This is a typical coefficient for natural convection in the flow regime expected in the aircraft cabin [13].

---

[12] Seigel, R. and Howell, J.R., Thermal Radiation Heat Transfer, McGraw-Hill, New York, 1972.

[13] Welker, J.R., and Sliepcevich, C.M. "Heat Transfer by Direct Flame Contact, Fire Tests - Phase 1," University Engineers, Inc., Report No. UE-122-FR, July 1971.

The heat flux on the bottom of a cushion above the flames from a fire on the floor and the heat flux on the ceiling above the flames of a fire on a seat are calculated by Equation 4-6 and combined with the background radiation level. If the resulting value is greater than the value of q_p for the material under consideration, the elements on the surface directly above the flame volume and the elements directly above elements which are within a distance of x_p laterally from the base of the fire are designed as being within the smoldering range of the fire.

The following state transitions occur for elements designated as being within the smoldering range of the fire:

- Elements in State 1 are changed to State 5
- Elements in State 6 are changed to State 5
- Elements in State 5 are changed to State 2 if they have been in State 5 for a time period greater than t_p.

The time t_p is an input parameter and is a function of the type of material comprising the element.

4.2.4 Transitions of Elements in the Smoldering or Flaming States

For each time step that an element is in State 2 (smoldering) or State 3 (flaming) a certain percentage of the total combustion products that can be emitted are emitted. For elements in State 2 this percentage is calculated by the equation

$$P_2 = \left(\Delta t / t_{pc}\right) 100 \qquad (4\text{-}7)$$

where Δt is the length of the time step and t_{pc} is an input parameter for each material defining the total time required for the element to become charred at a heat flux of q_p. For elements in State 3, the percentage is calculated by the equation

$$P_3 = \left(\Delta t / t_{fc}\right) 100 \qquad (4\text{-}8)$$

where t_{fc} is an input parameter defining the total time required for the element to become charred due to flaming combustion. The parameter t_{fc} is a function of material type and heat flux. The heat flux received by a flaming element is calculated by Equation 4-2.

Each time P_2 and P_3 are calculated for an element they are added to the total per cent of decomposition (P_T) for the element. The value of P_T is initially zero and increasing by P_2 or P_3 each time step that the element is in State 2 or State 3. When P_T for an element becomes equal to or greater than 100, the element state is changed from State 2 or State 3 to State 4 (charred).

While an element is in State 2, it emits smoke and toxic gases at rates which are input to the program for each material. While an element is in State 3, it emits heat, smoke, and toxic gases at rates which are determined from an input table of these rates versus heat flux. The heat flux used in this determination is q_2 which is computed by Equation 4-3.

Elements that are in State 2 are there because the heat flux being received by the element is greater than q_p. If an element in State 2 is found at some later time to be outside the smoldering range of a fire, it is no longer receiving a heat flux greater than q_p. In this case the element state is changed from State 2 to State 7. While in State 7 the element continues to smolder until it has been in this state for a time period t_{pe}. The time t_{pe} is an input parameter for each material. Once the element has been in State 7 for a time t_{pe}, it no longer smolders and its state is changed from State 7 to State 4. The change to State 4 occurs even though the element is not necessarily charred. Nonetheless, no other transitions are expected for the element since the time period for the simulation is normally not long enough for the fire to recede from a smoldering element and then to grow back to it again.

SECTION 5

CABIN ATMOSPHERE MODEL

The distribution of the smoke, toxic gases, and heat in the cabin section is estimated through the use of a lumped parameter, one-dimensional, dynamic model for the behavior of the cabin atmosphere. Dealing exactly with the fluid mechanics and heat transfer of an enclosed fire, such as that in a room or aircraft cabin, is a difficult and as yet unsolved problem. Principally, the difficulties stem from the turbulent character of the flow and the complexities of enclosure geometry and fuel combustion behavior. Consequently, it has been the practice [3, 14] when estimating smoke and toxic gas concentrations due to an enclosed fire to ignore the problem of the flow patterns and assume a uniform mixing of the airborne material throughout the enclosure at all stages of fire development. Recent developments in theoretical analysis of room fires, however, have made possible a more accurate model of the enclosure atmosphere which, while it is still a long way from a complete description of the thermofluid dynamics, does approach more closely the actual distribution of smoke, gases, and heat than the simple uniform mixing assumption. The primary assumption involved in the model described herein is the division of the cabin atmosphere into two separate horizontal volumes or zones.

The upper zone of the cabin atmosphere consists of combustion products and heated air which have risen to the ceiling by natural buoyancy. Below this volume is the lower zone which consists of cool, uncontaminated air originally in the cabin or that which enters during the simulation period. This "stratified" model is intended to describe the cabin atmosphere during the initial growth stages of the fire before significant vertical mixing can

---

[14] Robertson, A. F., "Estimating Smoke Production During Building Fires," Fire Technology, Vol. 11, No. 2, (May 1975), pp. 80-94.

occur. Since the emphasis of the cabin fire model is on conditions that may develop during an emergency evacuation, it is the initial stages of the fire which are of interest. The cabin atmosphere model, therefore, incorporates simple calculations to estimate the size of the upper and lower zones, the temperature in each zone, and the concentration of smoke and toxic gases within the upper zone.

5.1 DESCRIPTION OF THE CABIN ATMOSPHERE

As stated above, the cabin atmosphere model assumes the division of the interior atmosphere into two zones by the rise of hot combustion products and entrained air to the upper portion of the enclosure. As the fire continues, this upper zone or layer will grow and the interface between it and the relatively cool, clear lower zone will descend toward the floor. The distinction between the zones is, of course, not precise since some vertical mixing will always be taking place. The amount of mixing will depend on such factors as the temperature and density difference between the zones, the turbulence in each zone, the extent of ventilation, if any, and the time scale considered. For the model developed here, it has been assumed that the factors which tend to preserve the stratification dominate those that tend to mix the cabin atmosphere and, therefore, no gas exchange between the zones is assumed other than that caused by fires in the lower zone. Further, a uniform temperature is assumed for the gas in either zone, allowing simple computations of heat transfer to solid materials in the cabin and the position of the zone interface.

A typical wide-body aircraft cabin is not a single, large, long open space but is made up of sections connected by short passageways as seen in Figure 5.1a. One of these room-like sections, bounded by a galley unit at the rear and a lavatory unit at front, has been chosen as the volume for the atmosphere model, Figure 5.1b. The quantities computed in the model apply to the atmosphere in this section alone. Gas flow out through the

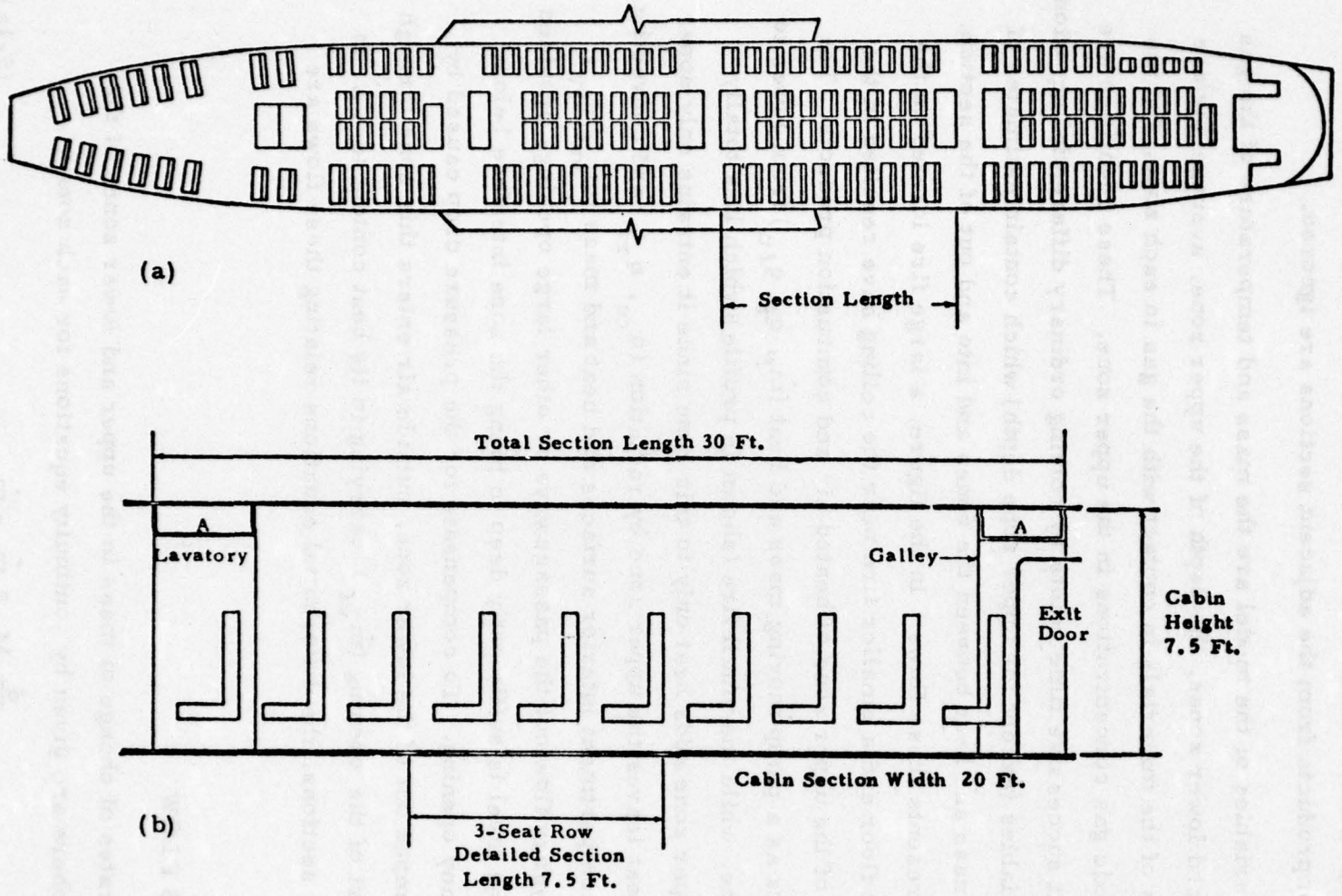

Figure 5.1 (a) Typical Wide-body Transport Aircraft Cabin Arrangement Showing the Location of the Cabin Section Used in the Model

(b) Longitudinal View of the Cabin Section and Location of the 3-Seat Row Detailed Region
All Seat Groups are not Depicted in this Simplified Representation
The Regions A are Soffits of the Passageways to the Adjacent Sections

passageways is taken into account but the conditions that would result from this flow in adjacent sections are not considered. Further, any backflows of combustion products from the adjacent sections are ignored.

The variables of the model are the mass and temperature of the gas in the upper and lower zones, the depth of the upper zone, average surface temperatures of the materials in contact with the gas in each zone, and the smoke and toxic gas concentrations in the upper zone. These quantities are determined at successive time points by solving ordinary differential equations for these variables (except for upper zone depth) which contain estimates of the flows of mass and heat between the zones and into and out of the section. Figure 5.2 presents these flows. In the figure, a large fire located on the compartment floor and a smaller fire near the ceiling have resulted in the development of the upper zone of heated air and combustion products. The floor fire acts as a pump moving mass and heat ($\dot{m}_f$, q_f, $q_{\ell u}$) from lower to the upper zone, while the small fire (shown in profile) which lies totally within the upper zone adds heat only to this zone since it entrains only upper zone gas. Heat leaves the upper zone by radiation (q_{ru}, $q_{r\ell}$) and convection (q_{hu}) to the compartment interior surfaces and heat and mass ($\dot{m}_{vu}$, q_{vu}) leave by buoyancy flow out the passageways or other large openings provided the upper zone level is sufficiently deep to bring the zone interface below the soffit of any opening. To compensate for the pressure drop caused by gas being pumped out of the lower zone, outside air enters this zone through the lower part of the opening ($\dot{m}_{v\ell}$) carrying in its heat content ($q_{v\ell}$). In the following sections, the differential equations relating these flows are described.

5.2 MASS FLOW

The rates of change of mass in the upper and lower zones of the cabin atmosphere are given by continuity equations for each zone

$$\frac{d}{dt} M_u = \dot{m}_f - \dot{m}_{vu} \qquad (5\text{-}1a)$$

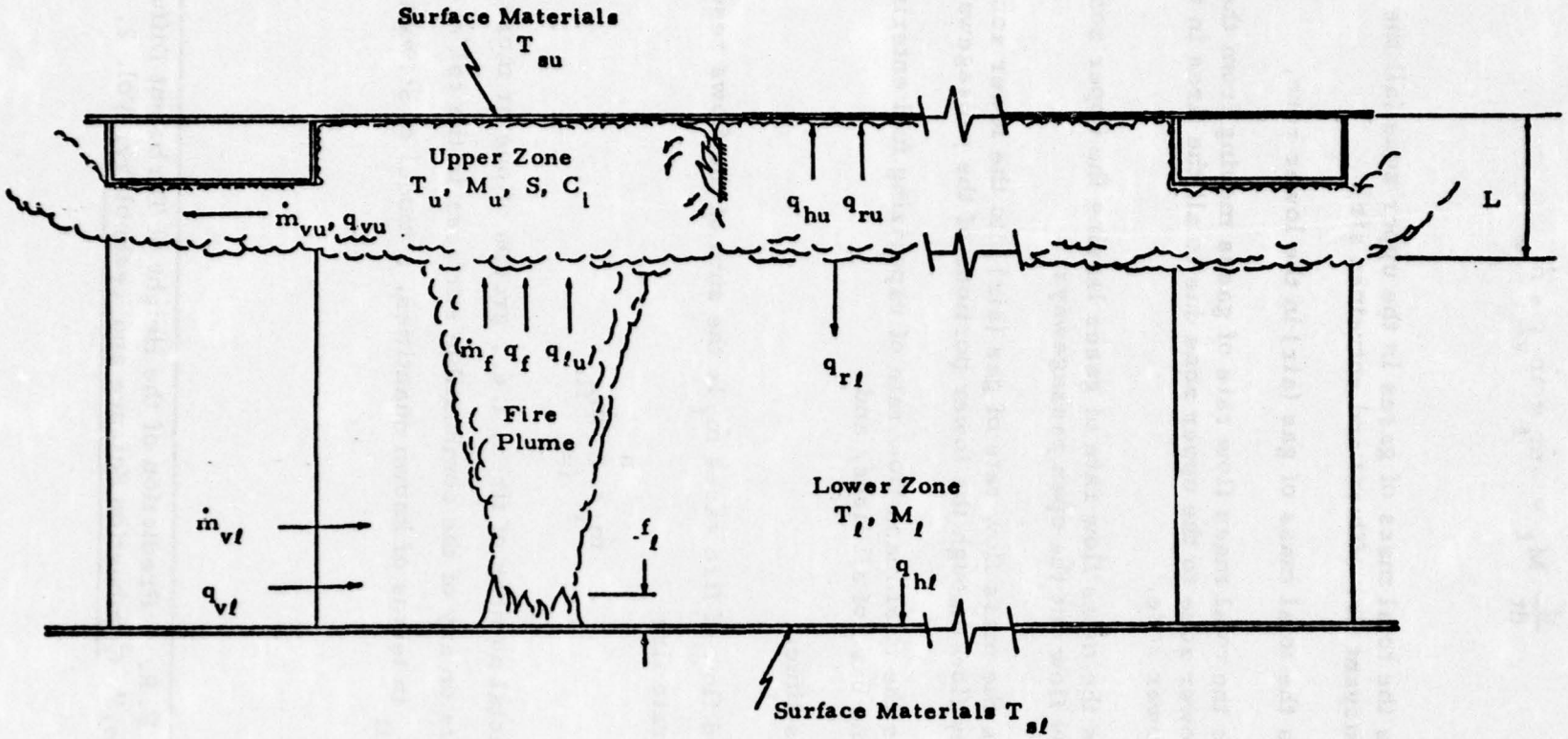

Figure 5.2 Mass and Heat Flows in the Cabin Atmosphere Model
(Symbols are defined in Sections 5.2 - 5.4)

$$\frac{d}{dt} M_\ell = -\dot{m}_f + \dot{m}_{v\ell} - \dot{m}_o \qquad (5\text{-}1b)$$

where

M_u is the total mass of gases in the upper zone (all the buoyant fire effluent and entrained air),

M_ℓ is the total mass of gas (air) in the lower zone,

$\dot{m}_f$ is the total mass flow rate of gases moving from the lower zone to the upper zone due to all the fires in the lower zone,

$\dot{m}_{vu}$ is the mass flow rate of gases leaving the upper zone by flow out the open passageways,

$\dot{m}_{v\ell}$ is the mass flow rate of gas (air) into the lower zone by flow through the lower portions of the passageways,

$\dot{m}_o$ is the total mass flow rate of vaporizing fuel entering the base of all fires, and

t is time.

The total upward flow of fire gases $\dot{m}_f$ is the sum of the flows resulting from each separate fire

$$\dot{m}_f = \sum_{i=1}^{n} \dot{m}_{fi} \qquad (5\text{-}2)$$

where n is the total number of fires, i.e., groups of one or more contiguous flaming elements on any of the combustible surfaces in the cabin. To express the values of $\dot{m}_{fi}$ in terms of known quantities, a model of Steward [15] and

---

[15] Steward, F.R., "Prediction of the Height of Turbulent Diffusion Buoyant Flames," Combustion Science and Technology, Vol. 2, (1970), pp. 203-212.

Fang [16] is used. The upward flow of gas above the group of flaming elements composing a fire is expressed by this model as

$$\dot{m}_{fi} = \dot{m}_o + \dot{m}_{ec} + \dot{m}_{ep} \qquad (5\text{-}3)$$

where

$\dot{m}_{ec}$ is the mass flow rate of laterally entrained air into the combustion zone, and

$\dot{m}_{ep}$ is the mass flow rate of laterally entrained air into the plume region above the combustion zone.

These flows are shown in Figure 5.3. The model assumes an axisymmetric flow of gases upward from the burning material. The radius of the fire column varies with height as air enters the column and the temperature in the column changes.

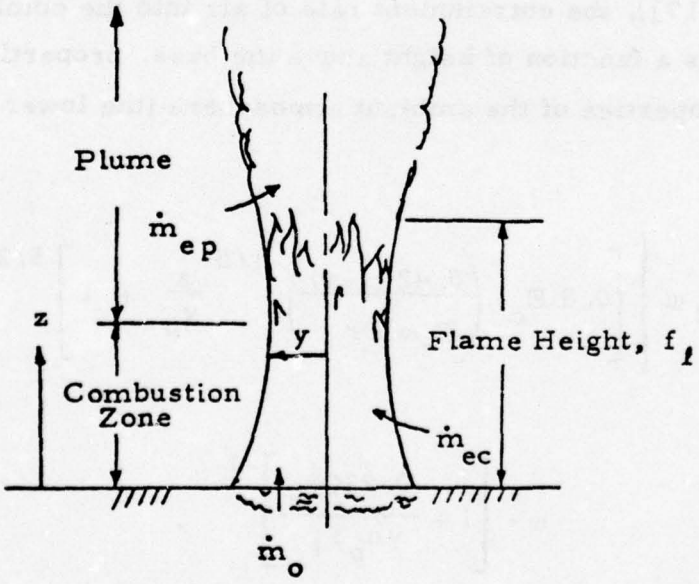

Figure 5.3. Mass Flow and Fire Structure in the Fire Model

[16] Fang, J. B., "Analysis of the Behavior of a Freely Burning Fire," NBSIR 73-115, Feb. 1973, U. S. National Bureau of Standards, Washington, D. C.

The mass flow rate of fuel vapor entering the base of the combustion zone is

$$\dot{m}_o = \rho_o u_o A_{fi} \tag{5-4}$$

where

ρ_o is the fuel vapor density (the average value of the densities of the gaseous species which constitute the fuel vapor),

u_o is the fuel vapor velocity as it leaves the fuel surface and enters the flame zone (a negligible flame "stand-off" distance is assumed over the entire burning area), and

A_{fi} is the base of area of the fire.

Above the fire base area, the combustion zone extends from the point at which burning of the fuel vapor starts to the height z at which a stoichiometric mixture of fuel and oxygen is reached. From Fang's analysis (see also Rockett [17]), the entrainment rate of air into the combustion zone can be given as a function of height above the base, properties of the fuel vapor and, properties of the ambient atmosphere (the lower zone air);

$$\dot{m}_{ec} = A_{fi} u_o \rho_\ell \omega \left\{ \left[0.8\, E_c \left(\frac{0.42\,(1-\omega)}{E_c \omega^3 Fr} \right)^{1/5} \frac{z}{y_o} + 1 \right]^{5/2} - 1 \right\} \tag{5-5}$$

where

$$\omega = \left[1 + \frac{0.23 Q^*_c}{\gamma c_p T_\ell} \right]^{-1} ,$$

$$Fr = u_o^2 / (g y_o) \quad , \quad \text{and}$$

---

[17] Rockett, J.A., "Fire Induced Gas Flow in an Enclosure," Accepted for Publication, Combustion Science and Technology.

where

ρ_ℓ is the lower zone air density,

E_c is an entrainment constant for the combustion zone,

z is the vertical length of the combustion zone which exists below the upper gas layer in the cabin,

y_o is the average radius of the fire base area,

Q^*_c is the adjusted heat of combustion of the fuel vapor,

γ is the stoichiometric oxygen to fuel mass ratio,

c_p is the specific heat of air (taken as 0.24 Btu/lbm$^\circ$R always),

T_ℓ is the lower zone temperature (absolute), and

g is the gravitational acceleration (32.174 ft/sec^2).

The height of the stoichiometric mixing point which defines the upper limit of the combustion zone is

$$b_c = 1.49\, y_o \left[\frac{\omega \left(\omega \rho_a / \rho_o + 4.32\gamma \right)^2}{E_c^{\,4} (1 - \omega)} \right]^{1/5} \left(\frac{\rho_o u_o}{\rho_a \sqrt{g y_o}} \right)^{2/5} . \qquad (5\text{-}6)$$

When the entire combustion zone lies below the boundary between the upper and lower cabin atmosphere zones (the thermal discontinuity), the value of b_c in Equation 5-6 is used for z in Equation 5-5. If the combustion zone extends into the upper zone, z in Equation 5-5 is taken to be the vertical distance from the fire base plane to the thermal discontinuity.

When the combustion zone of a fire does not extend into the upper hot gas layer in the cabin, air will be entrained into the plume region above the combustion zone. The amount of plume-entrained air is given by

$$\dot{m}_{ep} = \pi y_s^2 u_s \rho_\ell \left\{ \left[1.2E_p \left(\frac{0.625\left(1 - \rho_s/\rho_\ell\right)}{E_p Fs} \right)^{1/5} \frac{\left(z - b_c\right)}{y_s} + 1 \right]^{5/3} - 1 \right\} \tag{5-7}$$

where

y_s is the radius of the gas column at the top of the combustion zone,

u_s is the flow velocity at the top of the combustion zone,

E_p is an entrainment constant for the plume zone,

ρ_s is the gas density at the top of the combustion zone, and

$Fs = u_s^2/(gy_s)$.

The term $(z - b_c)$ in Equation 5-7 is the distance from the combustion zone top to the thermal discontinuity. The quantities y_s, u_s, and ρ_s may be written in terms of the properties at the fire base

$$y_s = 1.19 y_o \left[\frac{E_c}{\sqrt{\omega^3(1 - \omega)}} \right]^{1/5} \left[\frac{(1 + 4.32\gamma)^5}{\omega\rho_\ell/\rho_o + 4.32\gamma} \right]^{1/10} \left(\frac{\rho_o u_o}{\rho_\ell \sqrt{g y_o}} \right)^{2/5} \tag{5-8}$$

$$u_s = u_o \left(\frac{y_o}{y_s} \right)^2 \left[1 + 4.32\gamma/\left(\omega\rho_\ell/\rho_o\right) \right] \tag{5-9}$$

$$\rho_s = \rho_\ell \, \omega\left(1 + 4.32\gamma\right)/\left(\omega\,\rho_\ell/\rho_o + 4.32\gamma\right) \quad . \tag{5-10}$$

Some comments should be made concerning the Equations 5-5 through 5-10. First, the value of the adjusted heat of combustion of the fuel vapor Q_c^* is the actual heat of combustion of the fuel adjusted by a factor reflecting the loss of heat from the fire column by radiation. It is this simple accounting of radiative loss that allows the conservation equations (in which the physics of the problem is originally contained) to be solved analytically for the quantities given by Equations 5-5 through 5-10. Modak and Croce [18] have measured the total radiative heat loss from fires of the polymer polymethyl methacrylate (PMMA) in the size range 6 x 6 inches to 4 x 4 feet. Modak and Croce found that the radiative loss fraction expressed as a fraction of the total heat release (obtained from the mass burning rate and heat of combustion) is a remarkably constant 42% over the entire range of fire sizes observed. Since no other information of this type could be found on other types of polymers, the 42% value was used for all interior materials to adjust their heats of combustion for use in the model.

The values of E_c and E_p, the entrainment constants, represent a significant uncertainty in the model. Fang gives representative values for these parameters for various fuels of about 0.1 to 0.4 for E_c and 0.05 to 0.07 for E_p. Steward [15] and Quintiere [19] suggest values in the range 0.05 to 0.1 for E_c. The uncertainty connected in these values is relatively important since examination of Equations 5-5 and 5-7 shows that $\dot{m}_{ec}$ is approximately proportional to E_c^2 and $\dot{m}_{ep}$ is approximately proportional to $E_p^{1.3}$. Further, the effects of the fire location, orientation, and the general enclosure geometry on entrainment are unknown. The choice of values of E_c and E_p for the present model are $E_c = 0.300$ and $E_p = 0.250$.

---

[18] Modak, A. T., and Croce, P. A., "Influence of Flame Radiation on the Burning Rate of Plastic Pool Fires of Varying Scale," Paper Presented at the Ninth Fall Technical Meeting 1975, Eastern Section: The Combustion Institute, Nov. 6-7, 1975, SONY at Stony Brook, Long Island, NY.

[19] Quintiere, J., "The Growth of Fire in Building Compartments," Paper Presented at the ASTM-NBS Symposium on Fire Standards and Safety, National Bureau of Standards, Gaithersburg, Maryland, April 5-6, 1976.

These values were derived by comparing calculated flame heights with Modak and Croce's estimates of the flame heights of their PMMA fires, since the expression for the flame height in Fang's model includes both E_c and E_p (see below). The burning rates measured by Modak and Croce were used in these calculations. It should be emphasized that these results for the entrainment constants are not regarded as the final word on the subject; much work remains to be done on fire entrainment and mixing phenomena.

As stated above, the description of the fire convection column is based on the assumption of a horizontal, circular fire base and axial symmetry in the convection column. Since the description of the fire base area in the "elementized" model is a connected group of square elements, there is obviously no case in which a circular base will actually occur. Furthermore, the model allows fires to burn on vertical and downward facing horizontal surfaces, i.e., ceiling panels, etc., as well as upward oriented surfaces, such as the cabin floor, seat cushion tops, etc. There is, therefore, a need to modify the definition of y_o and to define the distance, z, "above" a vertical surface fire so that Equations 5-5 through 5-10 can be applied to these cases. The base radius y_o of the fire column is taken to be one half the hydraulic diameter of the base area

$$y_o = 1/2\left(4A_{fi} / P_{fi}\right) = 2A_{fi} / P_{fi} \qquad (5\text{-}11)$$

where P_{fi} is the perimeter of the fire base which is determined by summing the lengths of the open sides of the elements composing the base area. Fu [9] has shown that the flame height of rectangular fires shows approximately the same relationship to their hydraulic diameters as do circular fires to their diameters. Since the flame height is directly related to the quantities calculated above (see the flame height equation below), it appears that use of the hydraulic radius for y_o is a reasonable assumption.

For fires on vertical surfaces, the dimension z is measured from a computed horizontal midpoint of the burning area. The midpoint is determined by finding the maximum and minimum vertical extent of the fire and averaging the two values.

More than one fire can exist on a given surface. On the floor, each set of elements in State 3 that are contiguous (adjacent to each other or are touching at a corner), is considered to be one fire. On the ceiling, fires are separated by surfaces; that is, a fire overlapping two surfaces is treated as two fires, one on one surface and one on the other. On the sidewalls, the fires are not separated by surfaces; that is, contiguous elements in State 3 constitute a single fire even if the set of elements overlap any two or all three of the surfaces (lower sidewall panel, window transparency-window reveal surface, or upper sidewall panel). All elements in State 3 on a seat group are considered to be one fire whether they are contiguous or not.

The terms $\dot{m}_{vu}$ and $\dot{m}_{v\ell}$ of Equations 5-1 represent the mass flow rates of gases through the passageways leading from the section of fire origin to other sections of the cabin. Analyses of such flows have been made by Rockett and by Prahl and Emmons [20]. The expressions for the flows obtained in both works are physically equivalent; Rockett's expressions are used in the model because they are formulated in terms of the primary variables of the model. The flow terms are

$$\dot{m}_{vu} = \frac{2}{3} C \rho_{am} A_v \left[2gB \frac{T_{am}}{T_u} \left(1 - \frac{T_{am}}{T_u} \right) \right]^{1/2} \left(1 - D_d \right)^{2/3} \qquad (5\text{-}12a)$$

$$\dot{m}_{v\ell} = \frac{2}{3} C \rho_{am} A_v \left[2gB \left(1 - \frac{T_{am}}{T_u} \right) \left(D_d - D_i \right) \right]^{1/2} \left(D_d - D_i/2 \right) \qquad (5\text{-}12b)$$

---

[20] Prahl, J., and Emmons, H. W., "Fire Induced Flow Through an Opening," Technical Paper No. 12, Division of Engineering and Applied Physics, Harvard University, Cambridge, Mass., 1975.

where

C is the orifice coefficient (the correction factor for orifice flow effects, taken as 0.7 throughout),

ρ_{am} is the air density in the adjacent sections,

T_{am} is the air temperature in the adjacent sections,

A_v is the total area of all passageways through which flow is occurring,

T_u is the absolute temperature of the gas in the upper zone,

B is the passageway height, assumed equal for all passageways,

D_d is the distance from the cabin floor to the thermal discontinuity measured in the plane of the passageway opening and expressed as a fraction of the total passageway height, B, and

D_i is the floor to thermal discontinuity distance measured in the interior of the cabin section and expressed as a fraction of B.

Figure 5.4 illustrates the quantities involved in the flow calculation for a single passageway. Rockett's analysis was developed for flow out a single opening whereas this work applies the equations to multiple openings, four in the cabin section illustrated in Figure 5.1. The extension is straightforward, however, if the floor-to-soffit height is the same for all passageways or other openings. In this case, the value for A_v becomes the total area for all openings rather than area of a single opening. Assuming that the upper zone temperature and upper zone layer depth (discontinuity position) are known independently of Equations 5-12, these equations contain three unknowns, $\dot{m}_{vu}$, $\dot{m}_{v\ell}$, and D_d. To solve for these quantities, a third relationship is required. Assuming a steady-state flow over the period of integration of the cabin atmosphere model, the total inflow and outflow can be related by conserving mass within the section during the integration interval.

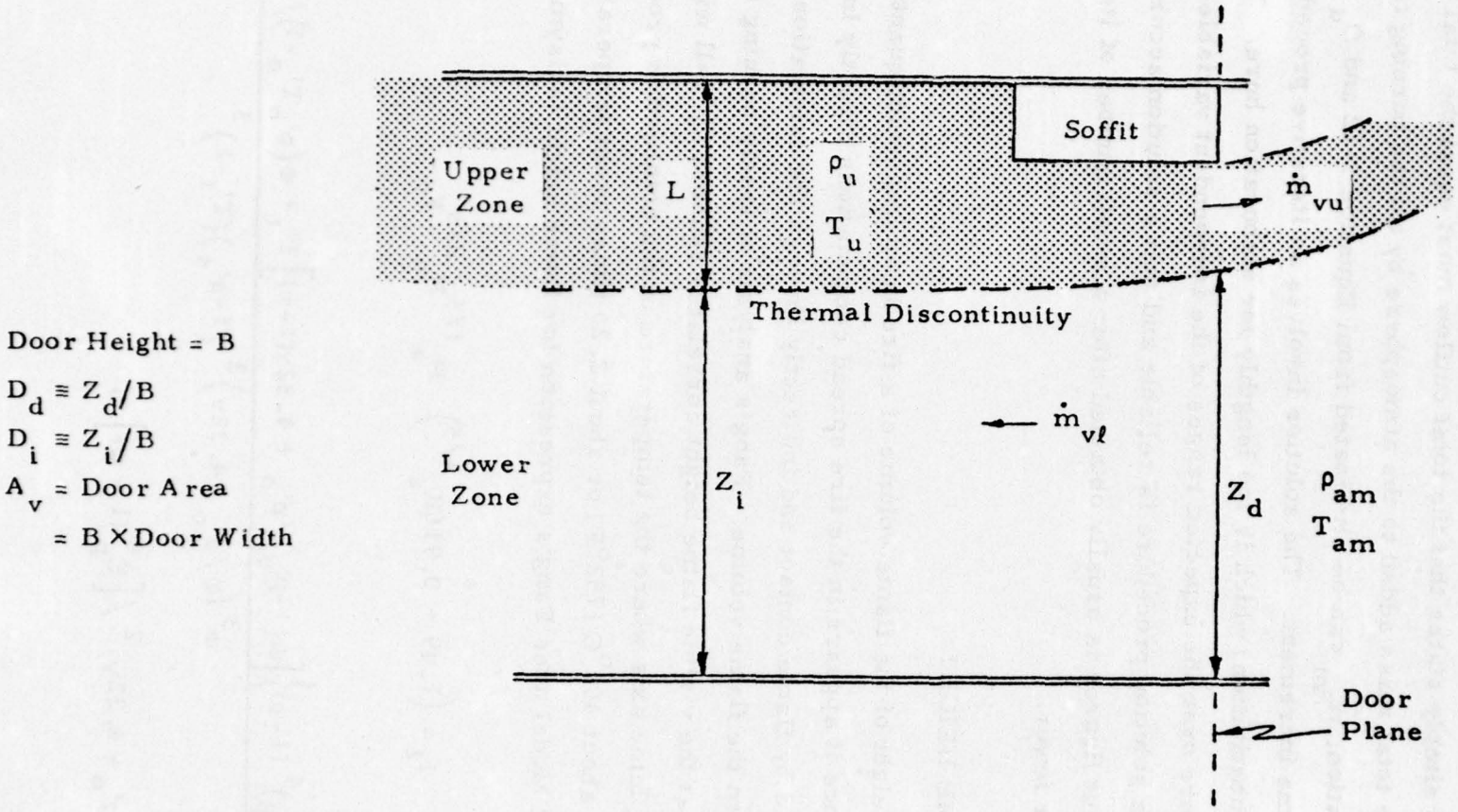

Figure 5.4. Convective Flow Out A Passageway (Door) into an Adjacent Section

$$\dot{m}_{vu} = \dot{m}_{v\ell} + \sum_{i=1}^{n} \dot{m}_{oi} \quad . \tag{5-13}$$

Equation 5-13 simply states that the total outflow must equal the total inflow of air plus the total mass added to the atmosphere by all the burning fuel, $\dot{m}_{oi}$. With this equation, $\dot{m}_{vu}$ can be eliminated from Equation 5-12 and D_d solved for at each time increment. The solution involves an iterative procedure (successive substitution) which is too lengthly for elaboration here. Tests of the procedure over the expected ranges of the independent variables have shown that the solution procedure is reliable and that a solution accurate to four significant figures is usually obtained after a small number of iterations, usually ten or fewer.

5.3 FLAME HEIGHT

The height of the flame volume of a fire is an important quantity in the model since it appears in the fire spread computations directly in determining spread by flame contact and indirectly through the calculation of the radiation from the flame volume. Fang's analysis of freely burning fires has shown that the visible flame height correlates reasonably well with the point on the plume axis where the temperature of the combustion products has fallen to about 400°C (752°F) or about 2.25 times room temperature. The DACFIR Model uses Fang's expression for flame height (axisymmetric case)

$$f_\ell = \left(1.49 + 0.916 K_a^{1/5}\right) P_a^{1/5} N_b^{2/5} y_o \tag{5-14}$$

where

$$K_a = \frac{\left(E_c / E_p\right)^4 (1-\omega)\left\{\left[\omega\left(1-p'_o\right)/\rho'_o + 4.32\gamma(1-\omega)\right] T'_t + \omega\left(\rho'_o T'_o - 1\right)/\rho'_o\right\}^3}{\omega^3 \left(\omega/\rho'_o + 4.32\gamma\right)^3 \left(1-\rho'_s\right)\left(T'_t - 1\right)^3} ,$$

$$P_a = \omega\left(\omega/\rho'_o + 4.32\gamma\right)^2 / \left[E_p^4 (1-\omega)\right] ,$$

$N_b = \rho_o u_o / (\rho_\ell \sqrt{g y_o})$,

$\rho'_o = \rho_o / \rho_\ell$, $T'_o = T_o / T_\ell$, $\rho'_s = \rho_s / \rho_\ell$,

$t'_t = T_t / T_\ell = 2.25$; and

T_o is the temperature of the fuel vapor entering the flame base. Other symbols in Equation 5-14 are as defined in Section 5.2.

5.4 HEAT TRANSFER AND GAS TEMPERATURE

Gas temperature in the upper and lower zones are computed by applying a heat balance to each zone. A constant pressure process is assumed for the transfer of heat during each integration step so that the change in enthalpy of the gas in each zone is equal to the heat added or lost. The reference temperature for zero enthalpy of the gas is taken to be absolute zero and the specific heat is assumed constant. The heat balance (energy conservation) equations for each zone are therefore

$$\frac{d}{dt}(H_u) = \frac{d}{dt}(M_u c_p T_u) = q_f - q_{hu} - q_{ru} - q_{r\ell} - q_{vu} + q_{\ell u} \qquad (5\text{-}15a)$$

$$\frac{d}{dt}(H_\ell) = \frac{d}{dt}(M_\ell c_p T_\ell) = q_{v\ell} - q_{h\ell} - q_{\ell u} \qquad (5\text{-}15b)$$

where

H_u is the total enthalpy of the upper zone gas;

H_ℓ is the total enthalpy of the lower zone gas;

T_u is the upper zone gas temperature;

T_ℓ is the lower zone gas temperature;

q_f is the total heat release rate for all fires in either zone;

q_{hu} is the convective heat transfer rate of the upper zone gas to the ceiling, upper sidewalls, and other surfaces which bound the upper zone;

q_{ru} is the net radiation exchange rate between the upper zone gas and the surfaces in contact with it;

$q_{r\ell}$ is the net radiation exchange rate between the upper zone gas and the surfaces bounding the lower zone;

q_{vu} is the rate of heat carried out of the upper zone by flow out the passageways;

$q_{\ell u}$ is the rate of heat transfer from the lower zone to the upper zone resulting from the entrainment of lower zone gas into the rising fire plumes;

$q_{v\ell}$ is the heat carried into the lower zone by the inflow of gas to the lower zone; and

$q_{h\ell}$ is the convective heat transfer rate of the lower zone gas gas to the solid surfaces bounding the lower zone.

The heat flow terms of Equations 5-15 are expressed in terms of the basic model variables as

$$q_f = \sum_{j=1}^{n} q_j A_{fj} \tag{5-16a}$$

$$q_{hu} = h_u \left(T_u - T_{su}\right) A_u \tag{5-16b}$$

$$q_{ru} = \sigma A_u \left(T_u^4 - T_{su}^4\right) + q_e A_u \tag{5-16c}$$

$$q_{r\ell} = \sigma A_\ell \left(T_u^4 - T_{s\ell}^4\right) + q_e A_\ell \tag{5-16d}$$

$$q_{vu} = \dot{m}_{vu} c_p T_u \tag{5-16e}$$

$$q_{\ell u} = \dot{m}_f c_p T_\ell \tag{5-16f}$$

$$q_{v\ell} = \dot{m}_{v\ell} c_p T_{am} \tag{5-16g}$$

$$q_{h\ell} = h_\ell \left(T_\ell - T_{s\ell}\right) A_\ell \tag{5-16h}$$

where

q_j is the heat release rate, per unit area, of the j^{th} interior material (the value appropriate for the applied heat flux),

A_{fj} is the total area of material j that is flaming,

h_u is the convective heat transfer coefficient for transfer between the upper zone gas and the upper surfaces,

T_{su} is the average surface temperature of the upper surfaces,

A_u is the total area of contact of the upper zone gas with the cabin interior surfaces,

q_e is an external "background" radiation,

σ is the Stefan-Boltzmann constant (4.761×10^{-13} Btu/ft^2 · sec · ^oR),

A_ℓ is the total area of contact of the lower zone gas with the cabin interior surfaces,

$T_{s\ell}$ is the average surface temperature of the lower surfaces, and

h_ℓ is the convective transfer coefficient for the lower zone gas.

The surface contact areas A_u and A_ℓ are given in terms of the cabin section dimensions

$$A_u = C_w C_\ell + 2L\left(C_w + C_\ell\right) \tag{5-17a}$$

$$A_\ell = 2\left[C_w C_\ell + C_\ell C_h + C_h C_w\right] - A_u \tag{5-17b}$$

where

C_w is the cabin section width,

C_ℓ is the cabin section length,

C_h is the cabin section height, and

L is the upper layer thickness.

For the convection coefficients, two expressions are used. The assumption is made that most surfaces in contact with the upper zone are horizontal and downward facing and that surfaces in the lower zone are horizontal and upward facing. Length scales for both cases is taken to be on the order of one foot. For the upper zone, the coefficient is

$$h_h = 5.55 \times 10^{-5} \left(|T_u - T_{su}| \right)^{1/4} \quad \left(\text{Btu/ft}^2 \cdot \text{sec} \cdot {}^\circ\text{R} \right) \tag{5-18a}$$

while for the lower zone

$$h_\ell = 1.05 \times 10^{-4} \left(|T_\ell - T_{s\ell}| \right)^{1/4} \quad \left(\text{Btu/ft}^2 \cdot \text{sec} \cdot {}^\circ\text{R} \right) \ . \tag{5-18b}$$

These coefficients are typical values for natural (free) convection from flat plates in air at atmospheric pressure [24].

The radiation terms q_{ru} and $q_{r\ell}$ assume that the upper zone gas is opaque and radiates as a black body at temperature T_u, that the lower zone gas is nonparticipating, that the cabin interior surfaces radiate as black bodies, and that the view factor for radiant exchange between the upper zone gas and lower zone surfaces is always unity. The background radiation term q_e is included to account for externally originating radiation that might come from, for example, a large external fuel fire. The specifics of the

[24] Hsu, S. T., Engineering Heat Transfer, D. Van Nostrand Co., Princeton, NJ, 1963.

entry of this radiation into the cabin are not detailed, and the radiation is assumed to be isotropic within the section. The numerical value q_e is assumed constant and is specified in the program input.

Some simplification of Equations 5-15 is possible by applying the chain rule of differentiation to the left hand side of each equation. In either case, the change in total enthalpy is then divided into change in mass and change in temperature terms:

$$\frac{d}{dt}\left(Mc_pT\right) = c_pT\,\frac{dM}{dt} + c_pM\,\frac{dT}{dt} \quad .$$

The change in mass dM/dt for each zone is known from Equations 5-1. Substituting these equations into Equations 5-15a and 5-15b gives

$$c_pM_u\,\frac{dT_u}{dt} + c_pT_u\left(\dot{m}_f - \dot{m}_{vu}\right) = q_f - q_{hu} - q_{ru} - q_{r\ell} - \dot{m}_{vu}c_pT_u + \dot{m}_fc_pT_\ell \qquad (5\text{-}19a)$$

$$c_pM_\ell\,\frac{dT_\ell}{dt} = c_pT_\ell\left(\dot{m}_{v\ell} - \dot{m}_f\right) + \dot{m}_{v\ell}c_pT_{am} - q_{h\ell} - \dot{m}_fc_pT_\ell \quad . \qquad (5\text{-}19b)$$

Cancellation of appropriate terms on each side of these equations gives the somewhat more simple relationships that are used in the computer code

$$c_pM_u\,\frac{dT_u}{dt} = q_f - q_{hu} - q_{ru} - q_{r\ell} + \dot{m}_f\,c_p\left(T_\ell - T_u\right) \qquad (5\text{-}20a)$$

$$c_pM_\ell\,\frac{dT_\ell}{dt} = \dot{m}_{v\ell}\,c_p\left(T_{am} - T_\ell\right) - q_{h\ell} \quad . \qquad (5\text{-}20b)$$

To determine the average temperature of the surfaces in contact with the gas in each zone, a simple approximation to the one-dimensional, unsteady state heat conduction problem is used. The approximation involves assuming that all heat supplied to the surface accumulates in a thin layer at the surface. A heat balance is performed on a unit area of the surface that includes terms for loss by conduction through the "back" of the thin layer in contact with the bulk of the wall material which is taken to be at the constant ambient temperature. The heat balance is expressed in two ordinary differential equations as

$$x\rho_m c_{pm} \frac{d}{dt} T_{su} = \left(q_{hu} + q_{ru}\right)/A_u - \frac{2k_m}{x} \left(T_{su} - T_{am}\right) + q_e \qquad (5\text{-}21a)$$

$$x\rho_m c_{pm} \frac{d}{dt} T_{s\ell} = \left(q_{h\ell} + q_{r\ell}\right)/A_\ell - \frac{2k_m}{x} \left(T_{s\ell} - T_{am}\right) + q_e \qquad (5\text{-}21b)$$

where

x is the material surface layer thickness,

ρ_m is the surface material density,

c_{pm} is the material specific heat,

k_m is the material thermal conductivity.

All of the above material thermal properties are assumed constant and identical for all materials. The choice of the surface layer thickness is somewhat arbitrarily chosen as 0.1 inch (0.0833 ft).

5.5 SMOKE AND TOXIC GAS CONCENTRATION AND UPPER ZONE LAYER DEPTH

The concentrations of smoke and toxic gases in the upper zone are determined by solving conservation equations for these quantities which involve the generation and loss rates of each quantity. The upper zone depth is derived by the assumption of equality of pressure across the interface

between zones at all times. For the smoke in the upper zone, the conservation equation is

$$\frac{d}{dt}\left(SV_u\right) = \sum_{i=1}^{n_s} r_{ssi}\, A_{si} + \sum_{i=1}^{n_f} r_{sfi}\, A_{fi} - S\,\dot{m}_{vu}/\rho_u \qquad (5\text{-}22)$$

where

S is the smoke concentration,

V_u is the volume of the upper zone,

n_s is the number of different material types on which smoldering combustion is taking place,

r_{ssi} is the rate of smoke generation per unit area in the smoldering state for the i^{th} material,

A_{si} is the total smoldering area of the i^{th} material,

n_f is the number of different material types on which flaming combustion is taking place,

r_{sfi} is the rate of smoke generation per unit area in the flaming state for the i^{th} material, and

A_{fi} is the total flaming area of the i^{th} material.

The last term on the right hand side of Equation 5-22 accounts for loss for smoke by the upper zone flows exiting the cabin section. Upper zone volume V_u is given in terms of the section dimensions and the upper zone layer depth as

$$V_u = C_w C_\ell L \quad . \qquad (5\text{-}23)$$

Units of smoke concentration in Equation 5-22 are "particles" per cubic foot. The definition of one "particle" of smoke, as introduced by Smith [10], is that amount of smoke which when confined in a unit volume reduces light transmission over unit length by 10%. Smoke concentration given in

particles per cubic foot is not easily envisioned by those not familiar with this unit. To provide a more widely known measure of smoke, the computer program reports the concentration in the output in optical density units. The conversion from particles per cubic foot to optical density is

$$O.D. \equiv \log_{10}\left(\frac{100}{\tau}\right) = \log_{10}\left(\frac{I_o}{I}\right) = k S \ell \qquad (5\text{-}24)$$

where

O. D. is the optical density,

τ is the percent light transmission through the smoke over a path length ℓ,

I_o/I is the ratio of initial light intensity to the intensity at ℓ, and

k is a converstion factor, which can be interpreted as the optical cross section of a smoke particle.

The conversion factor k in Equation 5-24 has the numeric value 0.04576 ft^2/ particle.

For toxic gas concentration, equation is written for each toxic specie as

$$\frac{d}{dt}\left(C_i V_u\right) = \sum_{j=1}^{n_s} r_{gijs} A_{si} + \sum_{i=1}^{n_f} r_{gijf} A_{fi} - C_i \dot{m}_{vu}/\rho_u \qquad (5\text{-}25)$$

where

C_i is the concentration of the i^{th} toxic gas,

r_{gijs} is the generation rate per unit area of the i^{th} toxic gas by smoldering of the j^{th} material type, and

r_{gijf} is the generation rate per unit area of the i^{th} toxic gas by flaming combustion of the j^{th} material type.

The concentration of each toxic gas (a maximum of nine toxic gases are allowed by the program) is expressed in units of mass density (lbm/ft^3), and the generation rates are input as mass per unit area per unit time. Conversion of the computed concentrations to the more common unit of parts per million (ppm) is performed for the program output.

The final variable of the cabin atmosphere model is the thickness of the upper zone. This layer depth is computed by assuming the upper and lower zones to be in dynamic equilibrium; that is, the pressure is the same on either side of thermal discontinuity. Ignoring the pressure variation with height in the cabin interior, application of the gas law to both zones realtes the upper zone thickness to the temperatures and masses of each zone by the simple relationship

$$L = \left[\frac{C_h}{\frac{M_\ell \; T_\ell}{M_u \; T_u} + 1} \right] \quad . \tag{5-26}$$

With the definition of L by Equation 5-26, the set of variables of the atmosphere model is complete. The next section describes the solution procedure for the equations of the model and discusses methods of specifying ignition.

5.6 NUMERIC SOLUTION OF THE EQUATIONS

Nine equations constitute the basic set of relationships which is the cabin atmosphere model: Equations 5-1a and 5-1b for the mass of gas in each zone, 5-15a and 5-15b for the zone temperatures, 5-21a and 5-21b for the surface material temperatures, 5-22 for the upper zone smoke concentration, 5-25 for the concentration in the upper zone of each toxic gas, and 5-26 for

the upper zone depth. To solve these equations at consecutive time points, the straight-forward Eulerian numerical technique is employed. Finite difference equations are written as approximations to the differential equations, and the difference equations are rearranged to solve for the changes in the basic variables as functions of their previous values and the integration step-size Δt. The difference equations are

$$\Delta M_u = \left(\dot{m}_f - \dot{m}_{vu}\right)\Delta t \tag{5-27a}$$

$$\Delta M_\ell = \left(\dot{m}_{v\ell} - \dot{m}_f\right)\Delta t \tag{5-27b}$$

$$\Delta T_u = \frac{\Delta t}{C_p M_u}\left[q_f - q_{hu} - q_{ru} - q_{r\ell} + \dot{m}_f c_p \left(T_\ell - T_u\right)\right] \tag{5-27c}$$

$$\Delta T_\ell = \frac{\Delta t}{C_p M_\ell}\left[\dot{m}_v\ c_p\left(T_{am} - T_\ell\right) - q_{h\ell}\right] \tag{5-27d}$$

$$\Delta T_{su} = \frac{\Delta t}{\rho_m C_{pm} x}\left[\frac{\left(q_{hu} + q_{ru}\right)}{A_u}\right] - \frac{2k_m}{x}\left(T_{su} - T_{am}\right) + q_e \tag{5-27e}$$

$$\Delta T_{s\ell} = \frac{\Delta t}{\rho_m C_{pm} x}\left[\frac{\left(q_{h\ell} + q_{r\ell}\right)}{A_\ell}\right] - \frac{2k_m}{x}\left(T_{s\ell} - T_{am}\right) + q_e \tag{5-27f}$$

$$\Delta L = C_h \Big/ \left(M_\ell T_\ell \Big/ M_u T_u + 1\right) - L \tag{5-27g}$$

$$\Delta S = \frac{\Delta t}{C_w C_\ell L}\left[\sum_{n_s} r_{ssi} A_{si} + \sum_{n_f} r_{sfi} A_{fi} - \dot{m}_{vu}/\rho_u - C_w C_\ell \frac{\Delta L}{\Delta t} S\right] \tag{5-27h}$$

$$\Delta C_i = \frac{\Delta t}{C_w C_\ell L} \left[\sum_{n_s} r_{gijs} A_{si} + \sum_{n_f} r_{gijf} A_{fi} - C_i m_{vu} / \rho_u - C_w C_\ell \frac{\Delta L}{\Delta t} C_i \right] \quad (5\text{-}27i)$$

The products containing $\Delta L/\Delta t$ on the right hand sides of Equations 5-27h and 5-27i arise from the application of the chain rule to the left hand sides of Equations 5-22 and 5-26 and from the definition of $V_u = C_w C_\ell L$. These terms are the changes in each concentration resulting from the change in the upper zone volume.

The order of solution of Equations 5-27 is that in which they are presented. Changes in zone gas mass computed by Equations 5-27a and 5-27b are immediately used to update the total amounts by

$$M_u (t + \Delta t) = M_u (t) + \Delta M_u \quad (5\text{-}28a)$$

$$M_\ell (t + \Delta t) = M_\ell (t) + \Delta M_\ell \quad (5\text{-}28b)$$

The updated masses are then used in Equations 5-27c and 5-27d to compute the temperature changes of the zone gases. After the gas temperatures are updated by expressions analogous to Equation 5-28, these values are used in Equations 5-27e and 5-27f to obtain the changes in and the updated values of the surface temperatures. Next, the new gas masses and temperatures are used to compute the change in the upper zone depth in Equation 5-27g. Finally, ΔL is used to compute the new concentrations of smoke and toxic gases by Equations 5-27i and 5-27h and equations of the form of Equation 5-28.

5.7 COMBUSTION PARAMETERS

The mathematical equations of the DACFIR Model which describe fires on cabin interior surfaces and their influence on the cabin atmosphere employ seven parameters the values of which are assumed to be independently

known. For purposes of discussion, the quantities are called the combustion parameters of the cabin atmosphere model. They are: the entrainment constants E_c and E_p, the adjusted heat of combustion of the fuel material Q^*_c, the fuel vapor density ρ_o, the fuel vapor temperature T_o, the fuel vapor velocity u_o at the base of the flame, and the stoichiometric oxygen to fuel mass ratio γ. Unfortunately, values of these parameters for the types of sophisticated polymeric materials used in wide-body cabins are not available at present. To provide data for exercising of the model, values for these quantities have been estimated based on the available information from the fire research literature.

Since little comparative data on different types of polymers could be found, the present DACFIR code assumes constant values for the combustion parameters for all fires regardless of fire geometry or material type. The values assumed for the entrainment constants have been discussed previously in Section 5.2. For T_o, the assumed value is $1.6\ T_{am}$ as quoted by Fang for n-heptane liquid pool fires. Modak and Croce's study of PMMA fires provides the estimate of Q^*_c as 58% of the total heat of combustion of PMMA, or approximately 7000 Btu/lbm as the adjusted value. The stoichiometric fuel to oxygen ratio, γ, was estimated to be 2.0 which is in rough agreement with Quintiere's estimate of 7.0 for the fuel to <u>air</u> ratio of plastic fires. No direct estimates of either ρ_o or u_o could be found in the literature, but approximate limits on the values which these quantities may take can be inferred from Modak and Croce's burning rate data. The product of ρ_o and u_o is the mass burning rate per unit area $\dot{m}''_o$ (See Equation 5-4). The burning rate value measured for PMMA varied between about 0.0018 and 0.0041 $lbm/ft^2 \cdot sec$ depending on fire size. From these values, an estimate of 0.0035 $lbm/ft^2 \cdot sec$ was selected as typical. Assuming that the material vaporizes as a pure substance of molecular weight 60 (about that of butane) at a temperature of $850^\circ R$ ($1.6\ T_{am}$, where $T_{am} = 530^\circ R$ or $70^\circ F$), and at atmospheric pressure, the density of the fuel vapor would be about 0.1 lbm/ft^3. Therefore, u_o would have a value of 0.035 ft/sec to correspond to the assumed burning rate. These values have been used in the tests of the DACFIR Model.

5.8 IGNITION SOURCES

To start the simulation of a fire within the cabin section, some form of ignition method must be specified. The DACFIR program incorporates two methods by which ignition may be described. The first method involves initializing elements on any surface or surfaces to the flaming state at the start of the run. The effect of this type of ignition is to assume that one or more fires of a given size have, by some means not specified, instantaneously ignited on the materials and that the materials form the only fuel for continued burning. This method does not consider, on the part of computations in the program at least, questions of the method by which these fires might be ignited in an actual cabin fire incident. Many state-of-the-art aircraft interior materials will not ignite or propagate flames when exposed to low externally applied heat fluxes, so that small fires created on surfaces of these materials may not provide sufficient heating to grow. While this is an interesting result in itself, the question of how a fire of such size came to be must be answered by the user who specifies the initial situation.

The second method of ignition used by the DACFIR program is the identification by the user of a group of "ignition source" elements which define a region where a separate ignition fuel is superimposed on a surface. The initial fire of the simulation burns over this ignition region and involves both the ignition fuel and the material on which it rests. Separate smoke, toxic gas, and heat generation rates can be specified for this ignition material; the total burning time can be controlled by giving the total amount of the ignition material present and the mass burning rate of the material (assumed constant). Four of the combustion parameters (Q_c^*, γ, ρ_o, u_o) described in Section 5.7 must also be specified for the ignition source material. The smoke, heat, and toxic gas release by the ignition source are added to that produced by the material which it covers, and the computation of the fire flame height and convective flow is adjusted to reflect the combined effect of the two fuels. This ignition method is designed to simulate a likely source, a spilled flammable liquid. Elements on the "host" surface adjacent

to the ignition source fire may be come involved if conditions are right for flame spread on this material. Any such fire surrounding the ignition source has the characteristics of the surface material only since the ignition fuel is not allowed to move from its originally specified location.

SECTION 6
COMPUTER PROGRAM

6.1 INTRODUCTION

This section briefly describes the DACFIR Program, the computer program which implements the mathematical model. A more complete flow chart of the program and instructions for its use may be found in Volume 3, Computer Program User's Guide.

The discussion here is included to demonstrate the general organization of the computations. The language of the program code is FORTRAN IV and conforms, except for a very few specific instances, to American National Standards Institute (ANSI) FORTRAN. The program has been successfully run on the UNIVAC 70/7 and CDC 6600 computers.

6.2 PROGRAM ORGANIZATION

Figure 6.1 presents a flow chart of the program. The small numbers identify specific processes or computational divisions, subroutines in most cases, designed to do specific tasks.

The program has a two-loop structure, a small loop of computations nested within a larger outer loop. Before entering the outer loop, the program reads the input data and initializes program variables. Subroutines INPUT G and INPUT M, 1 and 2 in the figure, read data cards specifying the size and orientation of the interior surfaces of the cabin section; the materials of which these surfaces are composed; and the flame spread rate data, time constants, and smoke, heat, and toxic gas release rate data for the materials. The combustion parameters: effective heat of combustion, stoichiometric ratio, fuel vapor density, and fuel vapor velocity are also read in for each material type. Subroutine INIT, step 3, initializes program variables as required; in particular the two large arrays containing the states and 'clocks' for each element are

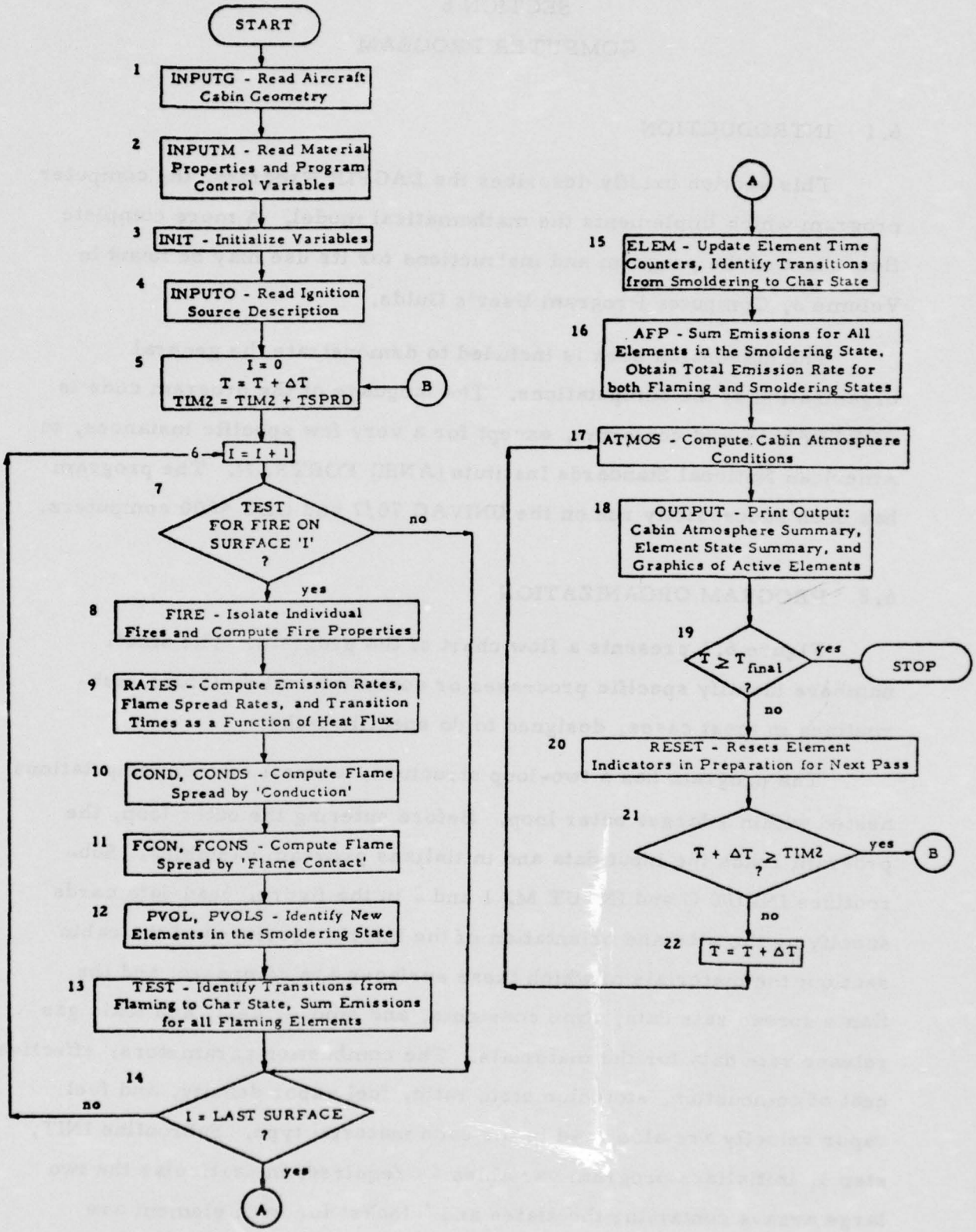

Figure 6.1 Program DACFIR Flow Chart

initially set here. Subroutine INPUTO, 4, reads the specific starting conditions: the location of the ignition source and its combustion parameters, and smoke and toxic gas generation rates. A level of background radiation above the normal may be input at this point. Selected elements may also be set to the charred state (burned out and thus inert), if desired, to study specific configurations that may not be easily designated by the general geometric or material descriptions.

At 5 in the figure the outer loop is entered. In this loop the growth of the fire is computed. The index 'I' counts the cabin surfaces examined in search of flaming elements. The simulation time T is advanced by the time step ΔT, the small or basic time step; and the flame-spread clock, TIM2, is advanced by TSPRD, the large time step representing the interval between element state transition calculations. At step 6, I is incremented (to the value one for the first pass). The test at step 7 determines if there are any flaming elements on surface I. The program contains an indicator for each surface that is set to a given value if a surface has one or more flaming elements.

Subroutine FIRE, 8, is called if surface I has at least one flaming element; if it does not, this surface is ignored. In FIRE surface I is examined in detail to find connected groups of flaming elements. These groups (which in some cases may be only one element) are defined as individual fires, a flame height and other parameters are calculated for each fire, and each fire is given a distinct identification number. Next, at process 9, the rates of emission of heat, smoke, and toxic gases, are calculated for the elements involved in each fire. The next four processes, 10 through 13, involve the computation of the fire spread to new elements, and the identification of new smoldering and charred elements. Subroutines COND (for the interior lining surfaces) and CONDS (for the surfaces of the seat groups) examine elements on the same surface as, and adjacent to, a fire to determine if the fire has spread to these elements in the time period TSPRD. When fire is at the

edge of a surface, the adjacent connecting surface is examined to account for spread across the boundary. Subroutines FCON and FCONS determine the flame spread by flame contact: the involvement of elements in the volume of flame above the fire. Transformation equations contained in these subroutines determine, given the height of the flames of a certain fire, which elements on other surfaces are touched by flames. If an element is involved for a sufficient length of time, its state will be changed to the flaming condition.

Subroutines PVOL and PVOLS perform a function similar to FCON and FCONS but, instead of transitions to the flaming state, transitions to the smoldering state are determined. Equations defining the heat flux from a fire are used to estimate the "smoldering range" of the fire. Within this range the heat flux level is sufficiently high that, taking into account the response time of the materials intruding the volume, transitions to the smoldering state can take place. The final process in the surface loop is the search for flaming elements that will burn out during this time interval. Subroutine TEST examines all the flaming elements on surface I and sets elements to the charred state if their percent of decomposition has reached 100 percent. Since this subroutine examines each flaming element, the emission of smoke, heat, and toxic gases from the elements are summed here to obtain total rates of emission for each quantity over all the fires on surface I. At the end of the surface loop, step 14 is the test to determine if all surfaces, both seats and lining surfaces, have been examined.

Step 15, subroutine ELEM, advances the clocks for each active element and determines which smoldering elements should now be set to the charred state. Subroutine AFP examines all smoldering elements and sums the emission rates for each smoldering material. The subroutine then sums the flaming and smoldering rates over all active materials to obtain the net rates of emission of smoke, heat, and toxic gases for the entire cabin section. These rates are passed to subroutine ATMOS, 17,

where they are incorporated into the equation set which models the cabin atmosphere dynamics. Once the updated values of the cabin atmosphere variables have been found, subroutine OUTPUT, 18, determines if a set of output variables are to be printed at this time step. If a set is to be printed, one of two options (determined by the choice of program control variables) is exercised. In the first option only the cabin atmosphere summary is printed. For the second option the print-out includes the atmosphere summary, a summary of the active elements, a list of the separate fires, and printer graphics of the location of all the elements in the flaming and smoldering states.

After leaving subroutine OUTPUT, a test is made, 19, to determine if the elapsed time is equal to the input time limit for this run. If the program is to continue, subroutine RESET resets indicators on the active elements. This "housekeeping" step is required because other portions of the program need to know which elements have changed state during the current pass and which were in their current state during the previous pass. RESET, therefore, equates all past state indicators with present state indicators. The test at 21 checks to see if the next increment of the simulation time by the small time step ΔT will result in the elapsed time being a multiple of the large time step, TSPRD. If a multiple of TSPRD will not be reached, the actual clock is updated, 22, and subroutine ATMOS is entered for another small step integration of the atmosphere differential equations. Flow around this shorter loop continues, output occurring at the proper times, until the test at 21 is passed (or the program stops by test 19). When $T + \Delta T$ becomes a multiple of TSPRD, control passes to 5 where the search for elements undergoing state transitions starts again.

Statistics on the program run time and memory requirements may be found in Volume III of this report.

SECTION 7
RESULTS FROM THE DACFIR MODEL

In this section the results of two simulations of cabin fires by the DACFIR Model are presented and discussed. The first simulation, Case 1, starts with a fire on the cabin floor in the left hand aisle which extends partially under two seat groups. This fire is initially fueled by a hypothetical, clean-burning, liquid fuel which produces no smoke or toxic gases by its own burning. The fuel is taken to be evenly distributed over four square feet of carpet and burns for about 170 seconds before it is exhausted. This initial fire situation could arise from the ignition of spilled cleaning fuel or other flammable liquids on the carpet. The second simulation, Case 2, starts with three square feet of the lower right sidewall and four and one-half square feet of the reveal/window/transparency strip above it set to the flaming state. This ignition method is chosen to approximate a burn-through of the fuselage skin and insulation batting which ignites the sidewall and reveal assembly from the outside. In both simulation cases the same material property data is used for all materials and all initial conditions other than the ignition description are identical.

7.1 INPUT DATA

The input data for a run of the DACFIR program may be divided into three groups: data describing the cabin geometry; data describing the material flammability properties; and data describing the ignition conditions, integration step-sizes, program run time, and output interval. For both cases the geometric description of the cabin section is that presented in Sections 3 and 5. This data is summarized in Table 7.1.

Flammability properties of the cabin materials form the most voluminous part of the program input. The twenty lining surfaces and nine seat groups are constructed of a total of seven separate material types. To describe a material under the DACFIR modeling scheme 19 + 2i properties of each

TABLE 7.1

SUMMARY OF GEOMETRIC INPUT DATA
Cases 1 and 2

1.	Cabin Section Dimensions (shown in Figure 5.1)	Length Width Height	30 feet 20 feet 7.5 feet
2.	Detailed Sub-section Dimensions (shown in Figures 3.1, 3.3, and 5.1)	Length Width Height	7.5 feet 20 feet 7.5 feet
3.	Lining Surfaces (shown in Figures 3.1 and 3.2)	20	Various dimensions
4.	Seat Groups (shown in Figure 3.3)	9	Various dimensions
5.	Passageways (Doors) (shown in Figure 5.1)	Number Height (floor to soffit) Width (2 left side) Width (2 right side)	4 7 feet (all) 5 feet 7 feet
6.	Element dimensions (all surfaces)	0.5 ft × 0.5 ft	

material must be known. The symbol i represents the number of toxic gases whose concentrations are to be computed. A maximum of nine is allowed by the computer code. Of these parameters, 8 + i must be known as functions of applied heat flux. Four of the flammability properties are the combustion parameters Q_c^*, γ, ρ_o, and u_o described in Section 5. Values for these quantities used in the simulations are those discussed in that section. Three thermal-physical properties are required for each material for use in the computation of average surface temperature: material density, ρ_m, specific heat, C_{pm}, and thermal conductivity k_m. Constant and identical values were used for all materials. The values are: $\rho_m = 35$ lbm/ft^3, $C_{pm} = 0.25$ Btu/lbm $\cdot$ ^oR, and $k_m = 8.4 \times 10^{-5}$ Btu/ft $\cdot$ sec $\cdot$ ^oR.

The material property input data for the simulation runs presented in this section consists of selected values obtained from laboratory tests on in-service, wide body cabin interior materials. A full description of the laboratory tests and the collected data is given in Volume II of this report subtitled "Laboratory Test Program". Figures from that volume are reproduced herein as Figures 7.1 through 7.12 which show the variation with applied heat flux of the following seven quantities: horizontal, vertical upward, and vertical downward flame spread rate; time to flame; time to char from the flaming state; heat release rate; smoke release rate (flaming state); and the release rates in the flaming state of the five toxic gases - hydrogen cyanide (HCN), hydrogen chloride (HCl), hydrogen fluoride (HF), carbon monoxide (CO), and sulphur dioxide (SO_2). This data was input to the program in the form of tables consisting of the coordinates of the points marked on the curves. The eighth function of heat flux, time to cease emission from the smoldering state (t_{pe}), was input as a constant value for each material in both runs because of the method by which this quantity was measured during the laboratory test program (see Volume II, Section 4). The values used for t_{pe} are given in Table 7.2.

The values of the nine material properties which are not functions of heat flux are given in Table 7.2. These quantities are all descriptive of the smoldering state, and were used for both cases.

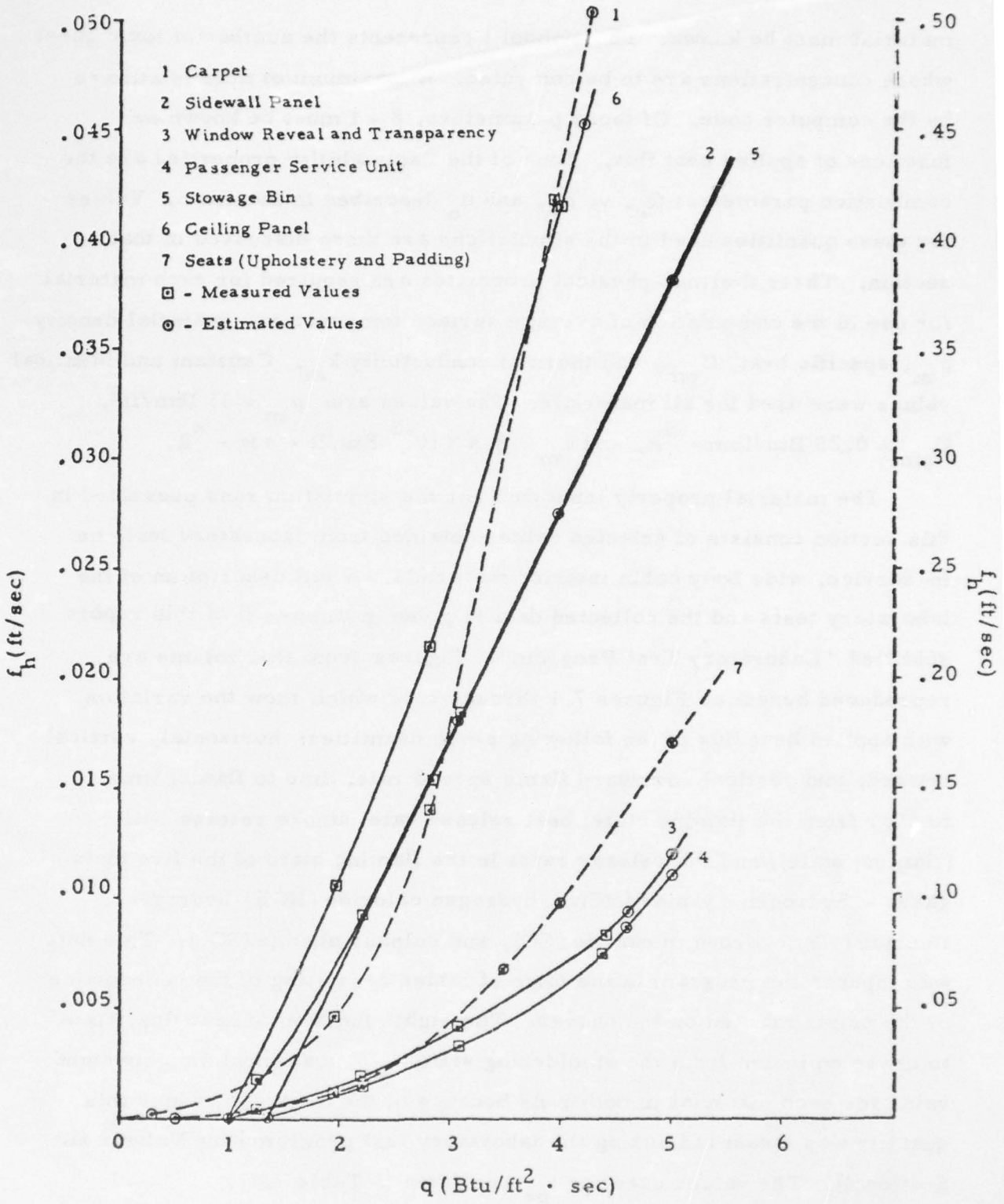

Figure 7.1 Horizontal Flame Spread Rate (f_h) Versus Heat Flux (q) (Dashed lines are based on the right-hand scale; solid lines are based on the left-hand scale)

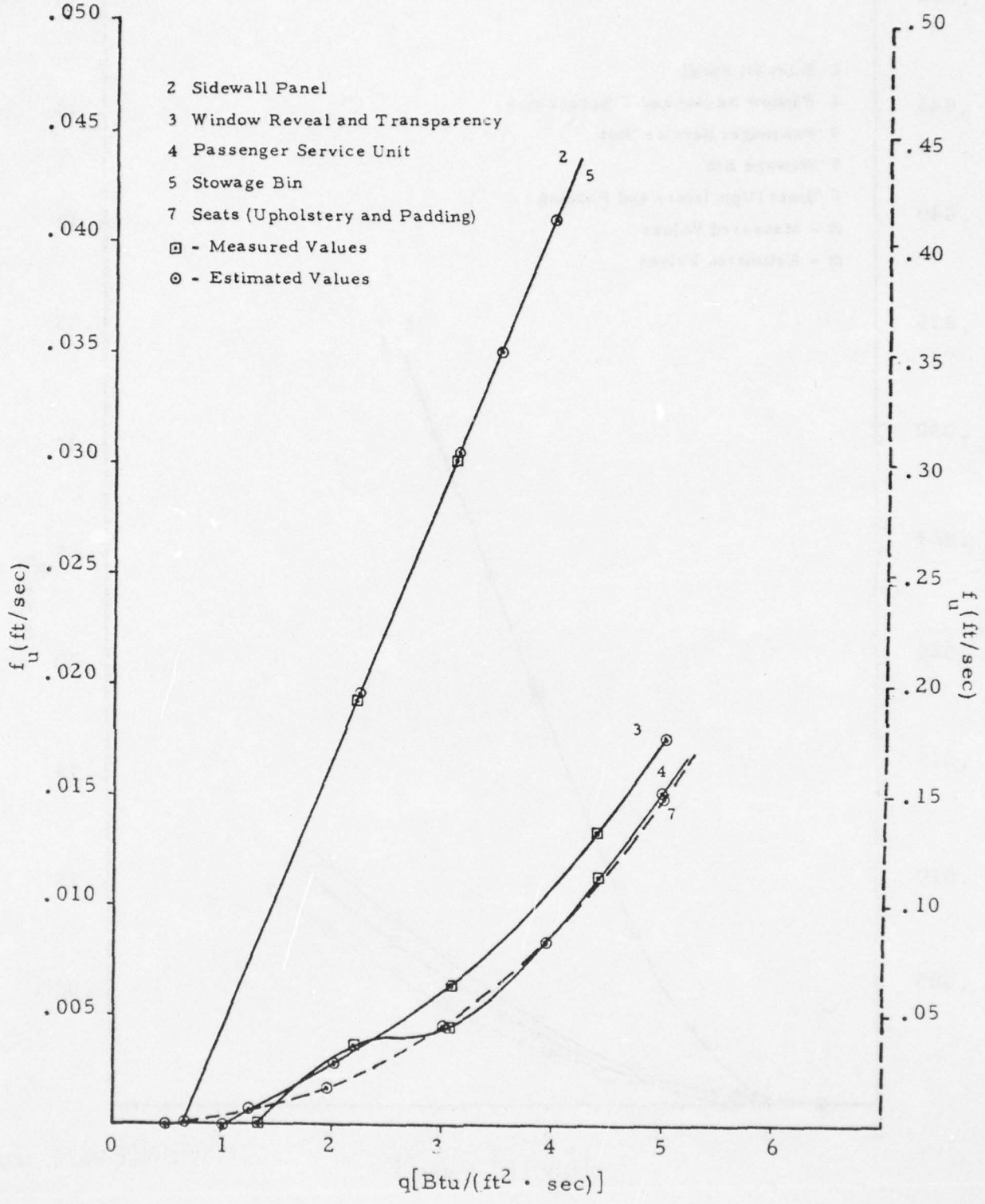

Figure 7.2 Vertically Upward Flame Spread Rate (f_u) Versus Heat Flux (q) (Dashed lines are based on the right-hand scale; solid lines are based on the left-hand scale)

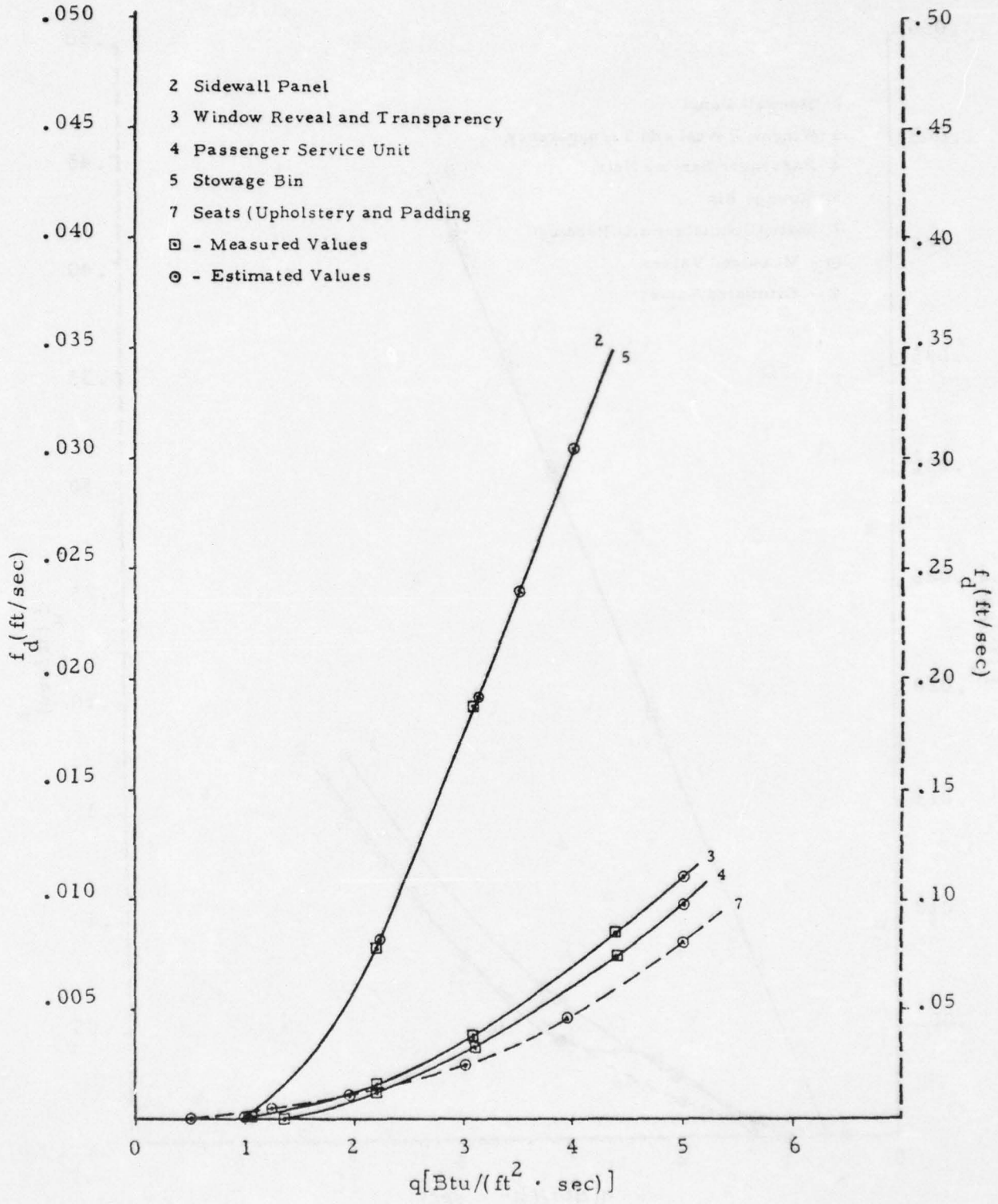

Figure 7.3 Vertically Downward Flame Spread Rate (f_d) Versus Heat Flux (q) (Dashed lines are based on the right-hand scale; solid lines are based on the left-hand scale)

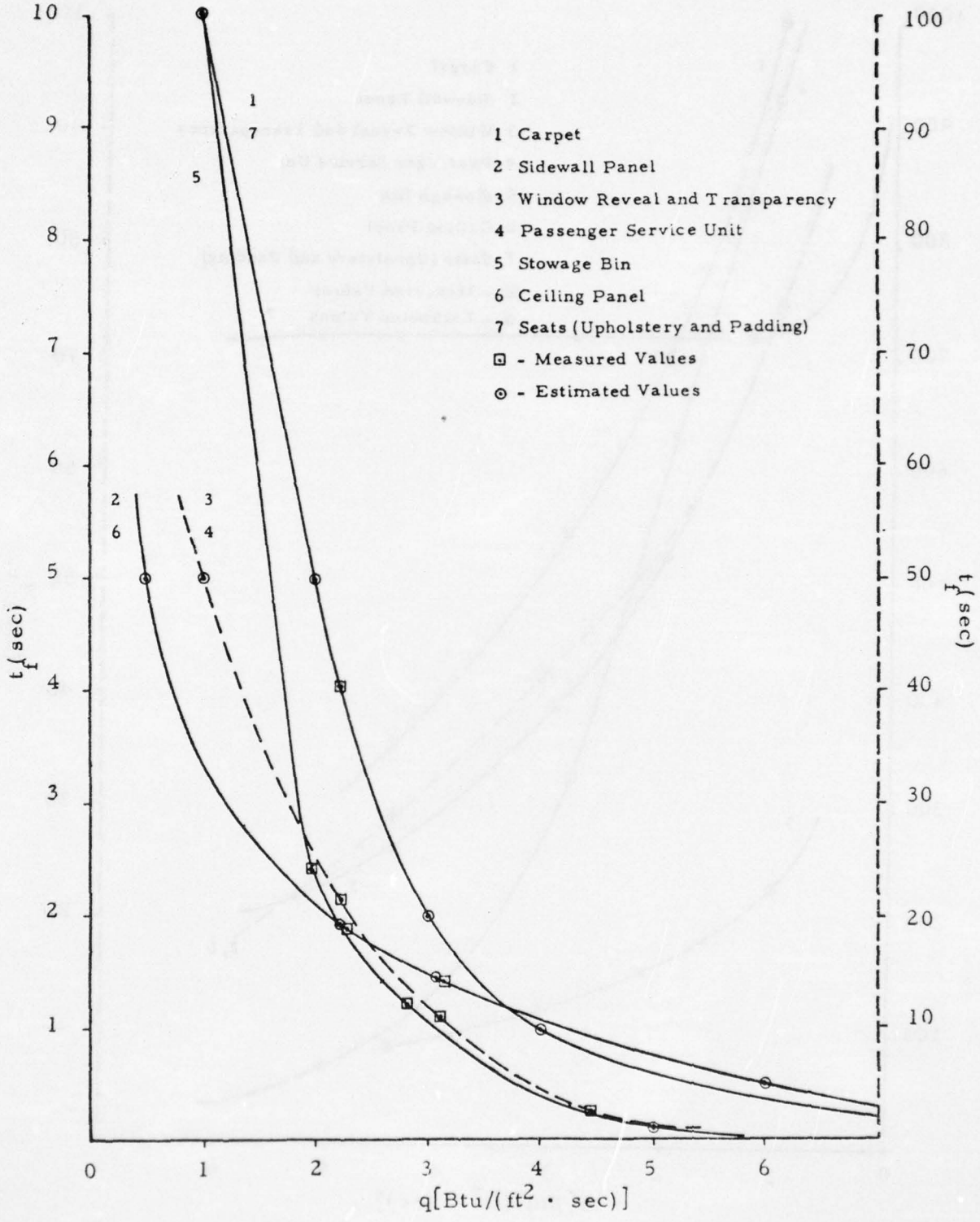

Figure 7.4 Time to Flame (t_f) Versus Heat Flux (q)
(Dashed lines are based on the right-hand scale;
solid lines are based on the left-hand scale)

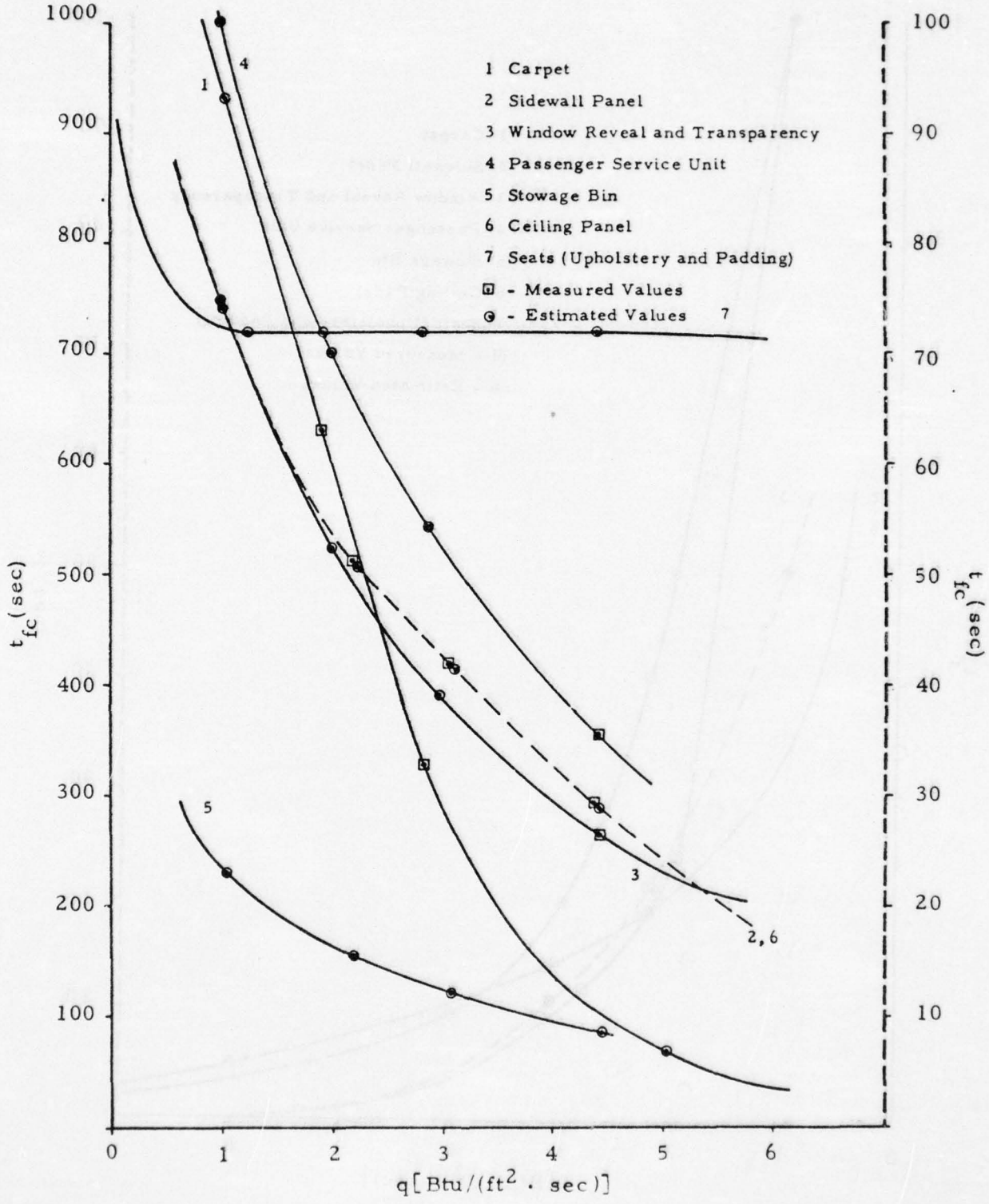

Figure 7.5 Time to Char from the Flaming State (t_{fc}) Versus Heat Flux (q)
(Dashed lines are based on the right-hand scale; solid lines are based on the left-hand scale)

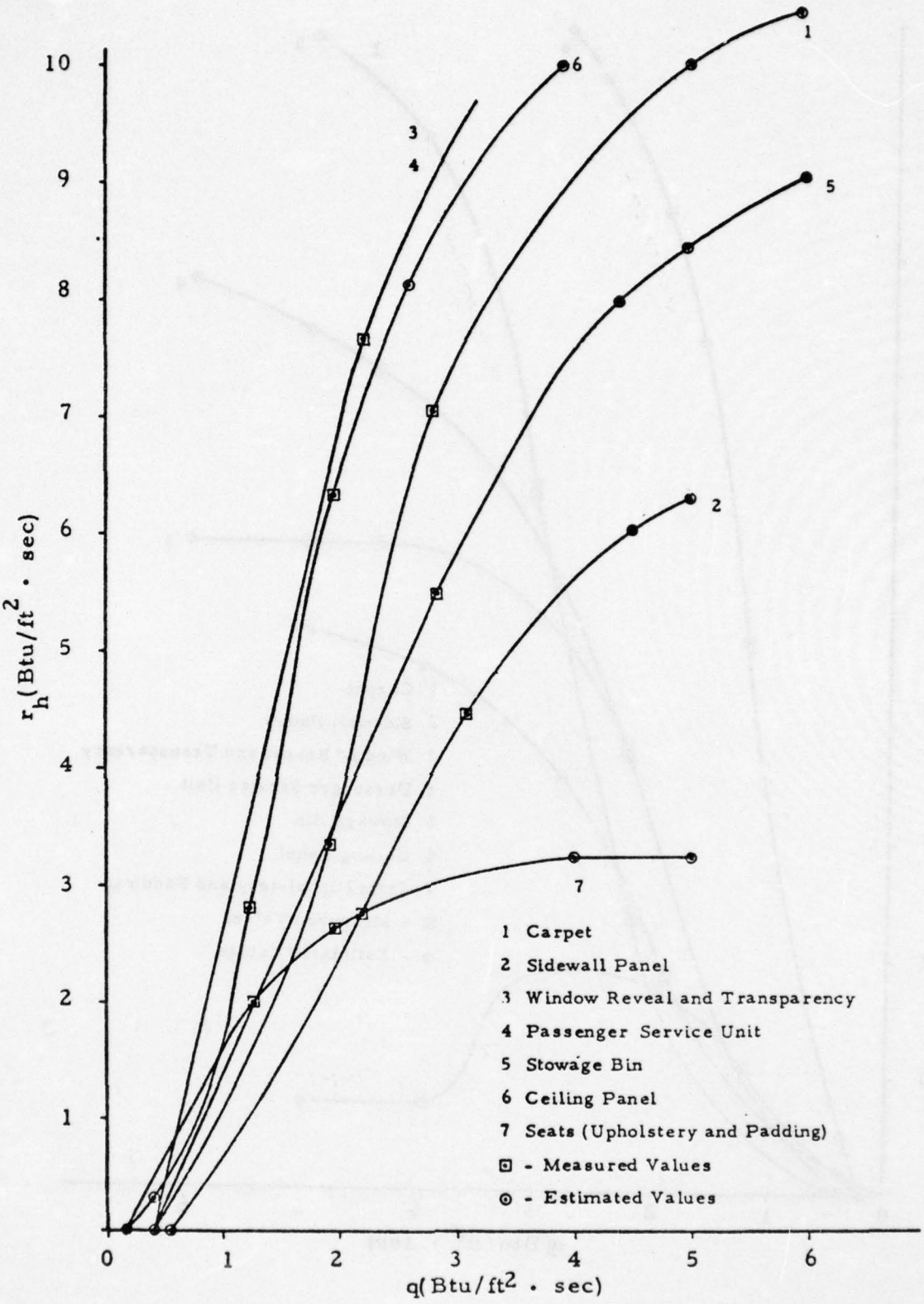

Figure 7.6 Heat Release Rate per Unit Area (r_h) Versus Heat Flux (q)

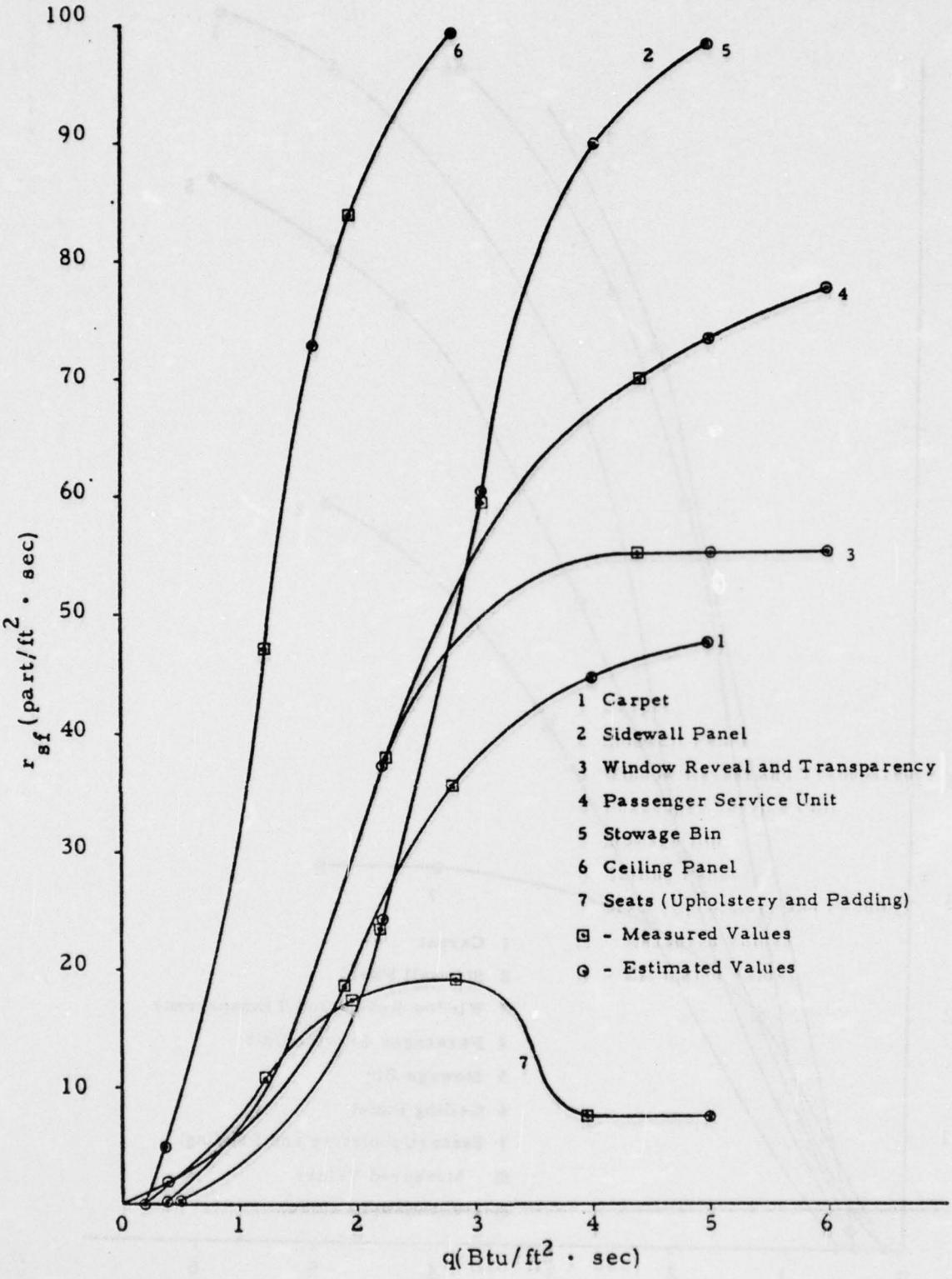

Figure 7.7 Smoke Release Rate per Unit Area in the Flaming State (r_{sf}) Versus Heat Flux (q)

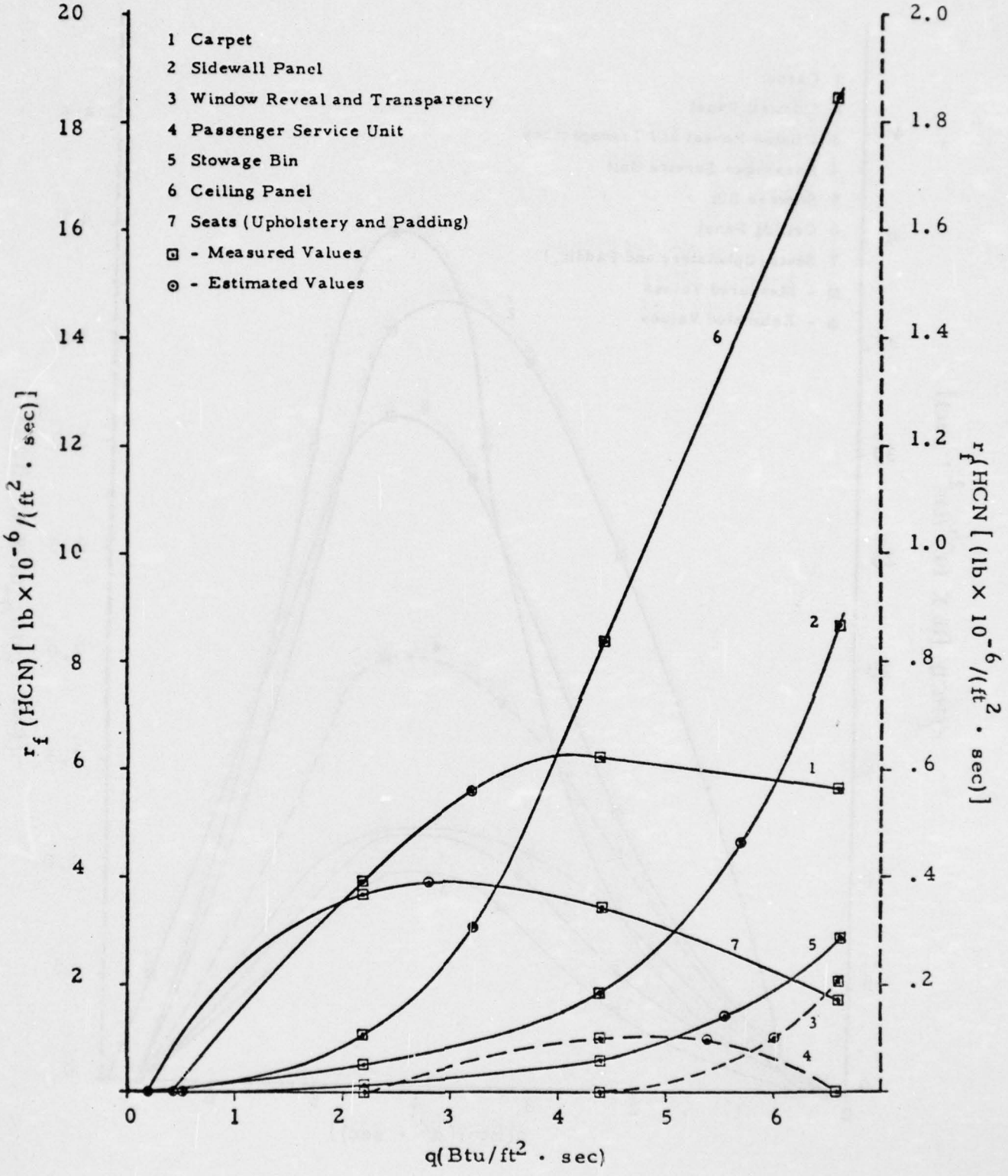

Figure 7.8 Release Rate per Unit Area of HCN in the Flaming State [r_f(HCN)] Versus Heat Flux (q)
(Dashed lines are based on the right-hand scale; lines are based on the left-hand scale)

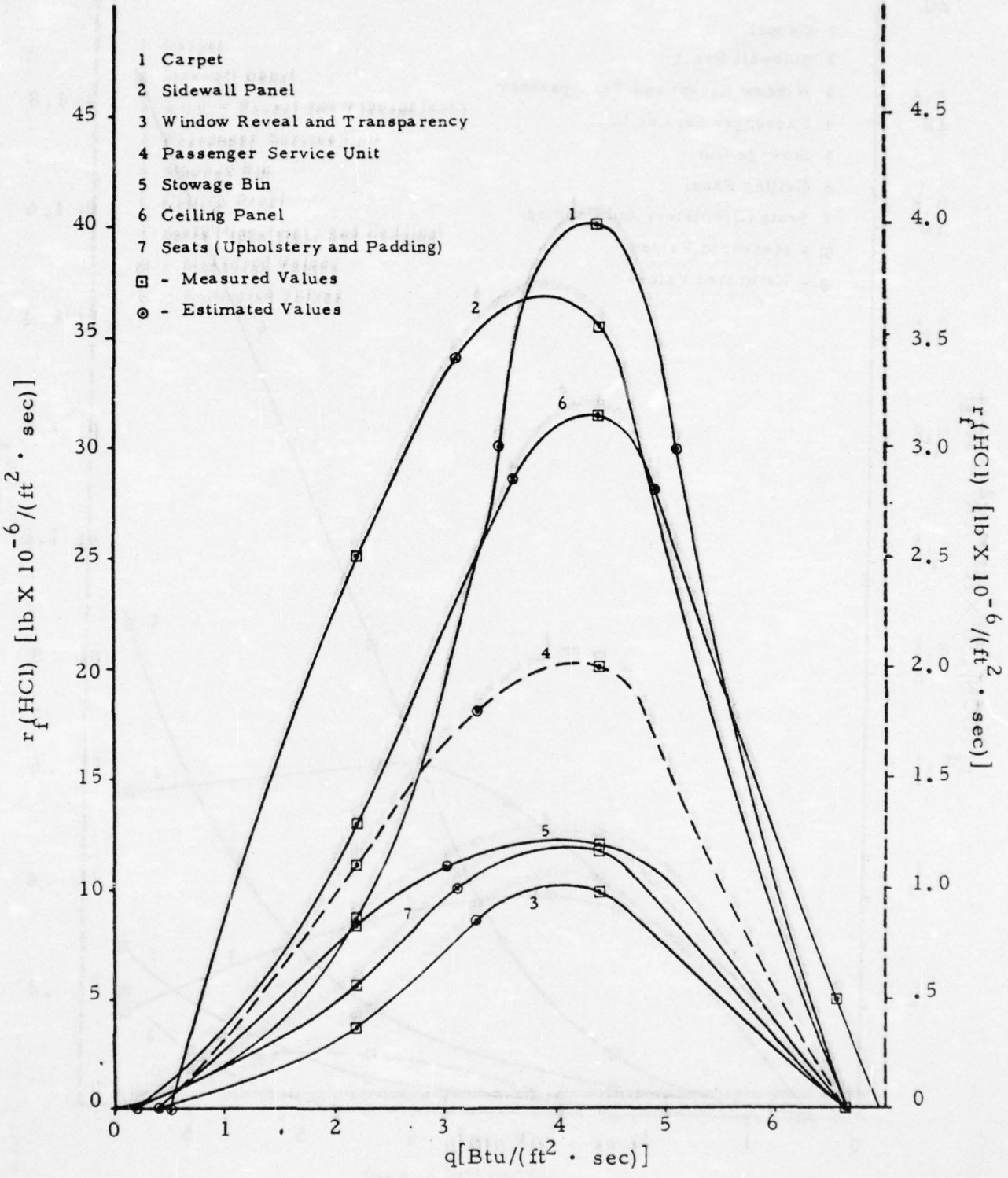

Figure 7.9 Release Rate per Unit Area of HCl in the Flaming State [r_f(HCl)] Versus Heat Flux (q)
(Dashed lines are based on the right-hand scale; solid lines are based on the left-hand scale)

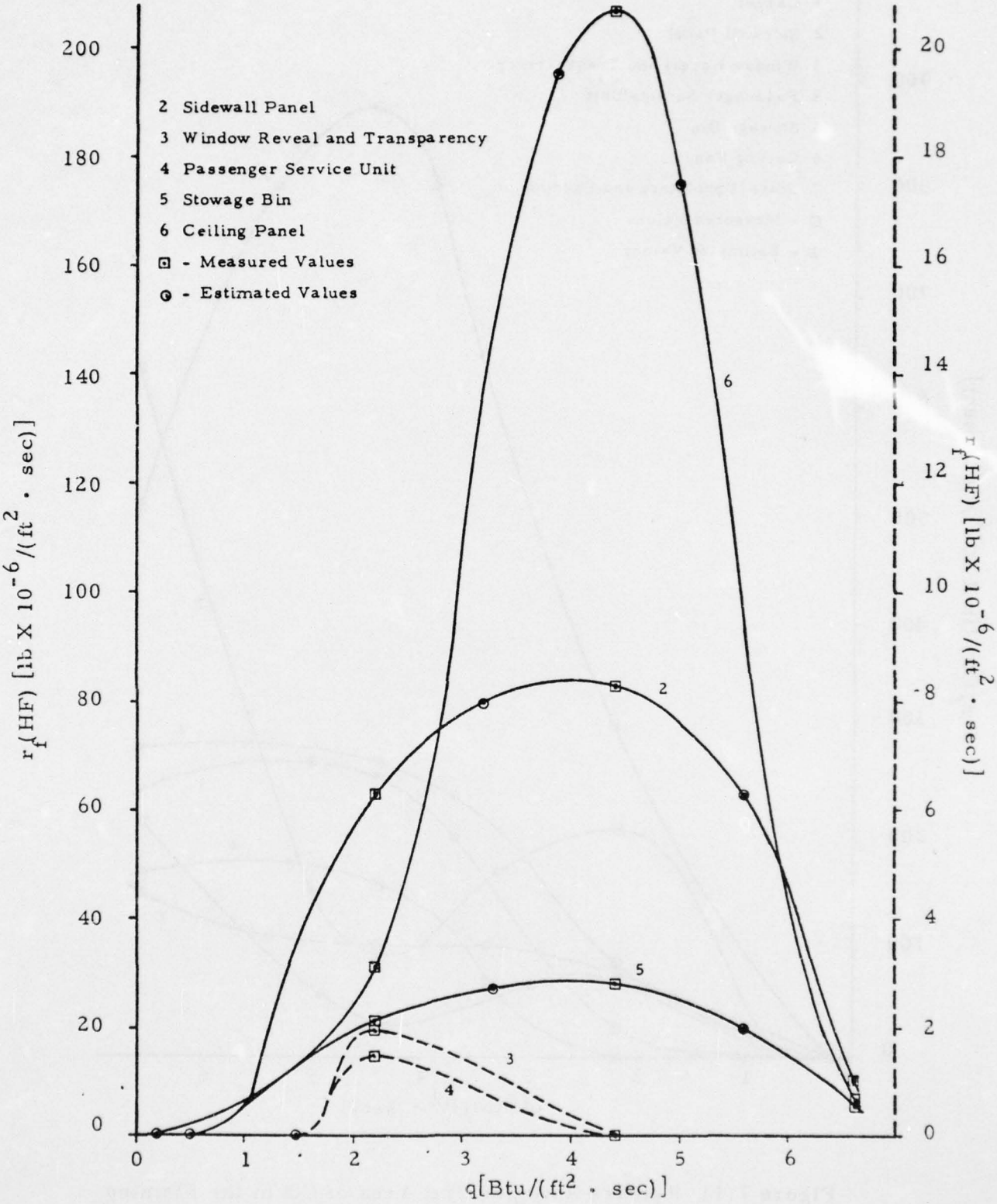

Figure 7.10 Release Rate per Unit Area of HF in the Flaming State [r_f(HF)] Versus Heat Flux (q) (Dashed lines are based on the right-hand scale; lines are based on the left-hand scale)

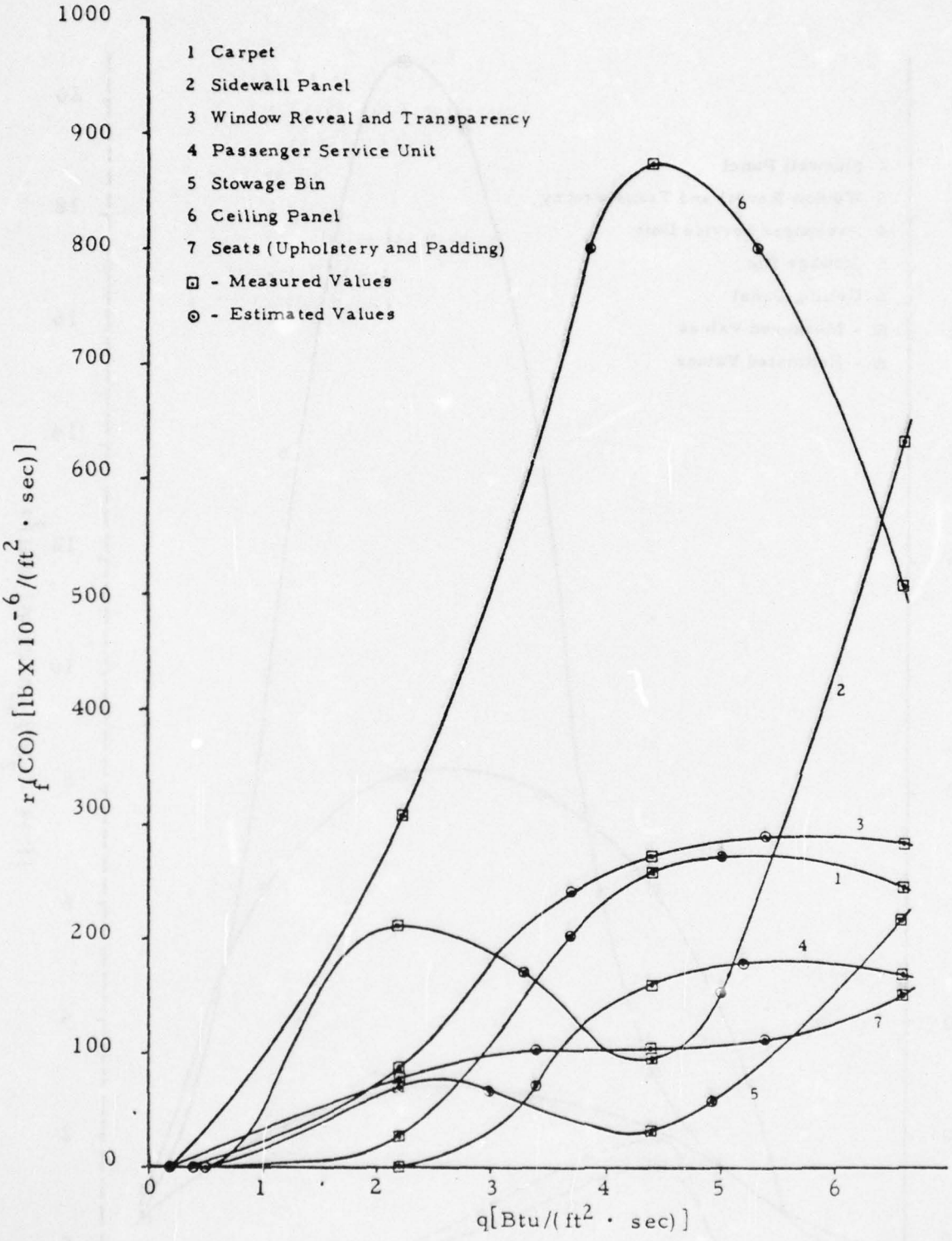

Figure 7.11 Release Rate per Unit Area of CO in the Flaming State [$r_f(CO)$] Versus Heat Flux (q)

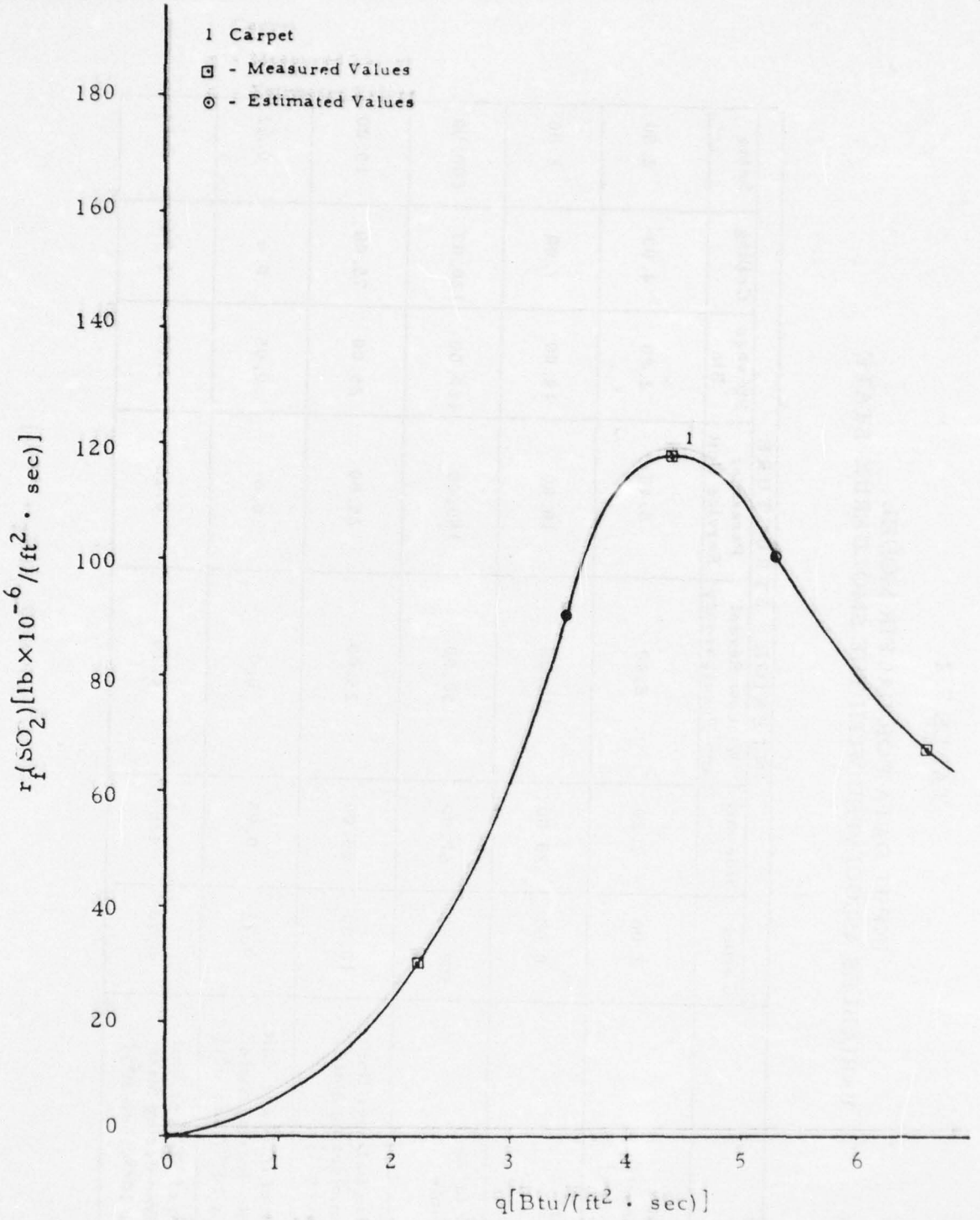

Figure 7.12 Release Rate per Unit Area of SO_2 in the Flaming State $[r_f(SO_2)]$ Versus Heat Flux (q)

TABLE 7.2

INPUT DATA FOR DACFIR MODEL
VARIABLES ASSOCIATED WITH THE SMOLDERING STATE

VARIABLE	INTERIOR STRUCTURE						
	Carpet	Sidewall	Window Reveal and Transparency	Passenger Service Unit	Stowage Bin	Ceiling	Seats
Heat Flux that Induces Smoldering q_p [Btu/(sec·ft^2)]	2.00	2.20	5.40	5.40	2.80	4.00	2.50
Time to Begin Smoldering t_p (sec)	8.00	20.00	12.00	10.00	14.00	7.00	8.00
Time to Char in the Smoldering State t_{pc} (sec)	500.00	67.00	150.00	150.00	180.00	120.00	600.00
Smoke Release Rate per Unit Area in the Smoldering State r_{ss} [part/(sec·ft^2)]	10.00	25.00	25.00	25.00	25.00	75.00	10.00
Release Rate of HCN per Unit Area in the Smoldering State r_s (HCN)[lb x 10^{-6}/(sec·ft^2)]	0.32	0.05	0.0	0.0	0.05	0.0	0.62
Release Rate of HCl per Unit Area in the Smoldering State r_s (HCl)[lb x 10^{-6}/(sec·ft^2)]	0.70	4.00	0.10	0.20	4.00	0.74	0.84

TABLE 7.2 (Continued)

INPUT DATA FOR DACFIR MODEL
VARIABLES ASSOCIATED WITH THE SMOLDERING STATE

VARIABLE	INTERIOR STRUCTURE						
	Carpet	Sidewall	Window Reveal and Transparency	Passenger Service Unit	Stowage Bin	Ceiling	Seats
Release Rate of HF per Unit Area in the Smoldering State r_s (HF)[lb x 10^{-6}/(sec·ft^2)]	0.0	6.00	0.0	0.0	6.00	2.00	0.0
Release Rate of CO per Unit Area in the Smoldering State r_s (CO)[lb x 10^{-6}/(sec·ft^2)]	2.00	30.00	16.00	16.00	30.00	4.00	10.00
Release Rate of SO_2 per Unit Area in the Smoldering State r_s (SO_2)[lb x 10^{-6}/(sec·ft^2)]	3.00	0.0	0.0	0.0	0.0	0.0	0.0
Time to Cease Smoldering When the Heat Flux is Reduced to Zero t_{pe} (sec)	10.0	13.5	1.8	1.2	2.4	6.6	2.4

AD-A033 682 DAYTON UNIV OHIO RESEARCH INST F/G 1/2
DAYTON AIRCRAFT CABIN FIRE MODEL. VOLUME I. BASIC MATHEMATICAL --ETC(U)
JUN 76 J B REEVES, C D MACARTHUR DOT-FA74WA-3532
UNCLASSIFIED FAA-RD-76-120-1 NL

2 OF 2
AD A033682

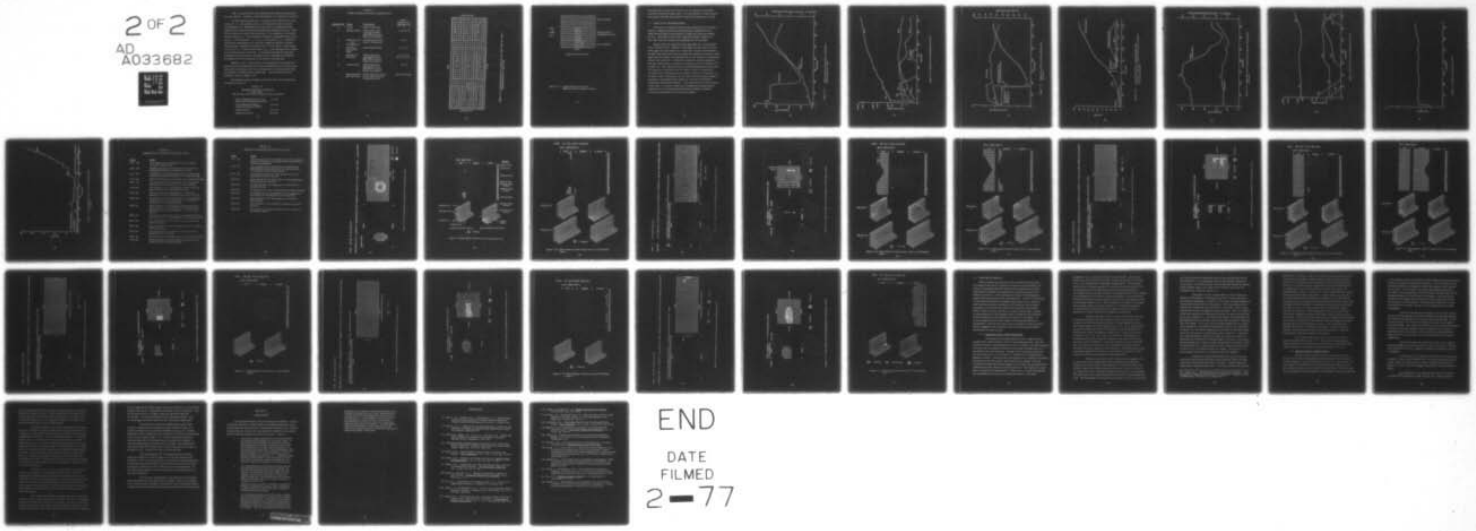

END

DATE FILMED
2-77

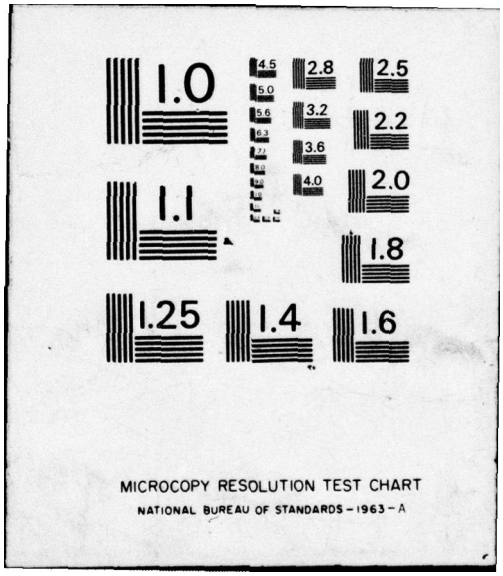
1.0
1.1
1.25
1.4
1.6
1.8
2.0
2.2
2.5
2.8
3.2
3.6
4.0
4.5
5.0
5.6
6.3
7.1
8.0
MICROCOPY RESOLUTION TEST CHART
NATIONAL BUREAU OF STANDARDS - 1963 - A

Table 7.3 describes the seven materials from which the flammability data was obtained. Complete material descriptions are contained in Volume II.

The third group of input data is comprised of the specification of the initial fire, i.e., the ignition source, and the program control variables. As mentioned above, the ignition source for Case 1 is a flammable liquid spilled on the carpet in the left aisle and partially beneath seat Group 1 in the first row and seat Group 4 in the second row. The distribution of the spill is shown in Figure 7.13. The combustion parameters of the ignition source fuel are Q^*_c = 13,000 Btu/lmb, γ = 3.5, ρ_o = 0.205 lbm/ft^3, u_o = 0.048 ft/sec. These values approximate a low molecular weight hydrocarbon or alcohol. The total mass of spilled fuel is taken to be 6.73 lbm, which, at the burning rate of 3.92 X 10^{-3} lbm/sec (the product of ρ_o, u_o and the spill area), results in a fire lasting about 172 seconds. In order that the smoke and toxic gas generation of only the interior materials could be examined the spilled fuel is assumed to have no generation rate of smoke or any toxic gas.

Ignition in Case 2 is described as an emerging fire on the right sidewall and reveal strip and does not involve an imposed fuel as in the first case. Seven and one-half square feet of the sidewall and reveal-transparency strip are initially set flaming by the program input. The distribution of these elements is shown in Figure 7.14.

The program control variables used in both cases were identical and are shown in Table 7.4.

TABLE 7.4

PROGRAM CONTROL VARIABLES
Cases 1 and 2
(See Sections 5 and 6 for discussion of these variables.)

Basic integration step-size (Δt) (step-size for the gas flow model)	1.0 sec
Time step-size for flame spread calculations (TSPRD)	10.0 sec
Output interval	10.0 sec
Maximum run time	730.0 sec

TABLE 7.3

CABIN INTERIOR MATERIALS DESCRIPTION

Material No.	Usage	Description	Cabin Surface No(s). (See Fig. 3.1)
1.	Carpet	wool, cut and loop	1
2.	Sidewall Panel	Tedlar/epoxy pre-impregnated fiber-glass/Nomex honey-comb core sandwich	2, 4, 18, 20
3.	Window Reveal and Transparency	polycarbonate reveal acrylic transparency	3, 19
4.	Passenger Service Unit (PSU)	polycarbonate sheet	5, 11, 17
5.	Stowage Bin (all sides)	Tedlar/epoxy pre-impregnated fiber-glass/Nomex honey-comb core sandwich	6, 7, 9, 10 12, 13, 15, 16
6.	Ceiling Panel	Tedlar/epoxy pre-impregnated fiber-glass/Nomex honey-comb core sandwich	18, 14
7.	Seat, Upholstery and Foam Pad	Nomex upholstery fabric, 4.0 in. thick Polyether Urethane foam pad	(all seat groups)

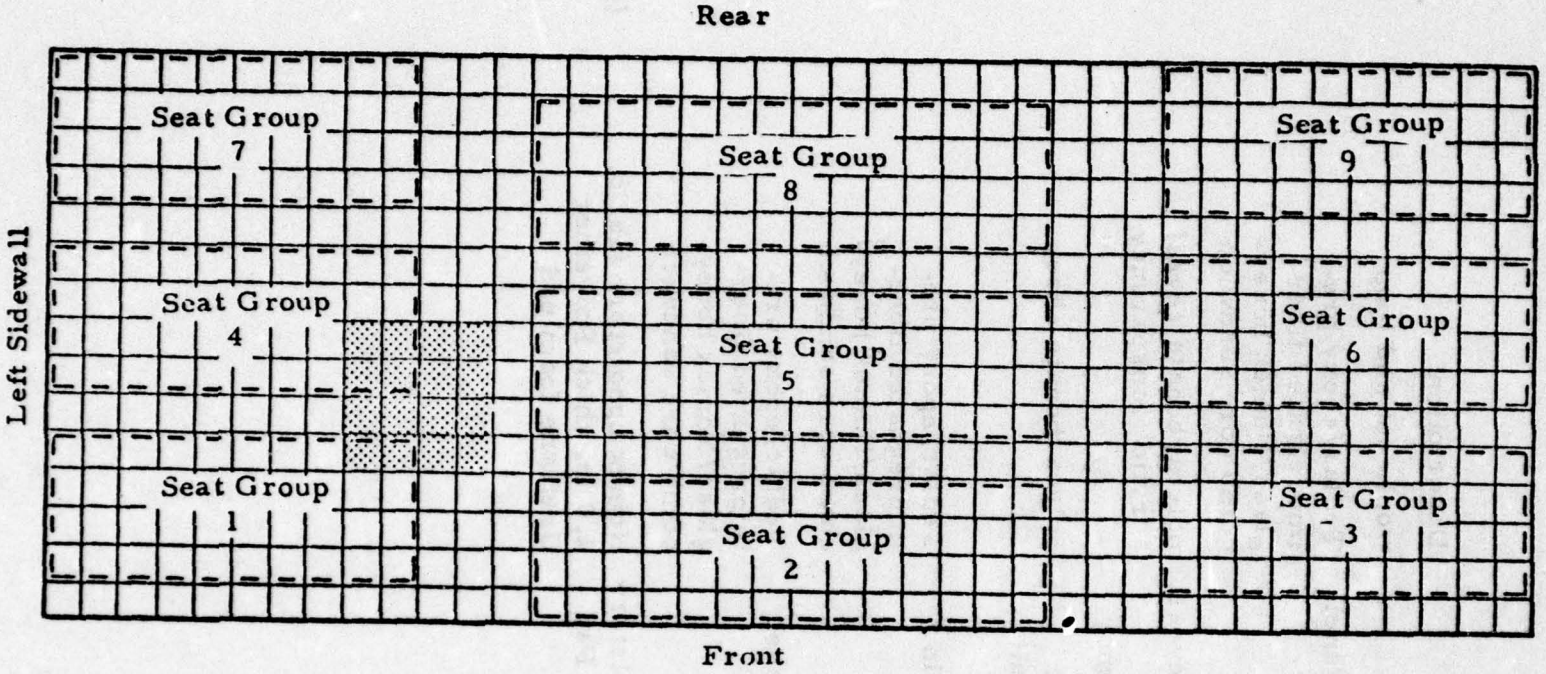

Figure 7.13 Initial Spill and Fire Location on the Cabin Floor for Case 1 Shading indicates the spill area.

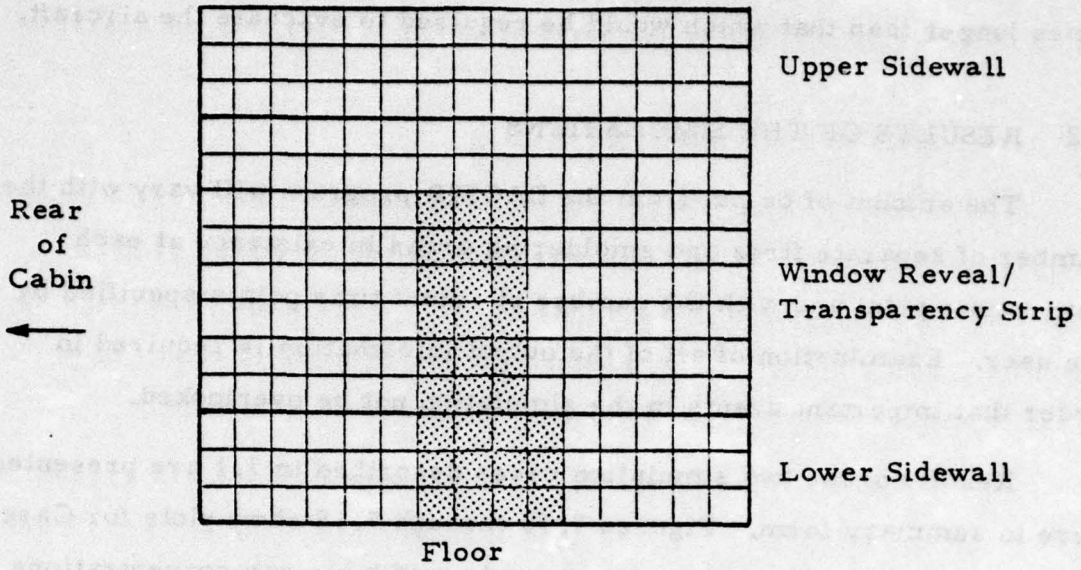

Figure 7.14 Ignition Pattern for Case 2
Shading indicates flaming elements.

The maximum run time of 730 seconds (12.16 minutes) was somewhat arbitrarily selected for these cases. This time period is at least several times longer than that which would be required to evacuate the aircraft.

7.2 RESULTS OF THE SIMULATIONS

The amount of output from the DACFIR program will vary with the number of separate fires and smoldering areas in existence at each output time point and with the number of output time points specified by the user. Examination of all of the output information is required in order that important events in the simulation not be overlooked.

Results of the two simulation cases described in 7.1 are presented here in summary form. Figures 7.15 through 7.18 show plots for Case 1 of the upper zone gas temperature, smoke and toxic gas concentrations in the upper zone (the model does not include these values for the lower zone), upper zone layer depth, total flaming area for each material, and total heat release rate versus time. These same quantities, with the exception of total heat release rate, are plotted versus time for Case 2 in Figures 7.19 through 7.22. The significant events concerning flame spread during each run are given in a narrative form in Tables 7.5 and 7.6 respectively. To further aid in visualization of fire spread, Figures 7.23 through 7.33, for Case 1, and 7.34 through 7.42, for Case 2, show the printer graphics produced by the program which display the locations of all flaming, smoldering, and charred elements. Three time points have been selected in each case. The printer results are accompanied by gridded figures (added here for clarity and not produced by the computer program) to aid in the interpretation of each printer graphic.

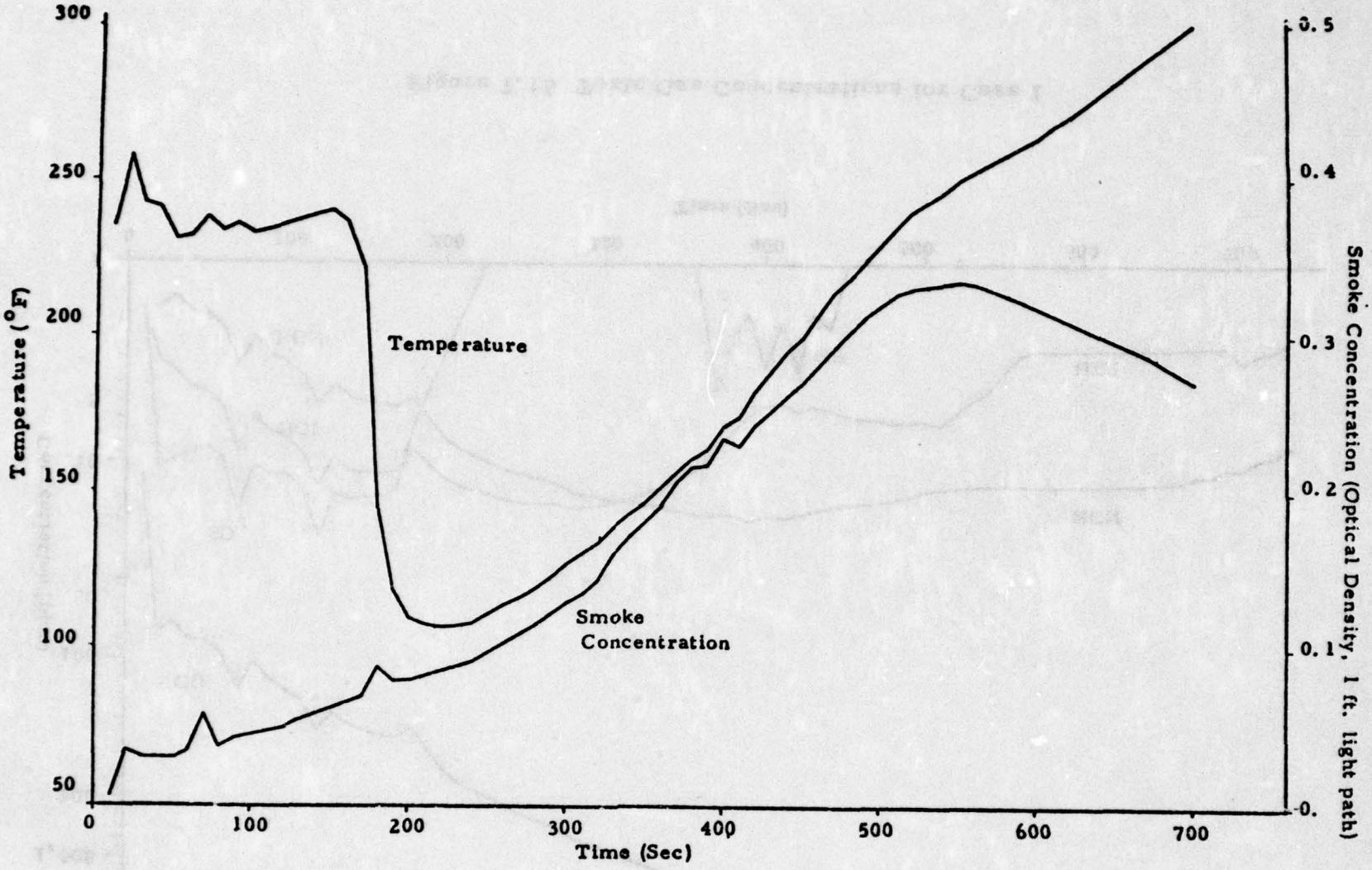

Figure 7.15 Upper Zone Gas Temperature and Smoke Concentration for Case 1

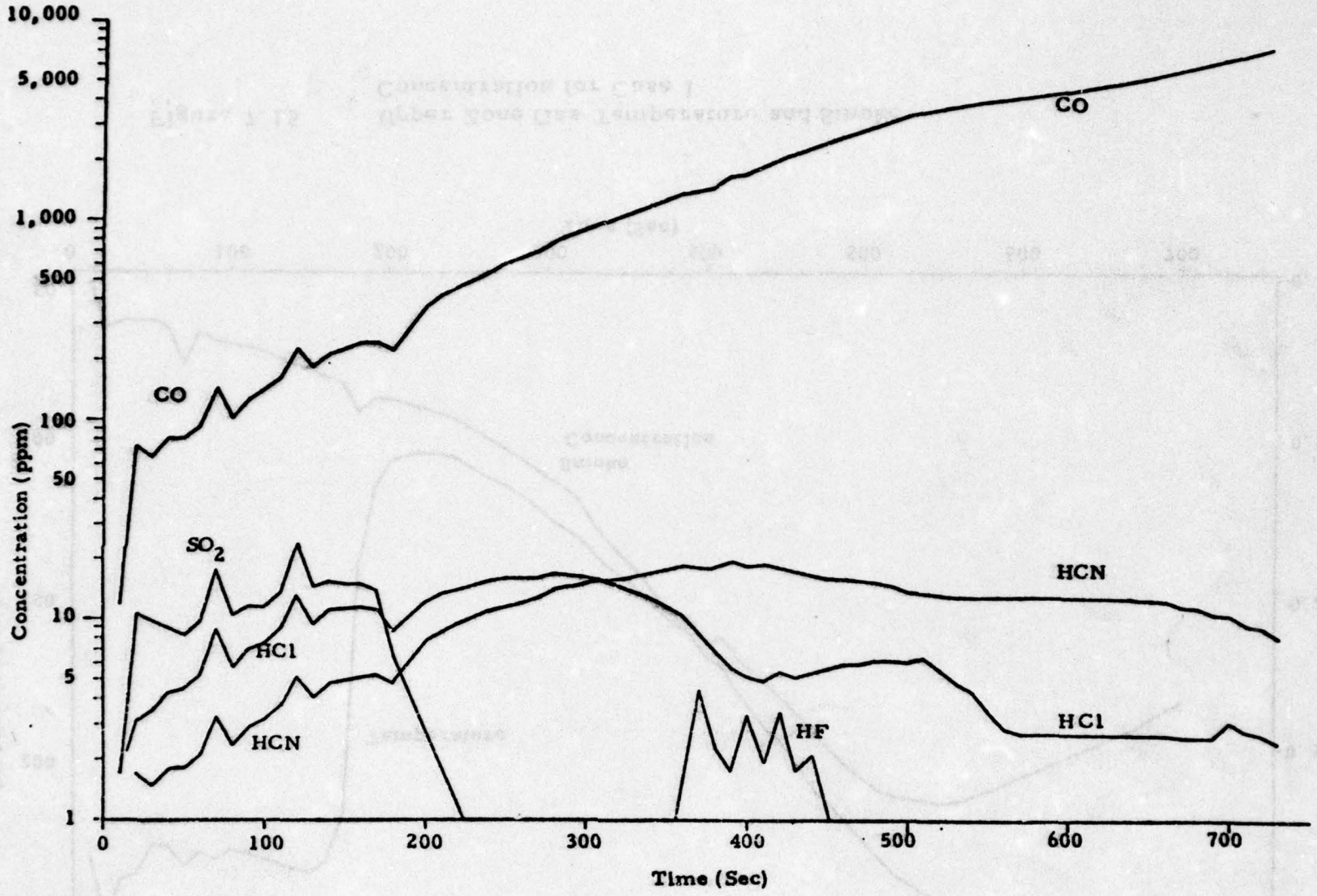

Figure 7.16 Toxic Gas Concentrations for Case 1

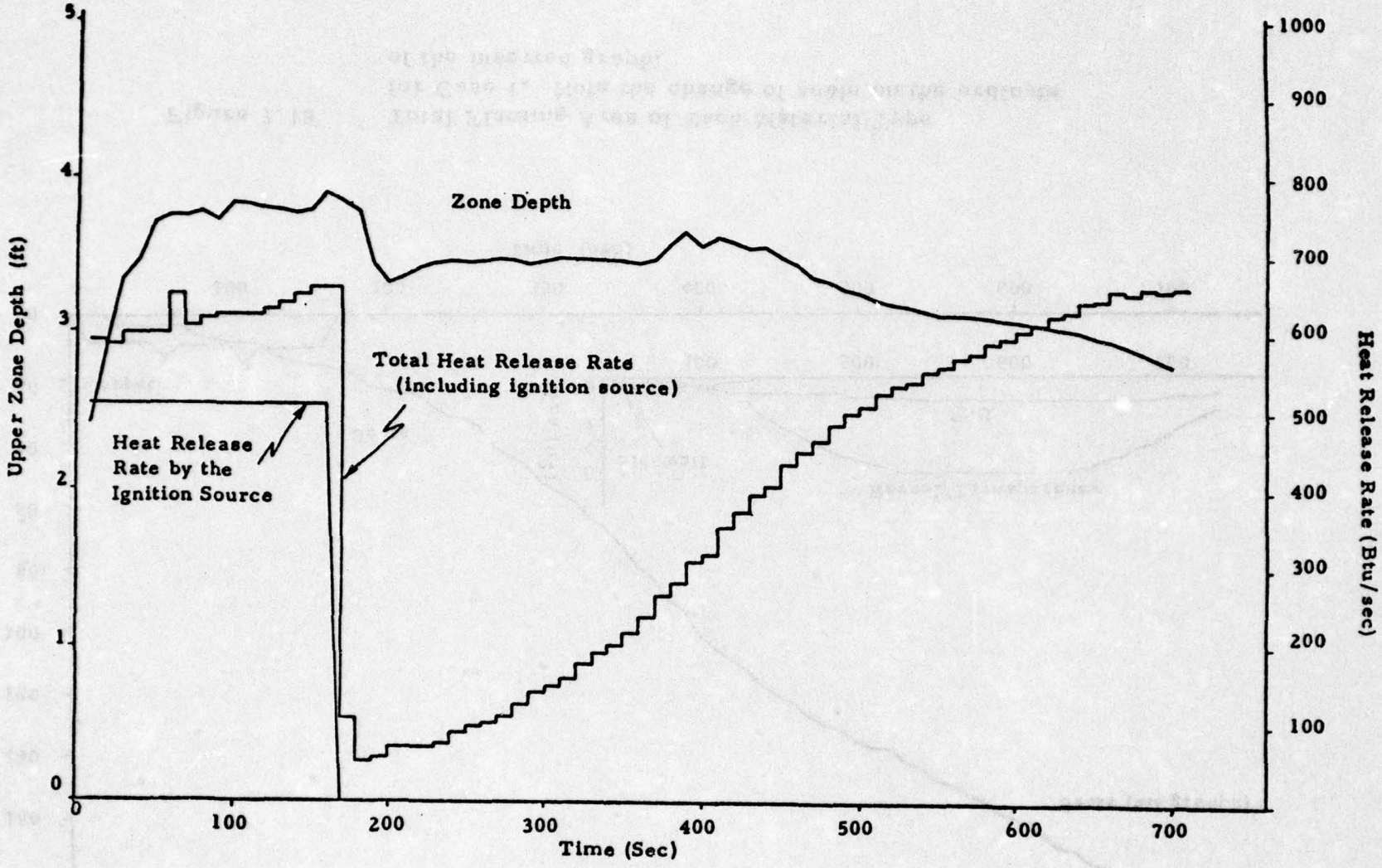

Figure 7.17 Upper Zone Depth and Heat Release Rate for Case 1

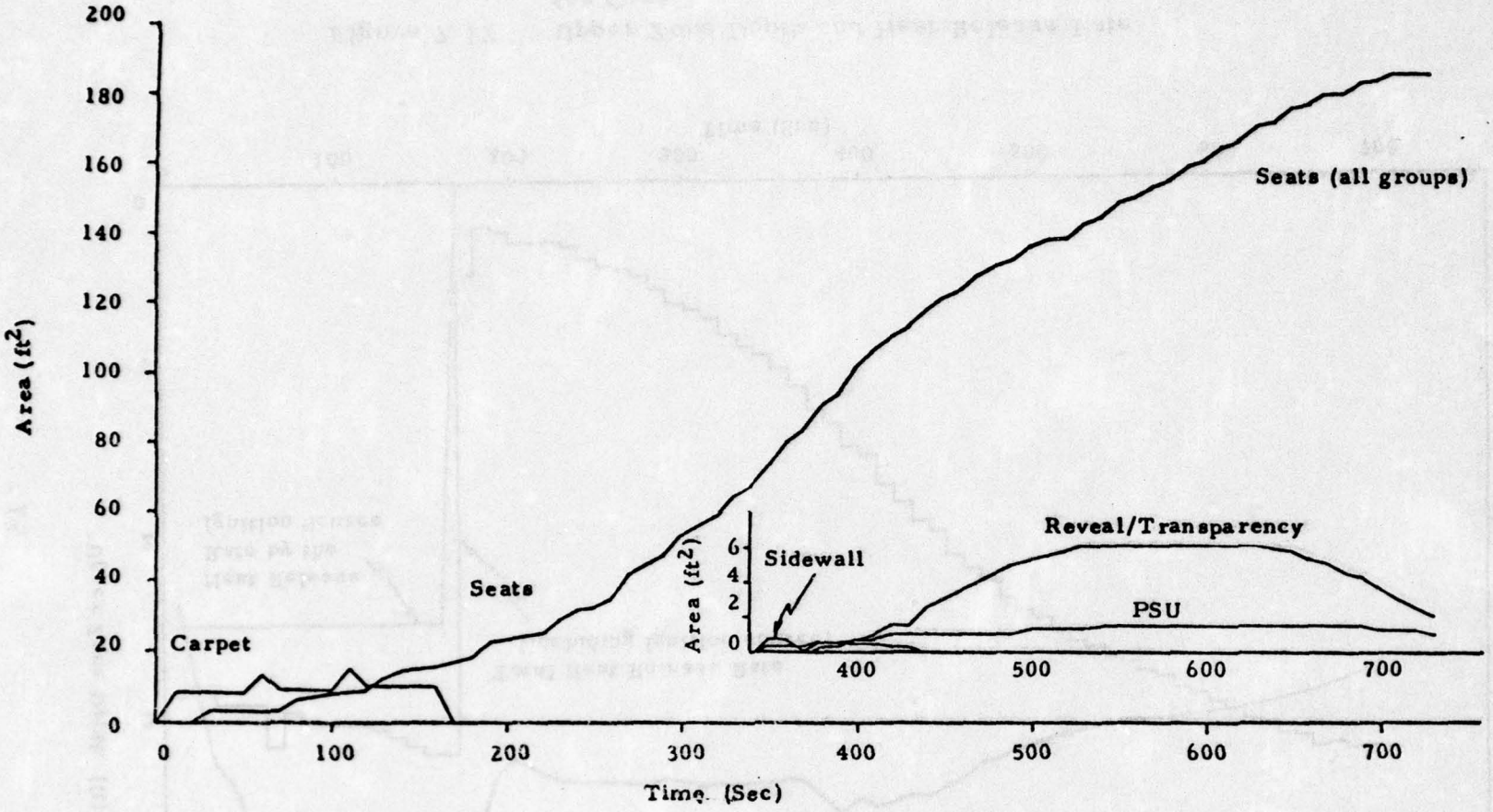

Figure 7.18 Total Flaming Area of Each Material Type for Case 1. Note the change of scale on the ordinate of the inserted graph.

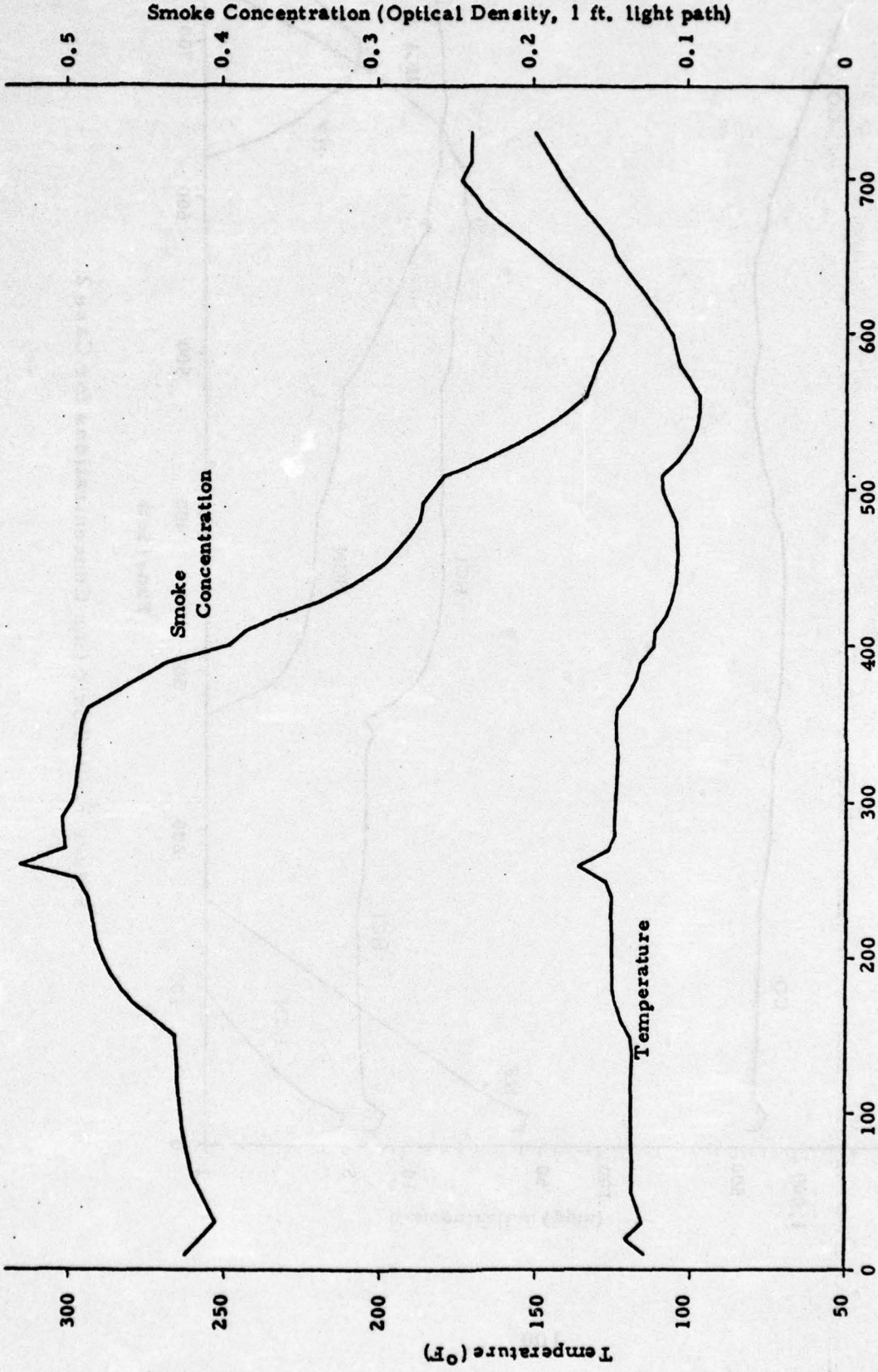

Figure 7.19 Upper Zone Gas Temperature and Smoke Concentration for Case 2

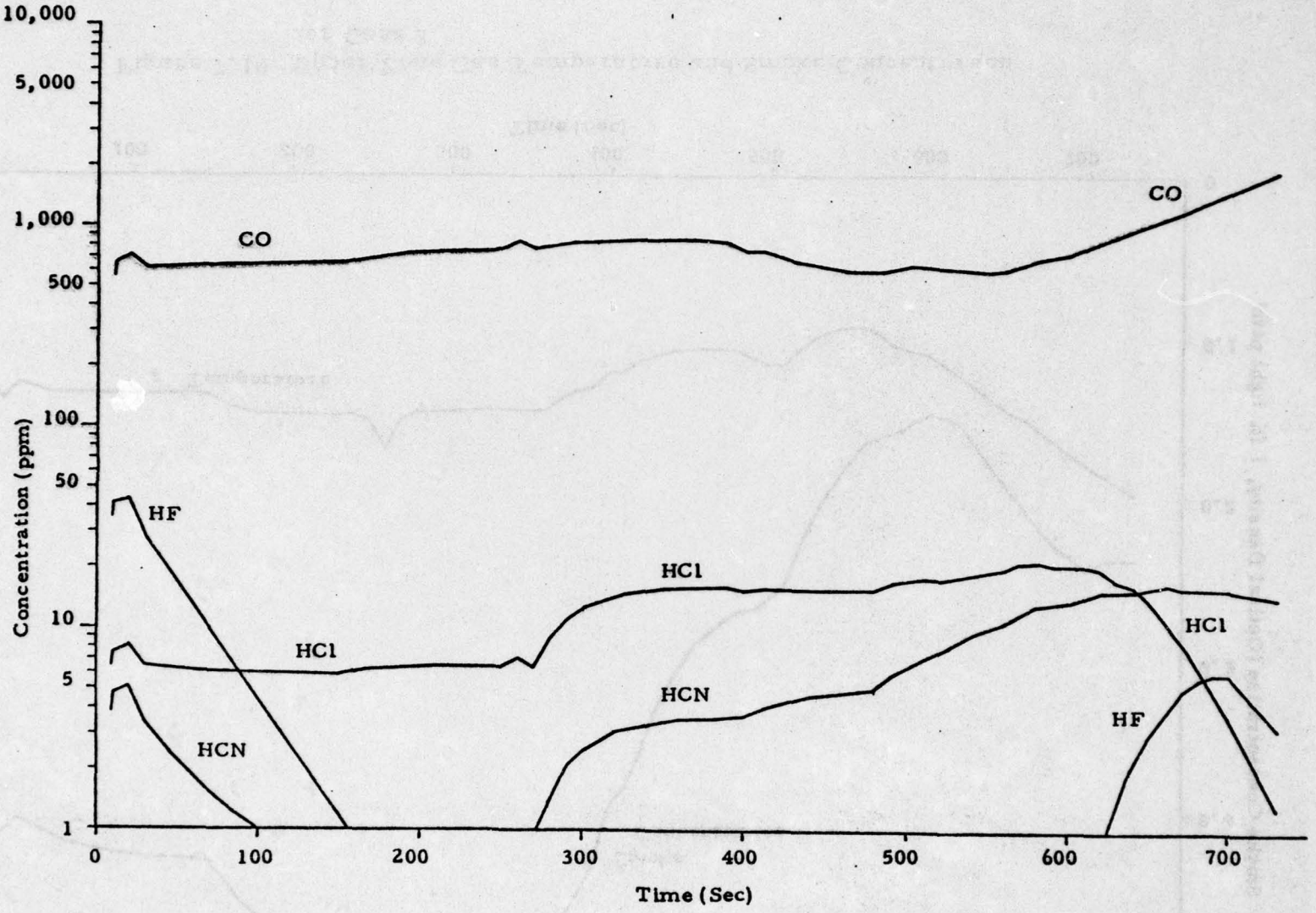

Figure 7.20 Toxic Gas Concentrations for Case 2

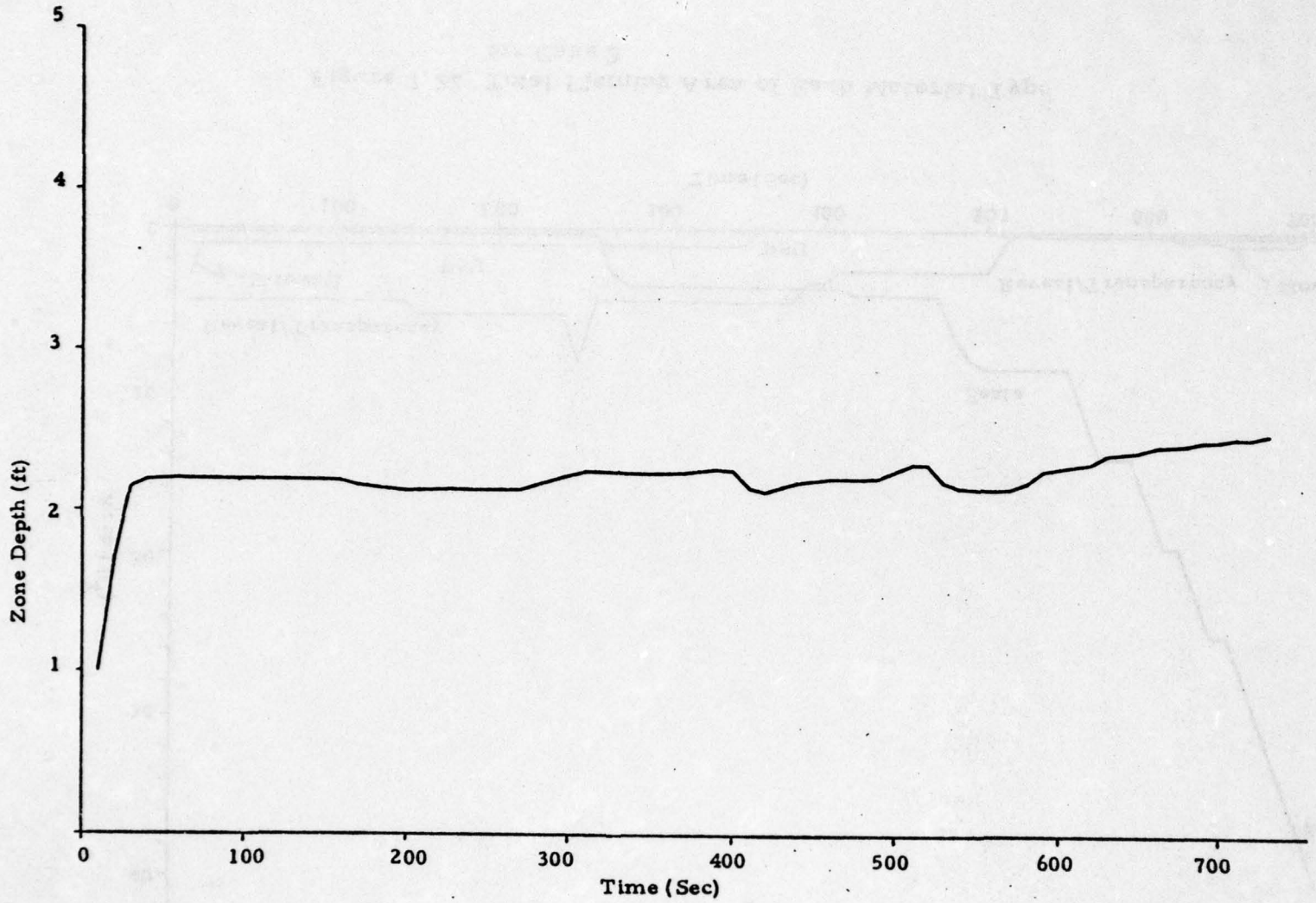

Figure 7.21 Upper Zone Depth for Case 2

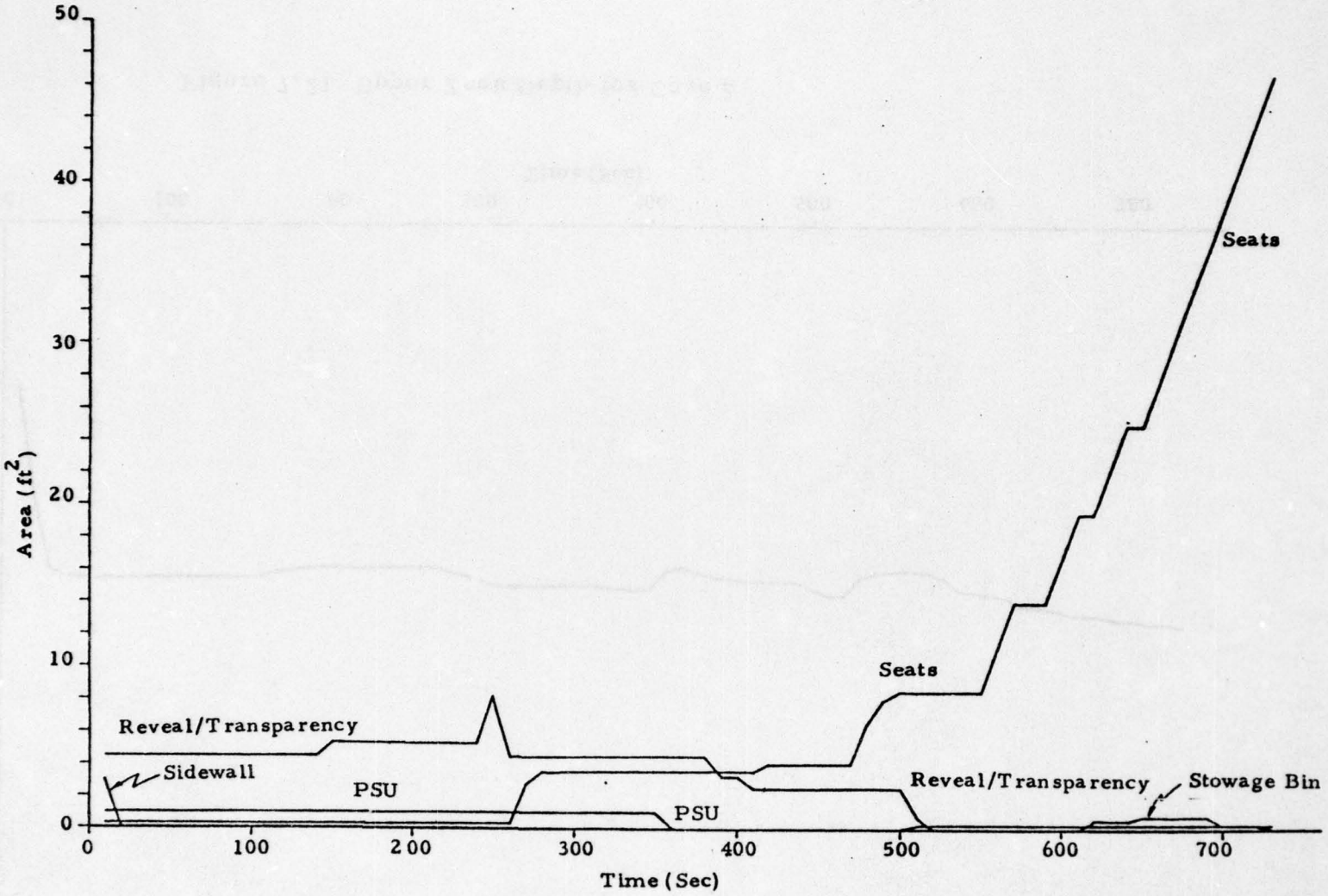

Figure 7.22 Total Flaming Area of Each Material Type for Case 2

TABLE 7.5

NARRATIVE OF SELECTED EVENTS IN CASE 1

Time	Event
0.0 sec	Fire begins with 16 elements on the floor carpet covered by burning fuel.
20.0 sec	Smoldering begins on the cushion bottom of the left seat group in both the first and second rows.
30.0 sec	Elements on the cushion bottom of the left seat group in both the first and second rows have begun flaming.
70.0 sec	Some of the elements on the carpet have become charred.
80.0 sec	Three elements on the cushion bottom of the middle seat group in the second row have begun flaming.
130.0 sec	One element on the cushion bottom of the middle seat group in the first row has begun flaming.
170.0 sec	The fire on the floor has gone out. A total of 76 elements on the floor burned during this time period.
350.0 sec	An element on the left PSU surface has begun flaming. Three elements on the upper edge of the left lower sidewall panel have begun flaming.
380.0 sec	Some elements on the left lower sidewall panel have become charred. One element on the bottom edge of the left window reveal-transparency strip has begun flaming.
440.0 sec	The elements on the left lower sidewall panel which at one time or another were flaming, have become charred.
480.0 sec	All of the elements on the left seat group in the first row are flaming.
520.0 sec	All of the elements on the left seat group in the second row are flaming.
650.0 sec	One element of the left window reveal-transparency strip has become charred.
700.0 sec	One element of the left PSU surface has become charred.
730.0 sec	Some elements on the left seat group in the first and second rows have become charred.

TABLE 7.6

NARRATIVE OF SELECTED EVENTS IN CASE 2

Time	Event
0.0 sec	The fire begins with 12 elements on the lower right sidewall and 18 elements on the right window reveal-transparency strip flaming.
10.0 sec	Four elements on the right PSU have begun flaming. One element on the cusion top of the right seat group in the second row has begun flaming.
20.0 sec	All elements on the lower right sidewall which were flaming have become charred.
260.0 sec	Some elements on the right window reveal-transparency strip have become charred.
360.0 sec	All elements that were flaming on the right PSU have become charred.
510.0 sec	An element on the lower right sidewall has begun flaming.
520.0 sec	All elements on the right window reveal-transparency strip which were flaming have become charred.
620.0 sec	Two elements on the right stowage bin bottom have begun flaming.
700.0 sec	Some elements on the stowage bin bottom have become charred.
720.0 sec	One element on the right seat group in the second row has become charred.

TIME= 100 SEC AFTER IGNITION

DISTRIBUTION OF FLAMING(F),SMOLDERING(S),AND CHARRED(C) ELEMENTS AT END OF FLAME SPREA. CALCULATIONS

FLOOR FIRES

X REAR X

FFFF
FCCCCF
FCFFFFCF
FCFFFFCF
FCFFFFCF
FCFFFFCF
FCCCCF
FFFF

X FRONT X

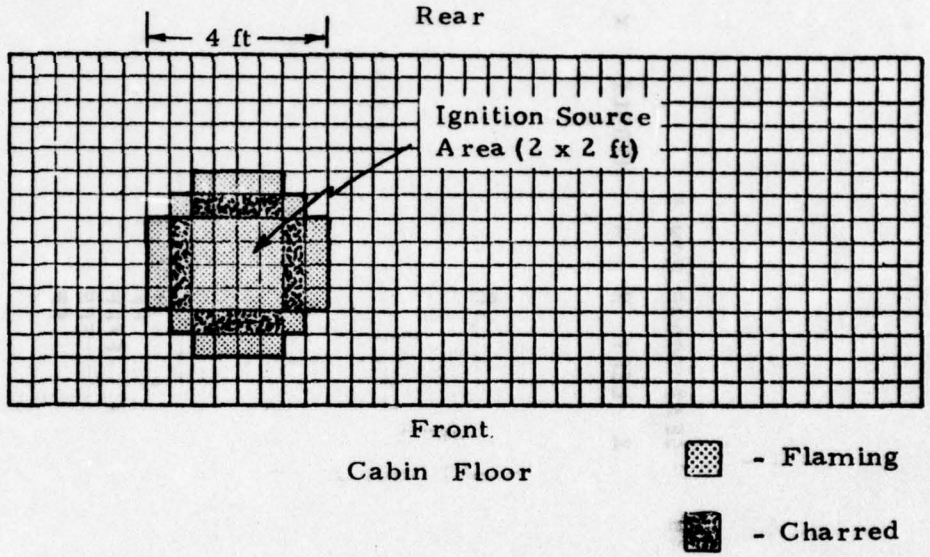

Figure 7.23 Flame Spread on the Cabin Floor at 100 Seconds, Case 1

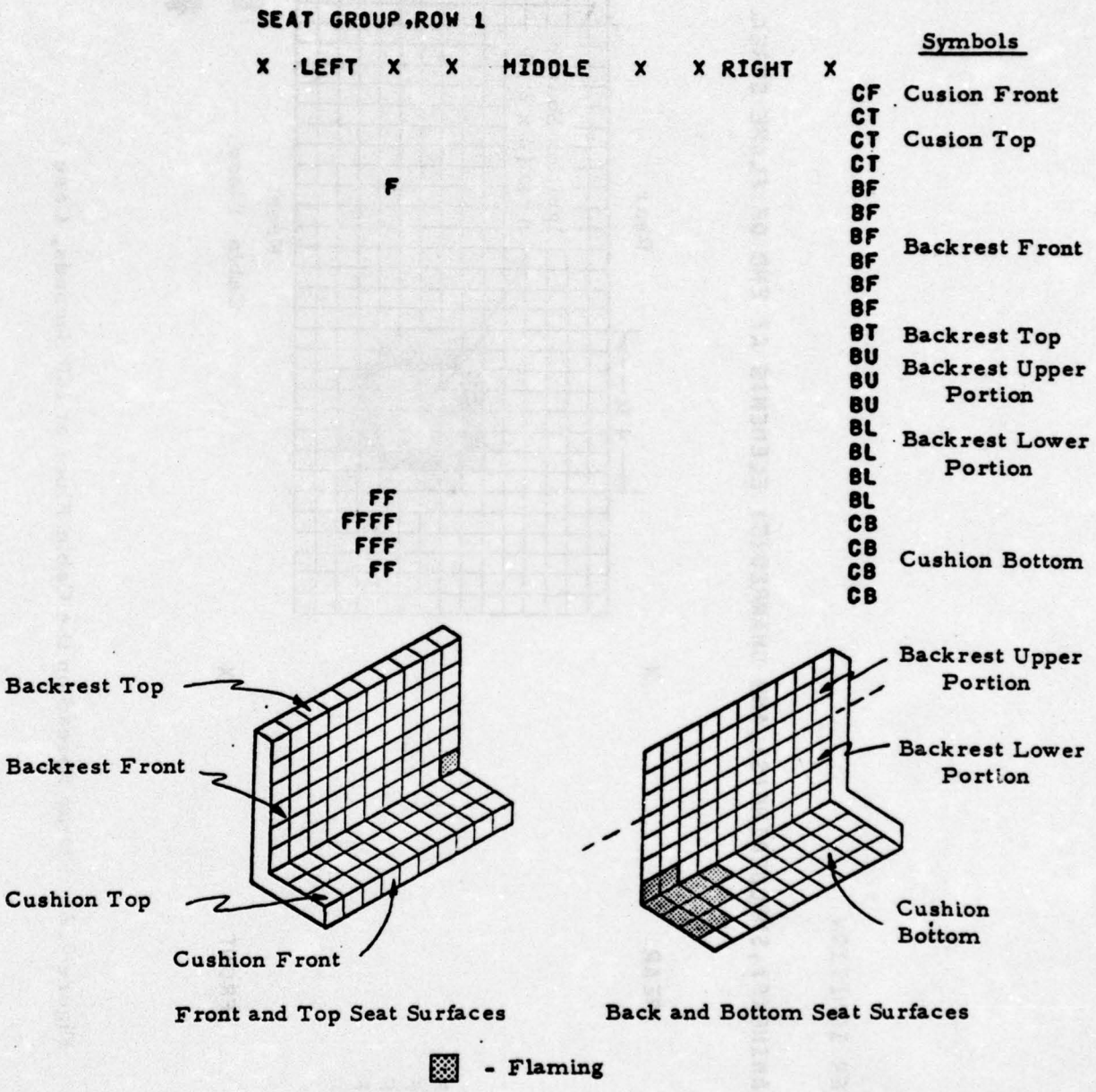

Figure 7.24 Flame Spread on Seat Group 1 at 100 Seconds, Case 1

TIME= 100 SEC AFTER IGNITION

SEAT GROUP,ROW 2

```
X  LEFT  X    X   MIDDLE   X    X RIGHT  X
      FFF                                  CF
        F                                  CT
        F                                  CT
        F                                  CT
                                           BF
                                           BF
                                           BF
                                           BF
                                           BF
                                           BF
                                           BT
                                           BU
                                           BU
                                           BU
                                           BL
                                           BL
                                           BL
                                           BL
       FF                                  CB
      FFF    F                            CB
     FFFF    F                            CB
     FFFF    F                            CB
```

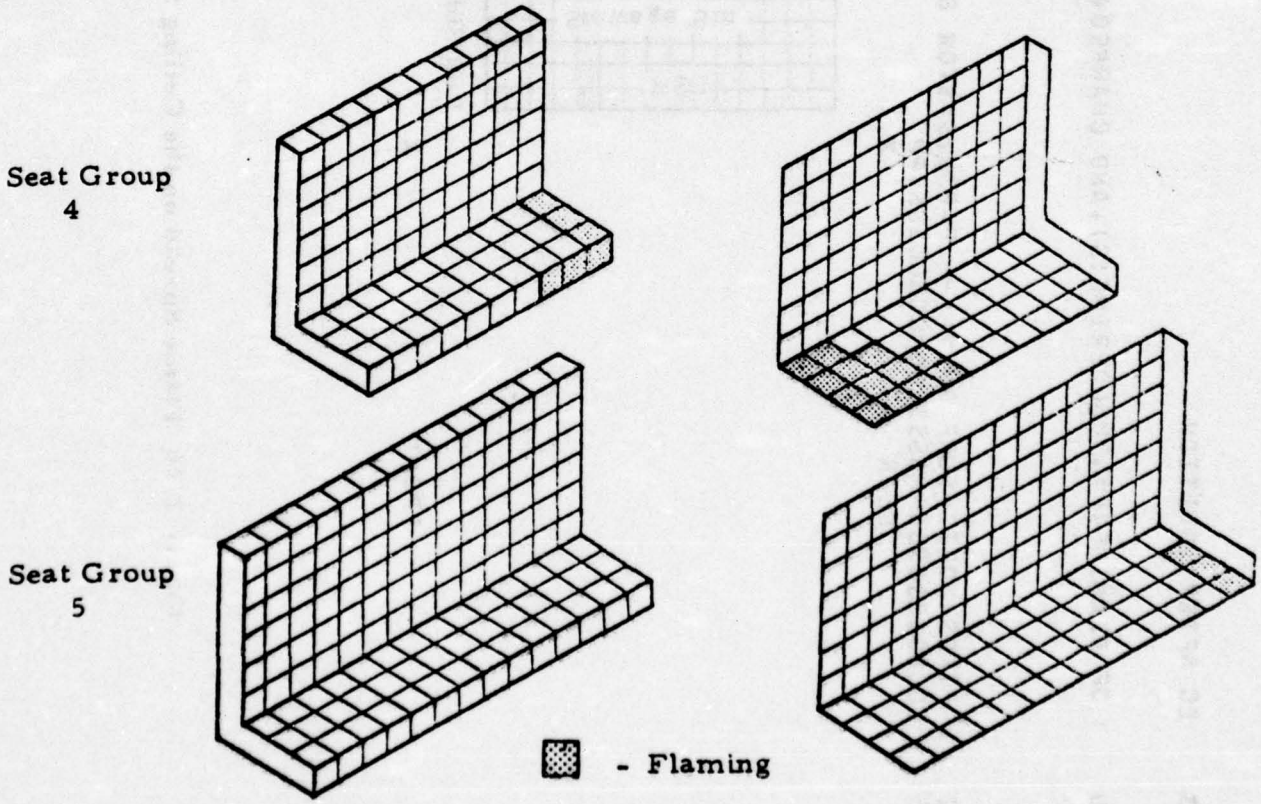

Figure 7.25 Flame Spread on Seat Groups 4 and 5 at 100 Seconds, Case 1

```
TIME=  3     EC AFTER IGNITION

DISTRIBU     OF FLAMING(F),SMOLDERING(S),AND CHARRED(C) ELEMENTS AT END OF FLAME SPREAD CALCULATIONS


     CEI     FIRES(HORIZ SURF ONLY) -- P=PSU,S=STOW BIN,C=CEILING PANEL
     PPS     CCCCCCCCSSSSPPSSSSCCCCCCCCCSSSSPP
     X                    REAR                    X

108


     FF


     X                    FRONT                   X
```

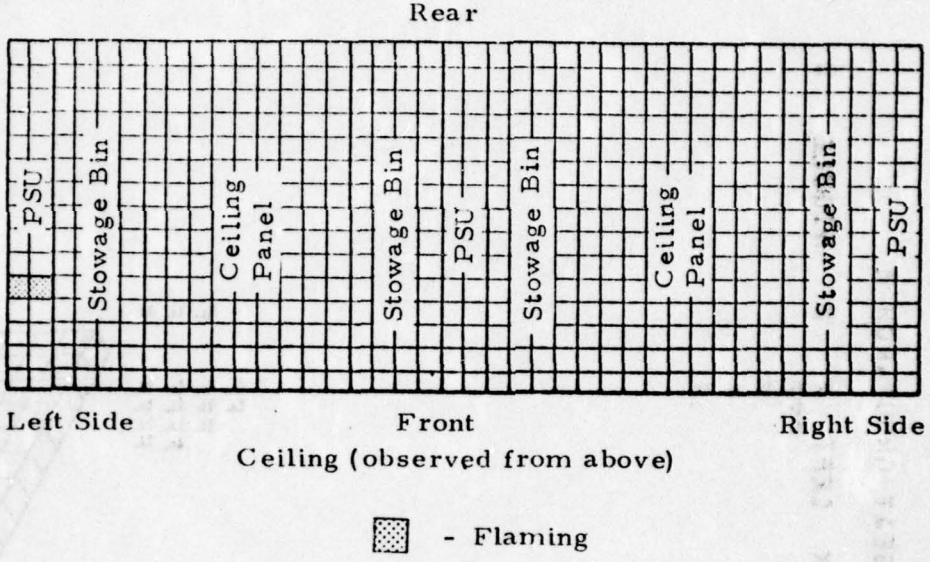

Figure 7.26 Flame Spread on the Ceiling Surfaces at 380 Seconds, Case 1

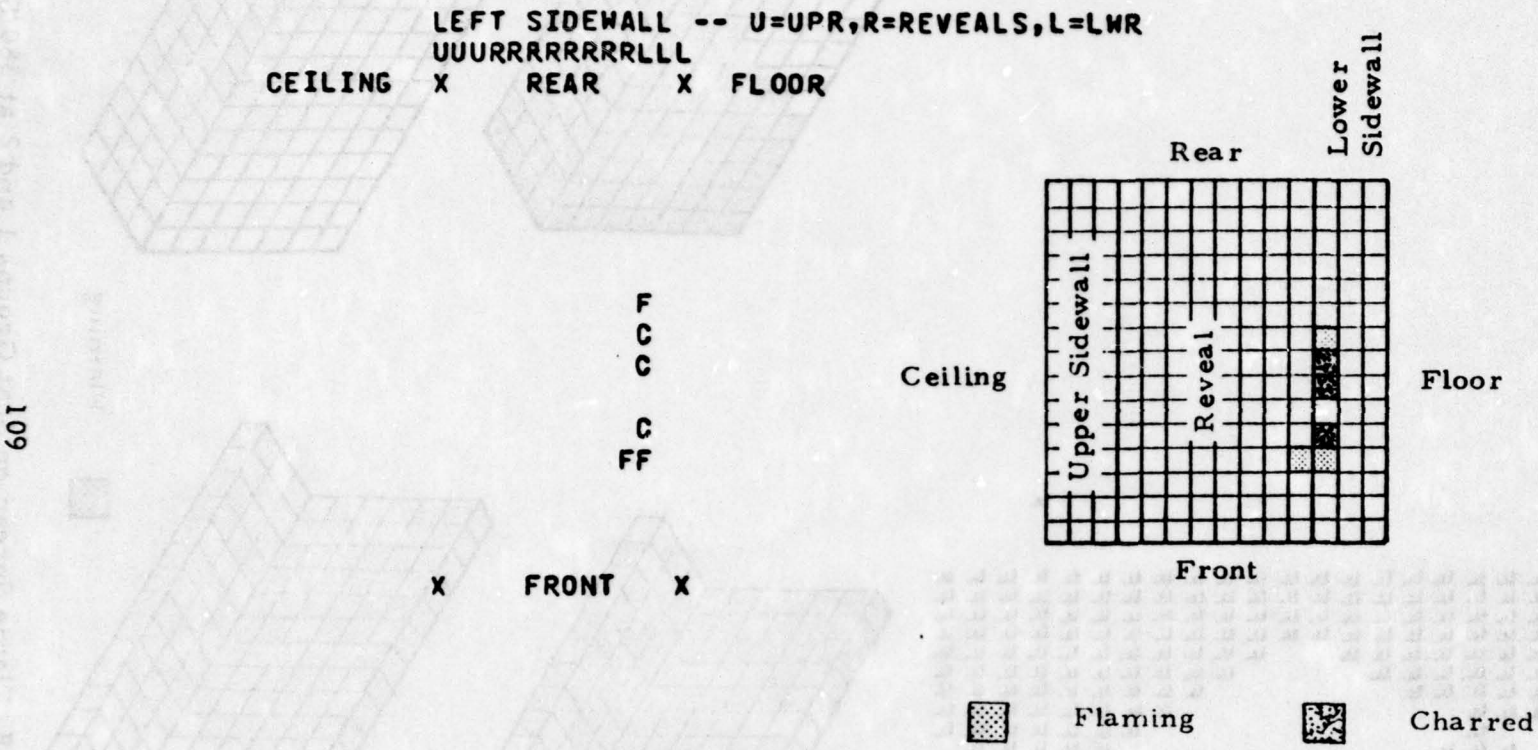

Figure 7.27 Flame Spread on the Left Sidewall at 380 Seconds, Case 1

TIME= 380 SEC AFTER IGNITION

SEAT GROUP,ROW 1

```
X  LEFT  X    X   MIDDLE   X    X RIGHT  X
  FFFFFFFF                                CF
   FFFFFFF                                CT
  FFFFFFFF                                CT
F FFFFFFFF                                CT
FFFFFFFFFF                                BF
F  FFFFFFF                                BF
   FFFFFFF                                BF
    FFFFFF                                BF
     FFFFF                                BF
      FFFF                                BF
      FFFF                                BT
     FFFFF                                BU
    FFFFFF                                BU
   FFFFFFF                                BU
  FFFFFFFF                                BL
 FFFFFFFFF                                BL
FFFFFFFFFF                                BL
FFFFFFFFFF                                BL
FFFFFFFFFF    F                           CB
FFFFFFFFFF                                CB
FFFFFFFFFF                                CB
 FFFFFFFFF                                CB
```

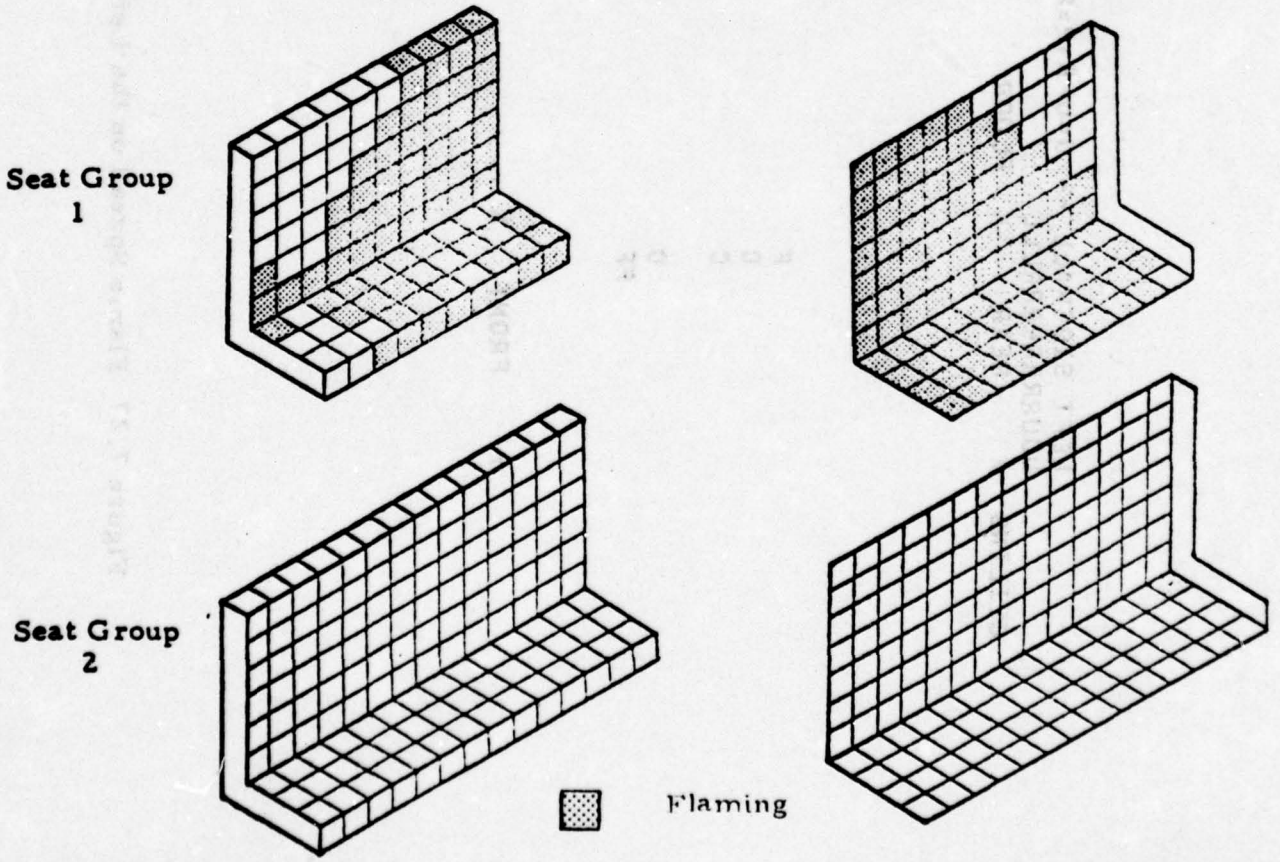

Figure 7.28 Flame Spread on Seat Groups 1 and 2 at 380 Seconds, Case 1

SEAT GROUP,ROW 2

```
X  LEFT  X    X   MIDDLE   X   X RIGHT  X
FFFFFFFFFF    FFF                      CF
FFFFFFFFFF    FFF                      CT
FFFFFFFFFF    FFF                      CT
F FFFFFFFF    FFF                      CT
  FFFFFFFF    FF                       BF
   FFFFFFF    F                        BF
    FFFFFF    F                        BF
     FFFFF                           BF
      FFFF                           BF
       FFF                           BF
        FF                           BT
       FFF                           BU
      FFFF                           BU
     FFFFF                           BU
    FFFFFF                           BL
   FFFFFFF    F                      BL
  FFFFFFFF    F                      BL
 FFFFFFFFF    FF                     BL
FFFFFFFFFF    FFF                    CB
FFFFFFFFFF    FFFF                   CB
FFFFFFFFFF    FFFF                   CB
FFFFFFFFFF    FFFF                   CB
```

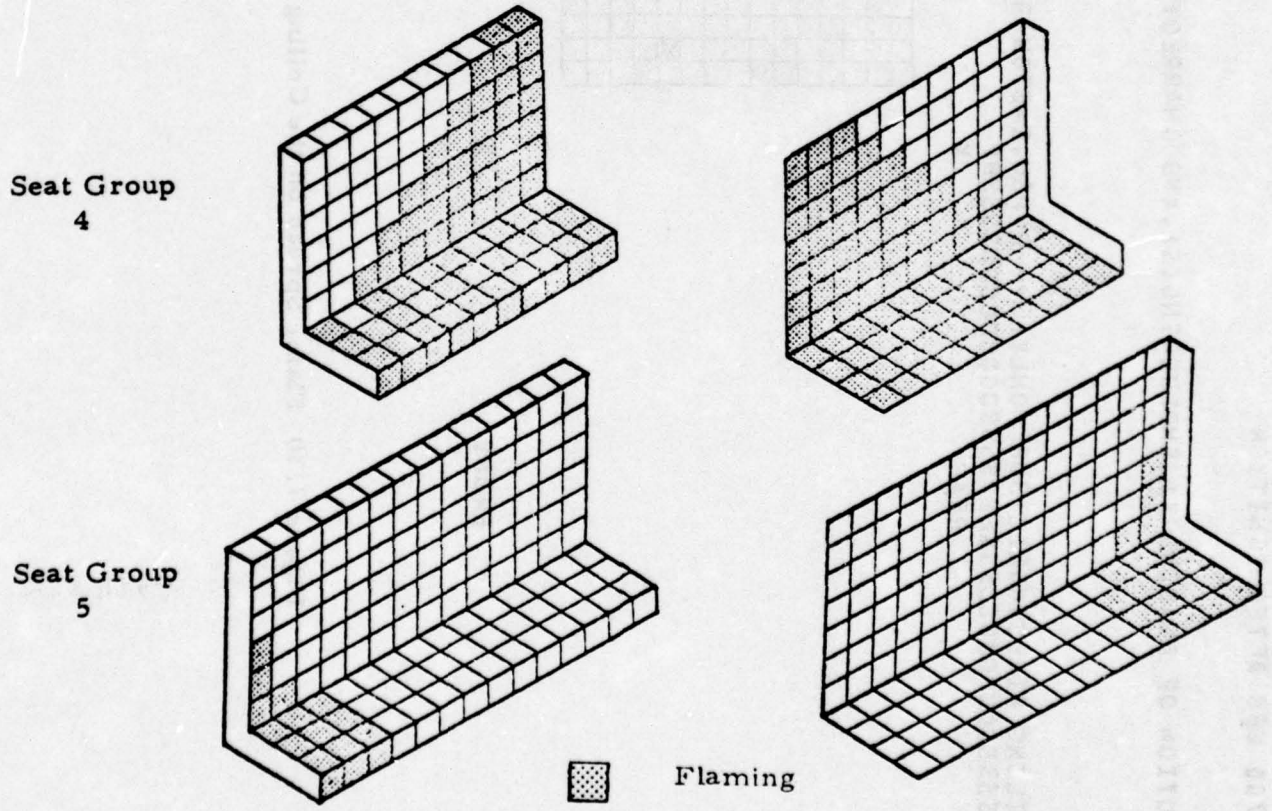

Figure 7.29 Flame Spread on Seat Groups 4 and 5 at 380 Seconds, Case 1

TIME= 700 SEC AFTER IGNITION

DISTRIBUTION OF FLAMING(F),SMOLDERING(S),AND CHARRED(C) ELEMENTS AT END OF FLAME SPREAD CALCULATIONS

CEILING FIRES(HORIZ SURF ONLY) -- P=PSU,S=STOW BIN,C=CEILING PANEL
PPSSSSCCCCCCCCSSSSPPSSSSCCCCCCCCSSSSPP
X REAR X

FF
F

FC
F

X FRONT X

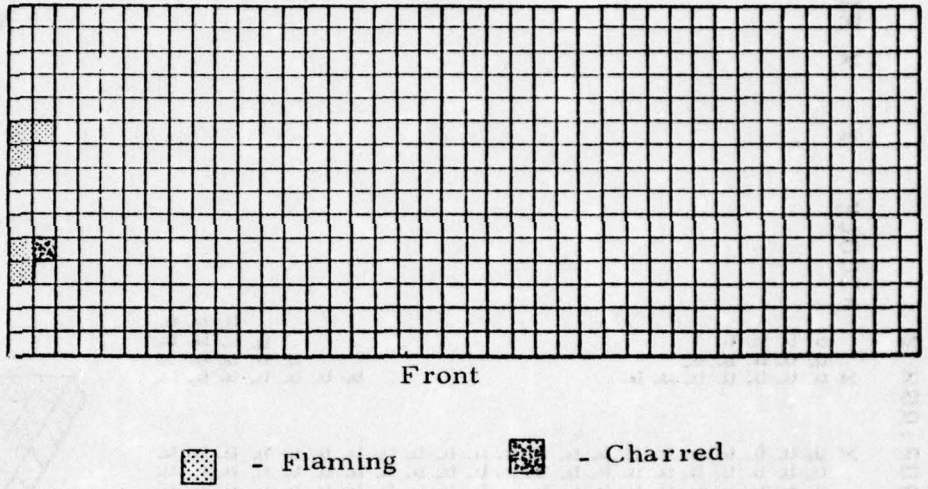

Figure 7.30 Flame Spread on the Ceiling Surfaces at 700 Seconds, Case 1

```
          LEFT SIDEWALL -- U=UPR,R=REVEALS,L=LWR
          UUURRRRRRRRLLL
CEILING   X     REAR     X  FLOOR

                FFFFFCC
                FFFFCCC
                     C
                     C

                FFFCCCC
                FFCCCCC
                     C
                     C

          X     FRONT    X
```

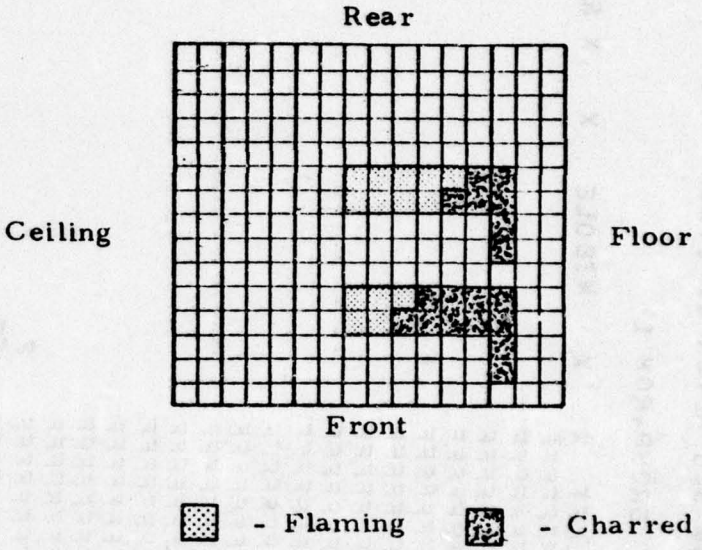

Figure 7.31 Flame Spread on the Left Sidewall at 700 Seconds, Case 1

TIME= 700 SEC AFTER IGNITION

SEAT GROUP,ROW 1

```
X  LEFT  X    X    MIDDLE    X    X RIGHT  X
FFFFFFFFFF                                  CF
FFFFFFFFFF                                  CT
FFFFFFFFFF                                  CT
FFFFFFFFFF                                  CT
FFFFFFFFFF    F                             BF
FFFFFFFFFF                                  BF
FFFFFFFFFF                                  BF
FFFFFFFFFF                                  BF
FFFFFFFFFF                                  BF
FFFFFFFFFF                                  BF
FFFFFFFFFF                                  BT
FFFFFFFFFF                                  BU
FFFFFFFFFF                                  BU
FFFFFFFFFF                                  BU
FFFFFFFFFF                                  BL
FFFFFFFFFF                                  BL
FFFFFFFFFF                                  BL
FFFFFFFFFF    F                             BL
FFFFFFFFFF    FF                            CB
FFFFFFFFFF    F                             CB
FFFFFFFFFF                                  CB
FFFFFFFFFF                                  CB
```

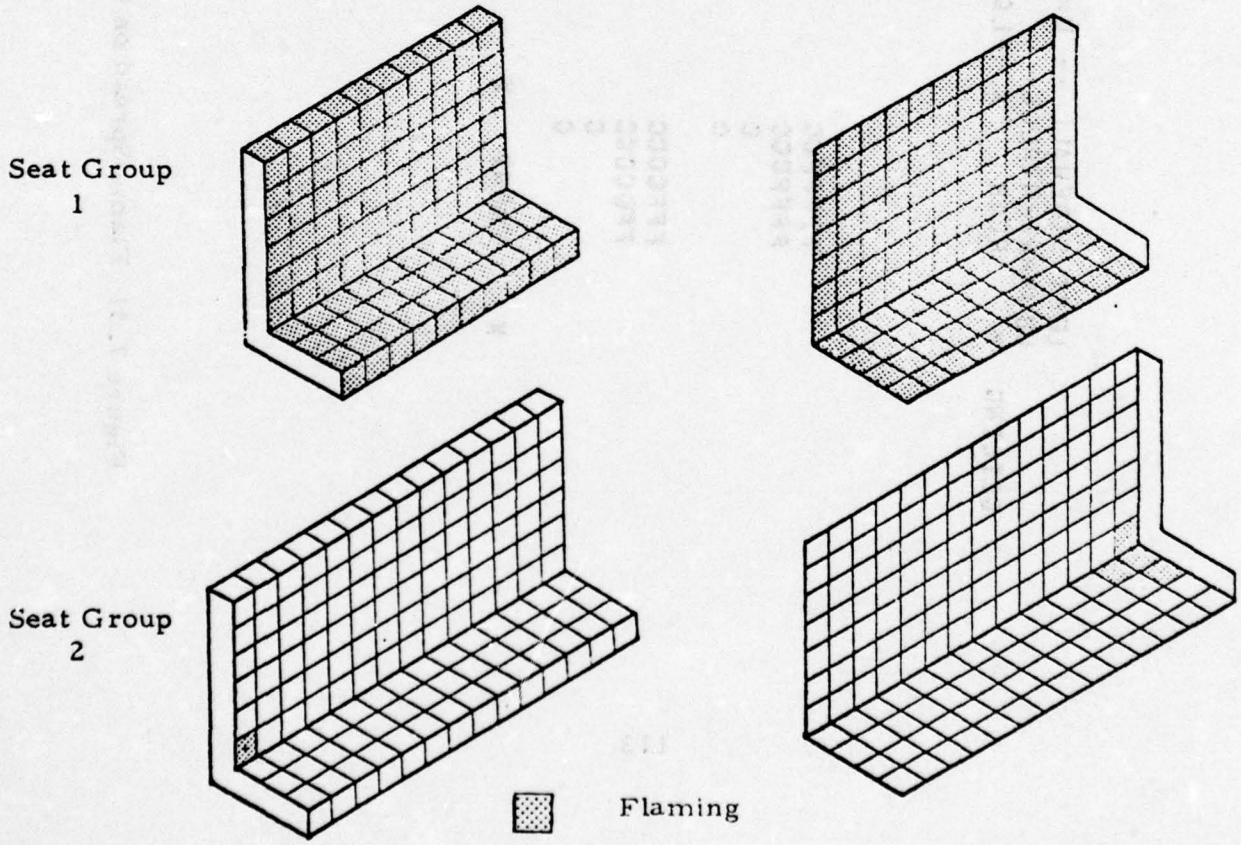

Figure 7.32 Flame Spread on Seat Groups 1 and 2 at 700 Seconds, Case 1

SEAT GROUP,ROW 2

X LEFT X	X MIDDLE X	X RIGHT X	
FFFFFFFFFF	FFFFFFFFFFFFFF		CF
FFFFFFFFFF	FFFFFFFFFFFFFF		CT
FFFFFFFFFF	FFFFFFFFFFFFFF		CT
FFFFFFFFFF	FFFFFFFFFFFFFF		CT
FFFFFFFFFF	FFFFFFFFFFFFFF		BF
FFFFFFFFFF	FFFFFFFFFFFFFF		BF
FFFFFFFFFF	FFFFFFFFFFFFFF		BF
FFFFFFFFFF	FFFFFFFFFFFFF		BF
FFFFFFFFFF	FFFFFFFFFFFF		BF
FFFFFFFFFF	FFFFFFFFFFF		BF
FFFFFFFFFF	FFFFFFFFFFF		BT
FFFFFFFFFF	FFFFFFFFFFF		BU
FFFFFFFFFF	FFFFFFFFFFFF		BU
FFFFFFFFFF	FFFFFFFFFFFFF		BU
FFFFFFFFFF	FFFFFFFFFFFFFF		BL
FFFFFFFFFF	FFFFFFFFFFFFFFF		BL
FFFFFFFFFF	FFFFFFFFFFFFFFF		BL
FFFFFFFFFF	FFFFFFFFFFFFFFF		BL
FFFFFFFFFF	FFFFFFFFFFFFFFF		CB
FFFFFFFFFF	FFFFFFFFFFFFFFF		CB
FFFFFFFFFF	FFFFFFFFFFFFFFF		CB
FFFFFFFFFF	FFFFFFFFFFFFFFF		CB

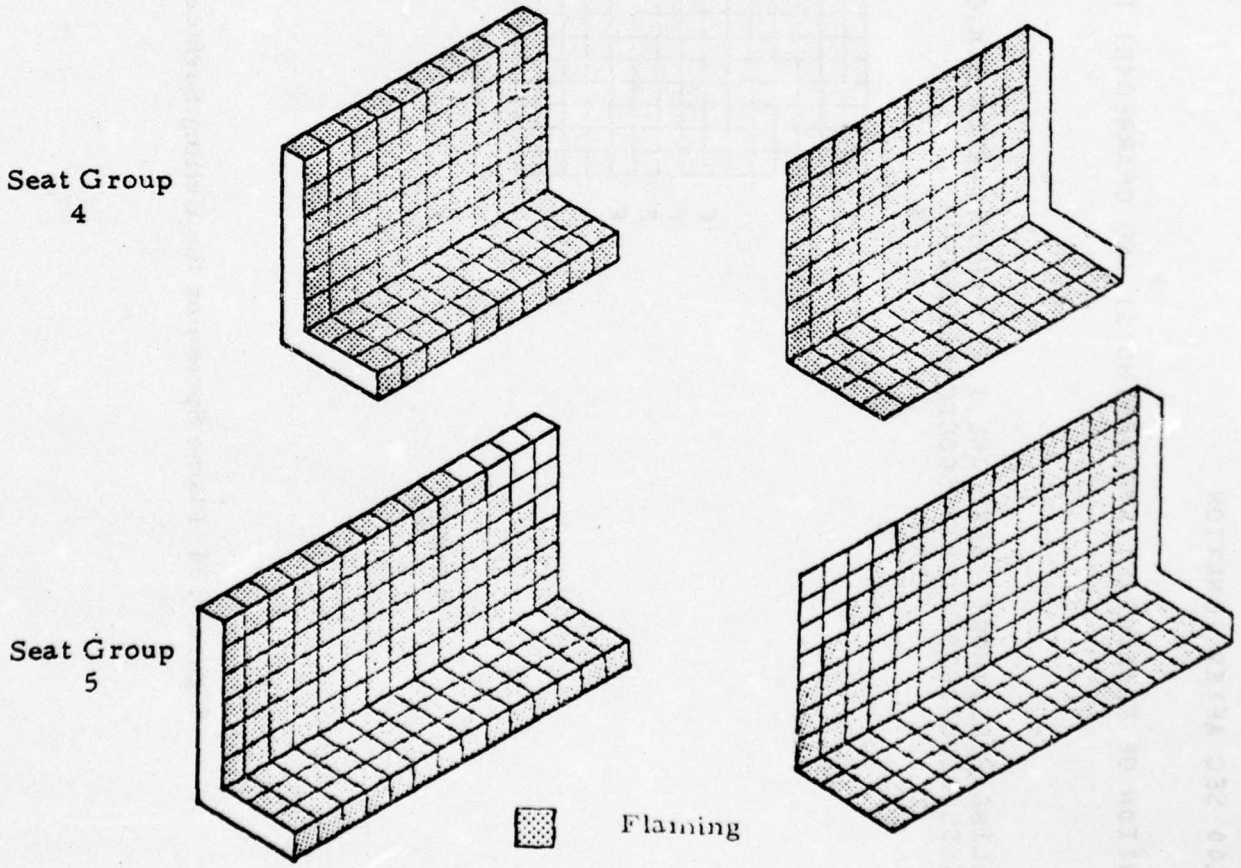

Figure 7.33 Flame Spread on Seat Groups 4 and 5 at 700 Seconds, Case 1

TIME= 100 SEC AFTER IGNITION

DISTRIBUTION OF FLAMING(F),SMOLDERING(S),AND CHARRED(C) ELEMENTS AT END OF FLAME SPREAD CALCULATIONS

CEILING FIRES(HORIZ SURF ONLY) -- P=PSU,S=STOW BIN,C=CEILING PANEL
PPSSSSCCCCCCCCSSSSPPSSSSCCCCCCCCSSSSPP
X REAR X

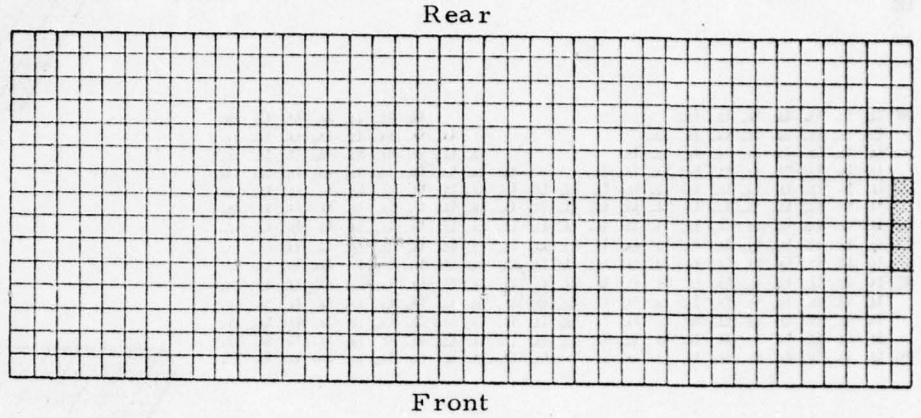

X FRONT X

Ceiling (observed from above)

Flaming

Figure 7.34 Flame Spread on the Ceiling Surfaces at 100 Seconds, Case 2

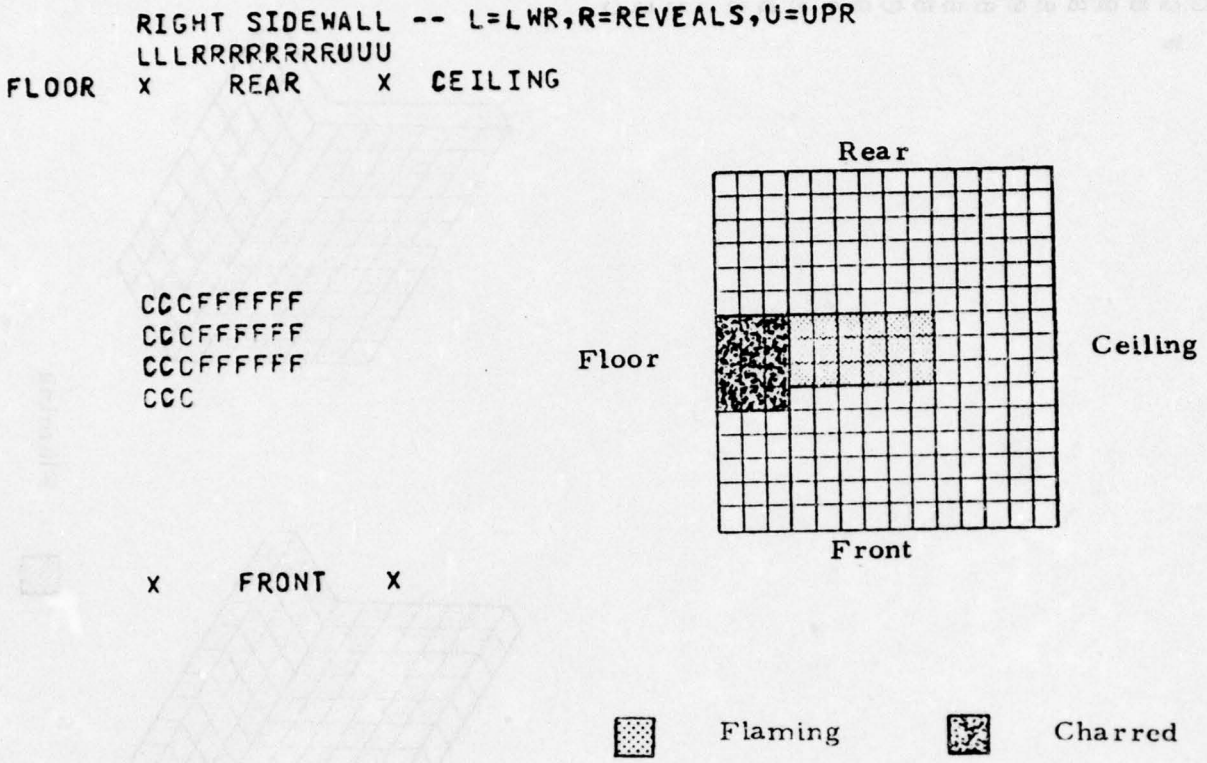

Figure 7.35 Flame Spread on the Right Sidewall at 100 Seconds, Case 2

TIME= 100 SEC AFTER IGNITION

SEAT GROUP,ROW 2

X LEFT X X MIDDLE X X RIGHT X

CF
CT
CT
F CT
BF
BF
BF
BF
BF
BF
BT
BU
BU
BU
BL
BL
BL
BL
CB
CB
CB
CB

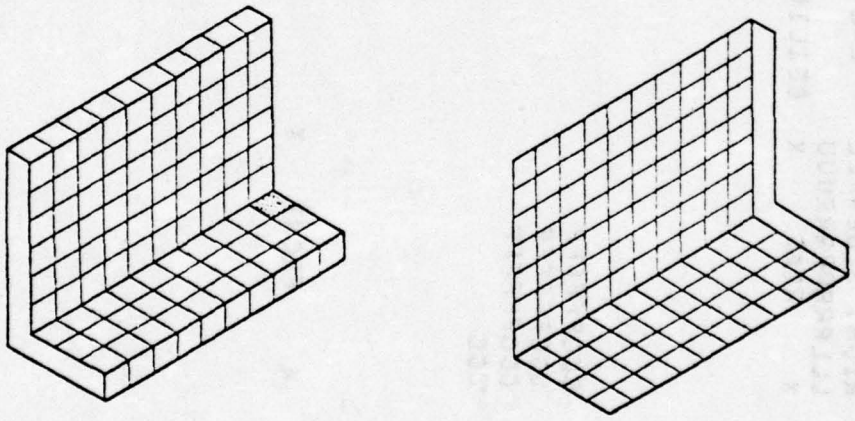

Flaming

Figure 7.36 Flame Spread on Seat Group 6 at 100 Seconds, Case 2

TIME= 350 SEC AFTER IGNITION

DISTRIBUTION OF FLAMING(F),SMOLDERING(S),AND CHARRED(C) ELEMENTS AT END OF FLAME SPREAD CALCULATIONS

CEILING FIRES(HORIZ SURF ONLY) -- P=PSU,S=STOW BIN,C=CEILING PANEL
PPSSSSCCCCCCCCCSSSSPPSSSSCCCCCCCCCSSSSPP
X REAR X

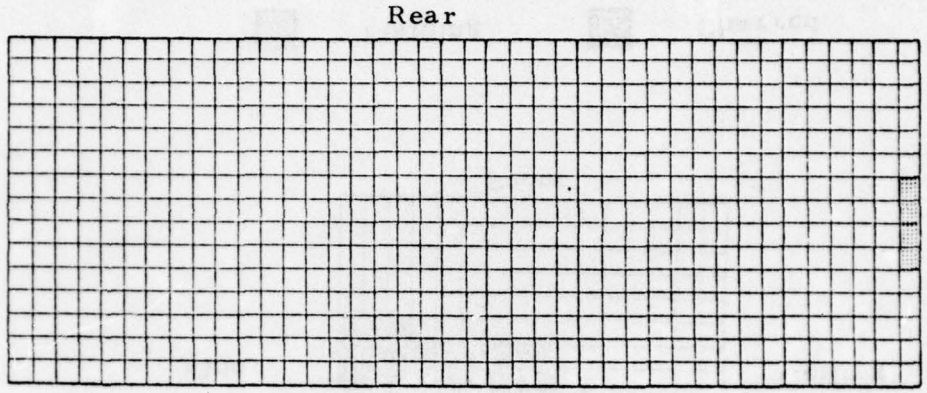

X FRONT X

Ceiling (observed from above)

Flaming

Figure 7.37 Flame Spread on the Ceiling Surfaces at 350 Seconds, Case 2

```
          RIGHT SIDEWALL -- L=LWR,R=REVEALS,U=UPR
          LLLRRRRRRRRUUU
FLOOR     X     REAR     X  CEILING
```

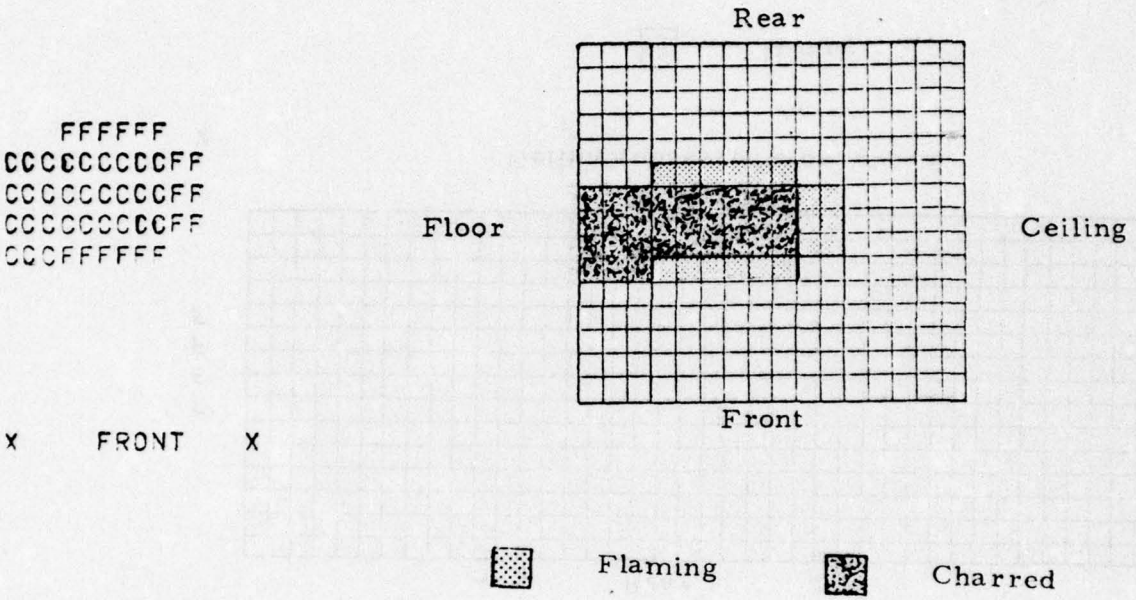

Figure 7.38 Flame Spread on the Right Sidewall at 350 Seconds, Case 2

TIME= 350 SEC AFTER IGNITION

SEAT GROUP,ROW 2

X LEFT X X MIDDLE X X RIGHT X

```
   CF
   CT
 F CT
FF CT
 F BF
 F BF
 F BF
 F BF
 F BF
   BF
   BT
   BU
 F BU
 F BU
 F BL
 F BL
 F BL
   BL
   CB
 F CB
   CB
   CB
```

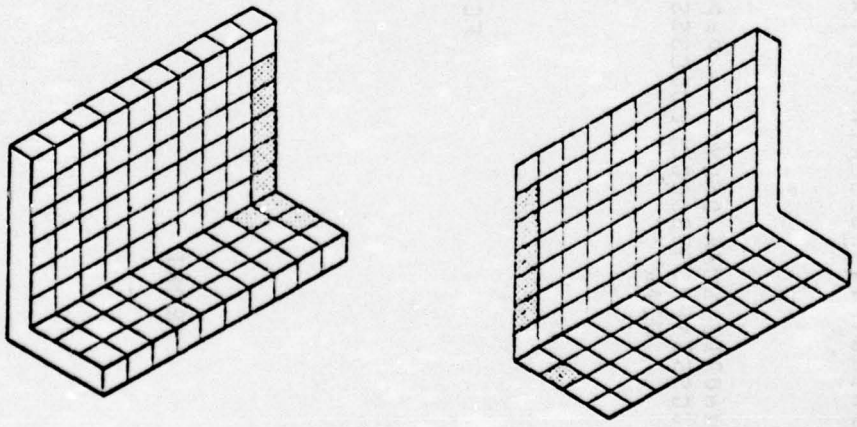

Flaming

Figure 7.39 Flame Spread on Seat Group 6 at 350 Seconds, Case 2

TIME= 720 SEC AFTER IGNITION

DISTRIBUTION OF FLAMING(F),SMOLDERING(S),AND CHARRED(C) ELEMENTS AT END OF FLAME SPREAD CALCULATIONS

CEILING FIRES(HORIZ SURF ONLY) -- P=PSU,S=STOW BIN,C=CEILING PANEL
PPSSSSCCCCCCCCCSSSSPPSSSSCCCCCCCCCSSSSPP
X REAR X

122

FCC
C
C
C
C

X FRONT X

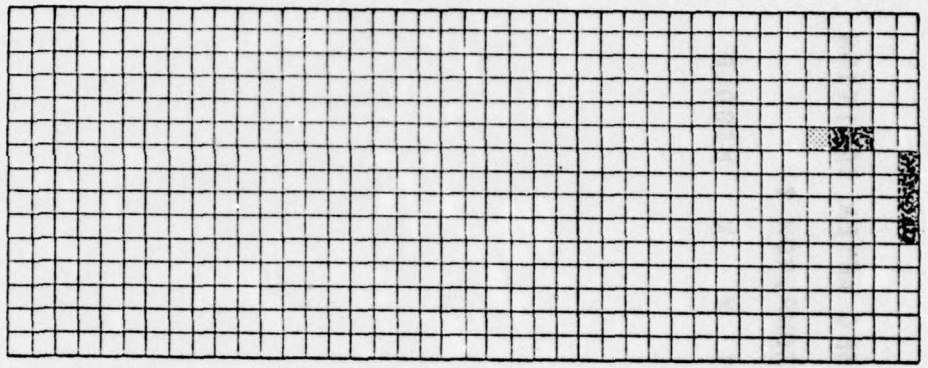

Ceiling (observed from above)

Flaming Charred

Figure 7.40 Flame Spread on the Ceiling Surfaces at 720 Seconds, Case 2

RIGHT SIDEWALL -- L=LWR,R=REVEALS,U=UPR
LLLRRRRRRRRUUU
FLOOR X REAR X CEILING

FCCCCCC
CCCCCCCCCCC
CCCCCCCCCCC
CCCCCCCCCCC
CCCCCCCCC

X FRONT X

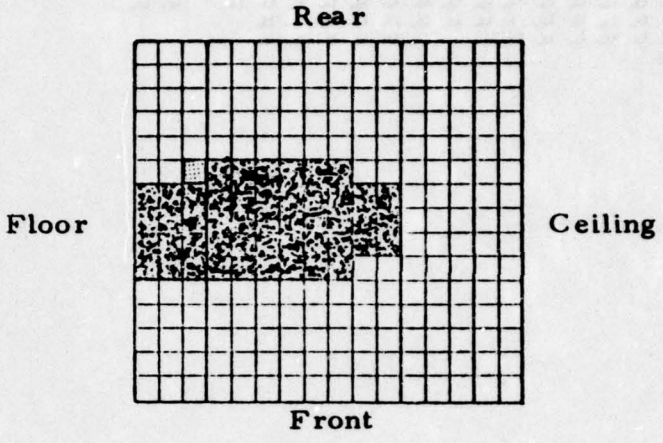

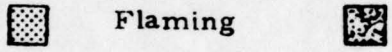

Figure 7.41 Flame Spread on the Right Sidewall at 720 Seconds, Case 2

TIME= 720 SEC AFTER IGNITION

SEAT GROUP,ROW 2

X LEFT X X MIDDLE X X RIGHT X

FFFFFF CF
SFFFFFFF CT
SFFFFFFFF CT
SFFFFFFFC CT
FFFFFFFFF BF
FFFFFFFFF BF
FFFFFFFFF BF
FFFFFFFFF BF
FFFFFFFFF BF
FFFFFFFF BF
FFFFFFFF BT
FFFFFFFF BU
FFFFFFFFF BU
FFFFFFFFF BU
FFFFFFFFF BL
FFFFFFFFF BL
FFFFFFFFF BL
FFFFFFF BL
FFFFFF CB
FFFFFFF CB
FFFFFFF CB
FFFFFF CB

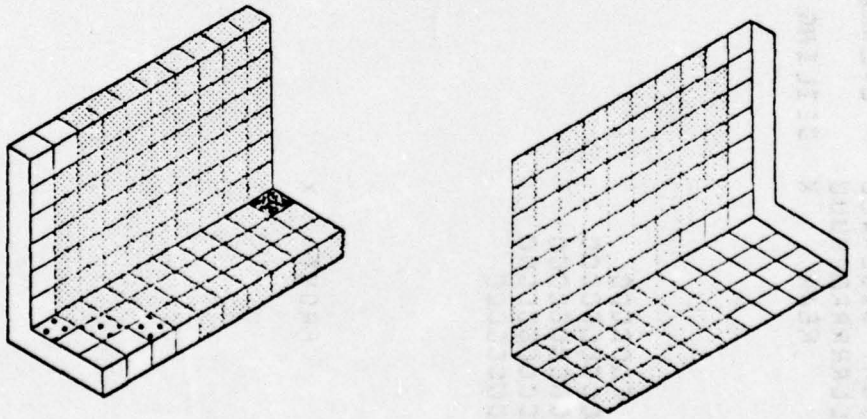

▨ - Flaming ▨ - Smoldering ▨ - Charred

Figure 7.42 Flame Spread on Seat Group 6 at 720 Seconds, Case 2

7.3 ANALYSIS OF RESULTS

Without specific mock-up tests results or data from actual cabin fire instances with which to compare the results of each simulation, few conclusive statements about the validity of the simulation can be made. Some general comments can be made however about the predicted fire behavior in each case. Such comments are made in the following paragraphs which briefly analyze each simulation case. Readers of this section are cautioned that while the simulation results shown are, (1) based on what the authors believe to be realistic fire scenarios, and (2) employ data taken on actual wide-body cabin interior materials, the DACFIR Model's validity is not as yet proven. Further, while the data collected on cabin materials for this program forms a valuable set of new flammability information on these materials, the data set is incomplete. To provide complete input for these sample cases some data items were extrapolated or inferred from other values in the data set where necessary. Specific judgements about wide-body cabin fire safety should therefore not be made from these results.

7.3.1 Analysis of Case 1, Floor Spill Ignition

Involvement of the cabin materials in Case 1 begins with the burning of the carpet material covered by the spilled liquid fuel. Since the fuel was described in the program input to have no smoke or toxic gas emissions of its own, the accumulation of smoke and toxic gases throughout the run is due totally to the cabin materials. Burning of the carpet can be seen from the heat release rate curve in Figure 7.17 during the 170 seconds that the ignition fire exists. During this period the ignition source material contributes the majority of the heat release, about 500 Btu/sec as shown. The first involvement of additional material appears at 10 seconds with the ignition of 16 elements on the floor adjacent to the liquid fuel fire. This spread is so quick that it is probably best interpreted as a "flame-over", a nearly simultaneous fire involvement over an area of the adjacent material. This rapid

propagation is due to the high radiation (about 5 Btu/(ft^2 · sec) from the ignition fire to the elements at its edge. Further involvement of the carpet occurs at 60 seconds when 20 additional elements ignite. By 70 seconds, however, the 16 elements ignited at 10 seconds burn out (see Figure 7.15). This phenomenon occurs again when a new ring of elements ignites at 110 seconds and the ring which started at 70 seconds burns out by 120 seconds. The development of the carpet fire follows this pattern of a ring of burning elements moving away from the ignition source fire at a decreasing rate due to decreasing radiation levels. When the ignition fire ended at 170 seconds, the remaining carpet fire has also burned out. The elements ignited at 110 seconds have been consumed and the radiation level at other floor elements is no longer sufficient for propagation to take place.

Burning of the seats in Case 1 starts at 20 seconds with seven smoldering elements on the seat cushion bottoms in Rows 1 and 2 (Seat Groups 1 and 4, the left groups in each row). These elements are set to this state by being in or near the ignition source fire. By 30 seconds these seven and six additional elements are flaming. From this point the fire quickly grows on both seat groups as shown at 100, 380, and 700 seconds in Figures 7.24, 7.25, 7.28, 7.29, 7.32, and 7.33. The thickness of the foam pad of the seats causes the elements on the seats to have a long burn time, about 720 seconds. Large fires therefore result as the flames move over the seat surfaces both up the backrests and around the front and sides of the seat cushions to the cushion tops. The middle seats in each row become ignited at 130 seconds by contact with the carpet fire which has grown by that time to a position beneath these seats.

When the fire on Seat Group 7 reaches the left sidewall at 350 seconds, some of the sidewall ignites and one element of the left PSU surface above the new sidewall fire ignites also. A short time later, 380 seconds, some of the sidewall elements have burned out; their burn times (t_{fc}) being rather short, especially for high heat flux levels. At 380 seconds the sidewall fire also involves an element of the window reveal-transparency strip. The development of the sidewall fires beyond this time is not dramatic

since the burn times for these materials are short and the flame spread rates fairly low. As a consequence, little of this material is flaming at any one time. On the PSU surface, only one additional element has ignited by 380 seconds, Figure 7.26, while at 700 seconds a total of five are burning and one is charred, Figure 7.30.

The behavior of the cabin atmosphere in Case 1 shows the influence of the changes in the burning areas of the various materials as the simulation progresses. In Figure 7.15 the upper zone gas temperature rises quickly to about 250 ^{o}F at the ignition. This value remains fairly constant until the ignition source goes out at 170 seconds, where it drops precipitously to about 100 degrees in several seconds. This is a reflection of the much reduced rate of heat production after the ignition source fires die as seen in Figure 7.17. The rate of heat release and consequently the gas temperature start to advance upward as the seat fires grow, especially after 200 seconds. At the end of the run the gas temperature has risen to above 300 degrees. The smoke concentration during the run, also shown in Figure 7.15, rises fairly constantly from the start to about 500 seconds where the concentration in optical density units is about 0.3. Lopez [22] has conducted studies of the effect of smoke on visibility in a wide-body cabin mock-up and found that "reasonably good visual acuity" is lost above optical densities of 0.1 (Lopez's smoke concentrations are stated in terms of optical density over a three-foot path so that, stated in his terms, the criterion is 0.3, the number quoted in his report). During Case 1 this level of optical density of 0.1 is reached at about 250 seconds.

Lopez has also noted that burning cabin interior materials can produce gases having sufficiently severe lachrymal effects such that viewers with unprotected eyes suffer "intolerable" irritation before the smoke density reaches the above level. Toxic gas concentrations attained

---

[22] Lopez, E.L., "Smoke Emission from Burning Cabin Materials and the Effect on Visibility in Wide-Bodied Jet Transports," Federal Aviation Administration, FAA-RD-73-127, March 1974.

during Case 1 are shown in Figure 7.16 where the concentrations are given in parts per million (ppm). Since the lowest levels of any toxic gas that may be said to definitely produce lachrymal or other detrimental physical effects over the exposure times considered here are not well established, no comparisons of such levels are made to the toxic gas results. An interesting fact to observe in Figure 7.16 is the rise and fall of the concentrations of two toxic gases, SO_2 and HF. Sulphur dioxide is produced by the carpet material only (see Figures 7.8 through 7.12) so that when this fire goes out the SO_2 concentration diminishes as gas leaves the upper zone. Hydrogen fluoride is produced by all materials except the seats and carpet (see Figure 7.10), but in large amounts only by the sidewall, ceiling, and stow bin materials. The first appearance of HF is thus seen at the time that the sidewall and reveal strip become involved in the fire, about 350 seconds. At 450 seconds what small amount of sidewall that was burning has burned out so that the HF concentration drops off sharply as the upper zone gas flows out into the adjacent sections. The concentrations of HCN and HCl fluctuate in response to the amounts of specific materials burning. Carbon monoxide, produced by all the materials in relatively large amounts, increases steadily as time goes by.

The stability of the upper gas layer is evidenced by the upper zone depth shown in Figure 7.17. The value stays approximately constant between three and four feet, meaning that about one half the cabin volume is filled with the combustion products throughout the run.

7.3.2 Analysis of Case 2, Sidewall Ignition

The fire in Case 2 begins with twelve elements flaming on the right lower sidewall and eighteen elements flaming on the right window reveal-transparency strip as illustrated in Figure 7.14. After ten seconds, four elements on the PSU above the sidewall fire and one element on the seat cushion top adjacent to the sidewall fire begin flaming. By 20 seconds, the 12 elements that were flaming on the lower sidewall have become charred.

At 150 seconds, the fire on the window reveal-transparency strip progresses upward to encompass these additional elements. At 250 seconds, this fire progresses outward to encompass six additional elements to the right and six to the left. At 260 seconds, the original eight flaming elements on the window reveal-transparency strip have become charred but the fire has progressed upward to include three more elements. Additional flaming elements on the window reveal-transparency strip become charred until this fire goes out at 520 seconds. Just before this fire goes out, an element of the lower sidewall is ignited, but the resulting fire is too small to propagate.

The fire on the seat does not begin to grow until 270 seconds at which point the elements on the backrest nearest the wall begin flaming. This includes both elements on the front and back of the backrest. As can be seen in Figure 7.22, the seat fire begins to increase in size rapidly after 540 seconds. This is due to the fact that, as more of the seat becomes involved, the increased radiation from this larger fire size causes the flame spread rate to accelerate. At the end of the simulation almost 50 square feet of fire area exists on the seat group adjacent to the original sidewall fire.

The PSU fire which was ignited very early in the simulation does not propagate and eventually goes out at about 350 seconds. Because of the small size of the fire, insufficient radiation is produced to cause it to propagate.

At 620 seconds, the stowage bin bottom above the burning seat is ignited. This fire grows slightly before the stowage bin material begins to char. Since this charring occurs within a relatively short time (see Figure 7.5), the fire does not propagate significantly over the stowage bin bottom.

The temperature of the upper gas layer rises very quickly to around 120^{o}F and remains roughly constant until it begins to decline

at 370 seconds when the PSU fires goes out and the window reveal-transparency fire begins to decline. These two materials have higher heat release rates per unit area than the other materials in the cabin as can be seen from Figure 7.6. The temperature begins to rise again as the seat fire becomes large after about 500 seconds.

The optical density of the smoke concentration in the upper gas layer is between 0.4 and 0.5 during the first 380 seconds of the run. It begins to decrease after the PSU fires goes out and the window reveal-transparency fire declines. As can be seen from Figure 7.7, the smoke release rate per unit area of the seats is less than that for the other materials and, thus, the smoke concentration does not begin to increase again until the seat fire becomes large. The optical density in the upper gas layer is greater than 0.1 during the entire simulation indicating that the smoke in this layer would considerably interfere with human vision. However, it should be noted that the upper gas layer thickness never exceeds about 2.5 feet. The thickness of this layer is relatively constant, as in Case 1, once gas begins to flow out the passageway opening at either end of the cabin section.

Initially the fire on the lower sidewall produces HCN which reaches a concentration in the upper gas layer of 5 ppm. This fire quickly goes out and the HCN concentration decreases due to the natural ventilation of the flow out the passage-way. As seen in Figure 7.8, combustion of the window reveal-transparency and PSU materials produce only very small amounts of HCN. The HCN concentration in the upper gas layer begins to be noticeable again once the seat fire begins to grow at about 260 seconds.

The concentration of HCl in the upper gas layer is relatively constant at about 6.5 ppm until the seat fire begins to grow at 260 seconds. Then the concentration increases to about 20 ppm. The HCl concentration begins to decrease when the window reveal-transparency fire goes out and the seat fire becomes large. The decrease in HCl as the seat fire becomes

large is explained by the HCl release rate curve in Figure 7.9. The release rate per unit area for a seat peaks at a heat flux of about 4.2 Btu/(ft^2 · sec). As the seat fire grows, it begins to generate radiation larger than 4.2 Btu/(ft^2 · sec) and the production of HCl decreases rapidly. Flow out the passage-ways then reduces the HCl concentration appreciably.

The initial fire on the lower sidewall produces HF which reaches a concentration in the upper gas layer of almost 50 ppm very quickly but begins to decline when the sidewall fires goes out. The PSU and window reveal-transparency fires contribute very little to the production of HF as can be seen in Figure 7.10. The HF concentration becomes noticeable again after 620 seconds when the stowage bin fire begins to contribute significantly to the production of this gas. The decline in HF concentration after 700 seconds occurs because stowage bin fire begins to decrease in size. The seat fire does not produce any HF.

The concentration of CO in the upper gas layer remains relatively constant at around 700 ppm, for the first 600 seconds of the simulation. This is due to the fact that, as the window reveal-transparency fire declines and therefore begins to produce less CO, the seat fire grows and begins to produce more CO. When the seat fire becomes large, the CO concentration begins to increase and reaches almost 2000 ppm at the end of the simulation.

The toxic gas concentrations in the upper gas layer probably reach sufficient levels to at least become irritants. However, as pointed out for the first case, the effects of these gases are not well enough defined to know the level of harm that should be associated with these concentrations.

SECTION 8

CONCLUSIONS

The DACFIR Model has not been experimentally validated. Specific conclusions, therefore, cannot be made concerning the agreement of predicted results to actual fire tests. Some general conclusions can, however, be made about the model based on the experience gained in exercising the model on selected hypothetical cabin fire scenarios. They are:

1. The discrete element method shows excellent potential for tracking fire development in an aircraft cabin. If refinements of the technique are required to provide better agreement with actual fire tests in some cases, the refinements can be made easily with little or no change to the basic structure of the mathematical model. Such refinements might involve adding new states, new state transitions, or a revised set of characteristic properties (flame spread rates, etc.). Extension of the discrete element method to larger portions of a wide-body cabin, to alternate interior arrangements, or to aircraft of other sizes presents no serious difficulty.

2. The cabin atmosphere model adequately approximates the distribution of combustion products and the concentration of smoke and toxic gases within the cabin section. The predicted upper zone temperature and radiation loss to interior surfaces are lower than might be expected. Some modification of the thermal analysis of the upper gas zone is required based on comparison to fire tests.

   Extension of this "two-zone" atmosphere model to the analysis of conditions in adjacent cabin sections and to cabins with forced rather than natural ventilation conditions appears promising.

3. To conclusively validate the DACFIR Model, comparisons of simulation results to full-scale aircraft cabin fire tests are required. The results of tests already conducted in the past will be useful for verification of the model provided that sufficient information on the materials, procedures, and results of such past tests is available. The test information must allow for the

preparation of a proper set of input information for the simulation program and must contain quantitative test results which can be unambiguously compared to the program output. If such suitable past test results are not available or if more conclusive testing of the DACFIR Model is necessary, full-scale, wide-body cabin fire tests should be conducted. Careful coordination of test procedures and test simulation by the model will be required to best validate the model and/or suggest appropriate refinements.

REFERENCES

[1] Marcy, J.F., Nicholas, E.B., and Damaree, J.E., "Flammability and Smoke Characteristics of Aircraft Interior Materials," Federal Aviation Administration, FAA-ADS-3, January 1964.

[2] Marcy, J.F., "A Study of Air Transport Passenger Cabin Fires and Materials," National Aviation Facilities Experimental Center, FAA-ADS-44, December 1965.

[3] Gross, D., Loftus, J.J., Lee, T.G., and Gray, V.E., "Smoke and Gases Produced by Burning Aircraft Interior Materials," National Bureau of Standards, June 1968.

[4] "Flaming and Self-Extinguishing Characteristics of Aircraft Cabin Interior Materials," National Aviation Facilities Experimental Center, Report No. NA-68-30, July 1968.

[5] Smith, E.E., "Measuring Rate of Heat, Smoke, and Toxic Gas Release," Fire Technology, Vol. 8, No. 3, 1972, pp. 237-245.

[6] Smith, E.E., "Model for Evaluating Fire Hazard," Journal of Fire and Flammability, Vol. 5, July 1974, pp. 185-195.

[7] Smith, E.E., "Application of the Ohio State Release Rate Apparatus to Combustion Gas Studies," JFF/Combustion Toxicology, Vol. 1, May 1974, pp. 95-103.

[8] Dayan, A. and Tien, C.L., "Radiant Heating from a Cylindrical Fire Column," Combustion Science and Technology, Vol. 9, 1974, pp. 41-47.

[9] Fu, T.T., "Aviation Fuel Fire Behavior Study," U.S. Naval Civil Engineering Laboratory, AGFSRS 72-2, February 1972.

[10] Blinov, V.I. and Khudiakov, G.N., "Certain Laws Governing Diffusive Burning of Liquids," Academiia Nauk, SSR Doklady, Vol. 113, 1957, pp. 1094-1098.

[11] Hottel, H.C., "Review-Certain Laws Governing Diffusive Burning of Liquids by B.I. Blinov and G.N. Khudiakov," Fire Research Abstracts and Reviews, Vol. 1, No. 2, January 1959, pp. 41-44.

[12] Seigel, R. and Howell, J.R., Thermal Radiation Heat Transfer, McGraw-Hill, New York, 1972.

[13] Welker, J.R., and Sliepcevich, C.M. "Heat Transfer by Direct Flame Contact, Fire Tests - Phase 1," University Engineers, Inc., Report No. UE-122-FR, July 197[illegible].

[14] Robertson, A.F., "Estimating Smoke Production During Building Fires," Fire Technology, Vol. 11, No. 2, (May 1975), pp. 80-94.

[15] Steward, F.R., "Prediction of the Height of Turbulent Diffusion Buoyant Flames," Combustion Science and Technology, Vol. 2, (1970), pp. 203-212.

[16] Fang, J.B., "Analysis of the Behavior of a Freely Burning Fire," NBSIR 73-115, Feb. 1973, U.S. National Bureau of Standards, Washington, D.C.

[17] Rockett, J.A., "Fire Induced Gas Flow in an Enclosure," Accepted for Publication, Combustion Science and Technology.

[18] Modak, A.T., and Croce, P.A., "Influence of Flame Radiation on the Burning Rate of Plastic Pool Fires of Varying Scale," Paper Presented at the Ninth Fall Technical Meeting 1975, Eastern Section: The Combustion Institute, Nov. 6-7, 1975, SONY at Stony Brook, Long Island, N.Y.

[19] Quintiere, J., "The Growth of Fire in Building Compartments," Paper Presented at the ASTM-NBS Symposium on Fire Standards and Safety, National Bureau of Standards, Gaithersburg, Maryland, April 5-6, 1976.

[20] Prahl, J., and Emmons, H.W., "Fire Induced Flow Through an Opening," Technical Paper No. 12, Division of Engineering and Applied Physics, Harvard University, Cambridge, Mass., 1975.

[21] Hsu, S.T., Engineering Heat Transfer, D. Van Nostrand Co., Princeton, N.J., 1963.

[22] Lopez, E.L., "Smoke Emission from Burning Cabin Materials and the Effect on Visibility in Wide-Bodied Jet Transports," Federal Aviation Administration, FAA-RD-73-127, March 1974.